## Efficiently learning non-Markovian noise in many-body quantum simulators

Jordi A. Montañà-López, <sup>1, 2, \*</sup> Andreas Elben, <sup>3, 4</sup> Joonhee Choi, <sup>5</sup> and Rahul Trivedi<sup>6, 2</sup>

<sup>1</sup> Max Planck Institute of Quantum Optics, Garching bei München - 85748, Germany

<sup>2</sup> Department of Electrical and Computer Engineering, University of Washington - 98195, USA

<sup>3</sup> Laboratory for Theoretical and Computational Physics,

Paul Scherrer Institute, CH-5232 Villigen-PSI, Switzerland

<sup>4</sup> ETHZ-PSI Quantum Computing Hub, Paul Scherrer Institute, CH-5232 Villigen-PSI, Switzerland

<sup>5</sup> Department of Electrical Engineering, Stanford University, Stanford, CA, USA

<sup>6</sup> Max Planck Institute of Quantum Optics, Hans-Kopfermann-Straße 1, 85748 Garching, Germany

(Dated: November 24, 2025)

As quantum simulators are scaled up to larger system sizes and lower noise rates, non-Markovian noise channels are expected to become dominant. While provably efficient protocols for Markovian models of quantum simulators, either closed system models (described by a Hamiltonian) or open system models (described by a Lindbladian), have been developed, it remains less well understood whether similar protocols for non-Markovian models exist. In this paper, we consider geometrically local lattice models with both quantum and classical non-Markovian noise and show that, under a Gaussian assumption on the noise, we can learn the noise with sample complexity scaling logarithmically with the system size. Our protocol requires preparing the simulator qubits initially in a product state, introducing a layer of single-qubit Clifford gates and measuring product observables.

#### I. INTRODUCTION

Recent experimental progress in developing quantum simulators in different technological platforms [1–7] has opened up the possibility of using them to solve computationally challenging many-body problems. In order to both understand and characterize the accuracy of these simulators [8-11] as well as to effectively use error mitigation strategies [12-14], we would like to be able to learn an accurate noise model that captures their dynamics. As a first approximation, typically errors in a quantum simulator implementing a target Hamiltonian are modeled as Markovian. This can include errors modeled as either unwanted Hamiltonian terms or as jump operators in a master equation describing the simulator dynamics. However, the Markovian model is only an approximation — in many experimental quantum platforms, gates and Hamiltonian evolution are realized through global driving fields that couple multiple qubits simultaneously. This shared control introduces correlated noise and memory effects, giving rise to non-Markovian dynamics. As both the size of the quantum simulators are increased and the noise rates are reduced, such non-Markovian effects are expected to become important and increasingly determine the noise floor in the quantum device. This opens up the theoretical question of developing efficient measurement protocols to learn non-Markovian noise models of quantum simulators.

For quantum devices containing only a few qubits, the quantum channel generated by its dynamics (including both the target Hamiltonian and unwanted errors) can be learned by performing quantum process tomography [15, 16]. In particular, for digital circuits, recent work has also developed "process tensor tomography" which generalizes process tomography to learn a non-Markovian noise model independent of the target evolution [17– 22]. However, these approaches usually require a number of samples that scale exponentially with the number of gubits and thus become infeasible to employ at large system sizes. For digital quantum simulators implementing a quantum circuit built out of a universal gate set, noise is often characterized by the average error rates of the individual gates used in the circuit, which can be extracted using the randomized benchmarking proto-

<sup>\*</sup> jordi.montana-lopez@mpq.mpg.de

col [23–30]. While traditionally randomized benchmarking was developed under the Markovian assumption, where individual gate errors are assumed to be independent and uncorrelated, it has recently been extended to the non-Markovian setting as well [31, 32]. Despite these significant advances, employing randomized benchmarking for learning noise models remains restricted to digital simulators and only furnishes an "average" measure of the noise rate as opposed to a more detailed model of the noise in the quantum device.

In analog quantum simulators, alternative approaches have been developed that leverage the natural system dynamics in the many-body regime to infer both the system Hamiltonian and Lindbladian noise processes [33-42]. Such strategies have been explored both for the closed system setting, where the unitary evolution of the simulator is generated by a Hamiltonian [33, 39], as well as in the Markovian open system setting, where dissipative evolution is described by a Lindbladian [34, 42]. The general strategy involves evolving the analog simulator for a short time starting from an initial product state and measure a set of local observables — since the evolution is performed only for a short time, the parameters of the Hamiltonian or the Lindbladian describing the simulator can be backed out from the measured observables. This can be done either by measuring the observables at a single, sufficiently small, time and using a non-linear equation solver [33] or by measuring timetraces of the observables and employing a robust fitting strategy [34]. For Markovian geometrically local models, it has also been rigorously proven that the sample complexity of a learning protocol employing either of these strategies scales at-most logarithmically with the system size and attains the standard-quantum-limit scaling with respect to the desired precision in the simulator parameters [34]. Furthermore, for the case of Hamiltonian learning, a strategy that combines long-time evolution and Pauli operator reshaping has also been developed to attain Heisenberg scaling in the sample complexity with respect to the desired precision [40, 43]. However, the development of these strategies beyond the Markovian approximation still remains an experimentally relevant open question and has largely been considered only for

small systems [44–51].

In this paper, we address this question for geometrically local quantum simulators. We consider a reasonably general non-Markovian noise model, where the noise can act on multiple neighboring qubits in a correlated manner, with the only assumption being that the noise arises from an interaction with a stationary and Gaussian environment [52]. We provide a measurement strategy that uses short-time evolution to learn the two-point correlation functions of the non-Markovian environment to a desired precision. Similar to the algorithms available for the Markovian case, our strategy provably requires a number of samples scaling only logarithmically with the system size, and the postprocessing time is similarly efficient. Furthermore, we provide an explicit construction of the initial states and observables that need to be measured for our protocol. In the worst case, while the sample complexity of our protocol scales exponentially with the size of the support of the system-environment coupling operators, it is independent of the locality of the terms in the system Hamiltonian.

Finally, we also adapt our strategy to a coherent noise model, where the errors are Gaussian random geometrically local terms in the Hamiltonian albeit with possible all-to-all correlations. Physically, this would be the case where a global control field is used to implement singleor two-qubit Hamiltonian terms in an experiment, but the control itself is noisy — then the laser noise would result in coherent errors that can be modeled as random, but coherent, terms added to the target Hamiltonian. On averaging the unitary evolution with respect to the noise realization, we in general still obtain a non-Markovian channel for the simulator dynamics. In this case, we show that even if the noise is all-to-all correlated, we can still learn the mean and covariance matrix of the noise model with almost the same experimental requirements as Hamiltonian learning.

This paper is structured as follows: in Section II we introduce the non-Markovian noise model, describing the non-Markovian effects via so-called memory kernels. In Section III we present our results for estimating the derivatives at t=0 of these memory kernels, on two classes of non-Markovian models that satisfy different lo-

cality assumptions. In Section IV we lay out the strategy to learn these derivatives from a linear system of equations and provide the set of measurements that need to be performed to invert it. In Section V we present numerical results for the performance of our protocol with both sparse non-Markovian kernels and in the case of correlated errors across all interaction terms. In Section VI we explain how this system of equations arises from a polynomial fit to the time traces of the measured observables and analyze the number of samples required to estimate the derivatives of the kernels to the desired precision.

#### II. DESCRIBING NON-MARKOVIAN NOISE

#### A. Model

We will model the quantum simulator as a system with N qubits interacting with a decohering environment. In the Pauli basis, the Hamiltonian describing the system-

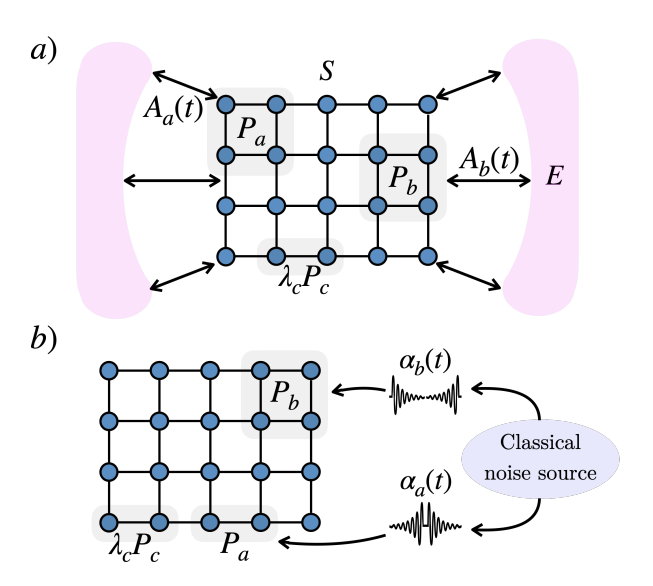


FIG. 1. Open system models considered in this paper. (a) The system S (blue circle lattice) is assumed to interact with an environment E (pink), with a coupling  $P_aA_a(t)$  between a Pauli string  $P_a$  acting on the system and a time-dependent Hermitian operator  $A_a(t)$  acting on the environment. (b) A non-dissipative environment, where the environment operators are commuting  $[A_a(t), A_b(s)] = 0$ , can be equivalently described by a noisy term in the system Hamiltonian  $\alpha_a(t)P_a$ , where  $\alpha_a(t)$  is a classical noise.

environment evolution can generically be written as sum of a static system Hamiltonian  $H_S$  and a time-dependent system-environment coupling  $V_{SE}(t)$ :

$$H(t) = H_S + V_{SE}(t), \tag{1a}$$

with

$$H_S = \sum_{a \in \mathcal{P}_S} \lambda_a P_a, \tag{1b}$$

$$V_{SE}(t) = \sum_{b \in \mathcal{P}_{SE}} P_b A_b(t), \tag{1c}$$

where  $\mathcal{P}_S$  and  $\mathcal{P}_{SE}$  are the index sets of Pauli operators (i.e., operators of the form  $\sigma_1 \otimes \sigma_2 \otimes \dots \sigma_N$  where  $\sigma_i \in \{1, \sigma^x, \sigma^y, \sigma^z\}$ ) appearing in the system Hamiltonian,  $H_S$ , and the coupling Hamiltonian,  $V_{SE}(t)$ , respectively. Note that we choose to express the coupling Hamiltonian directly in the interaction picture with respect to the environment Hamiltonian, which makes the Hermitian operator  $A_b(t)$  dependent on time. While the system-environment coupling will in general result in the system and the environment evolving into an entangled state, we will assume that initially the system and the environment are not entangled i.e.,  $\rho(0) = \rho_S \otimes \gamma_E$  where  $\rho_S$  and  $\gamma_E$  are the initial system and environment state, respectively. We assume that the state  $\gamma_E$  is the same for each realization of the experiment. This is reasonable as, for example, the environment could be evolving under a quadratic Hamiltonian and  $\gamma_E$  be its generalized Gibbs state. After a projective measurement on the system and turning off the system-environment coupling, the environment will equilibrate to  $\gamma_E$ .

From the Dyson expansion it follows that the state of the system at time t,  $\rho_S(t) = \text{Tr}_E(U(t,0))(\rho_S \otimes \gamma_E)U(0,t)$  where  $U(t,s) = \mathcal{T}\exp(-i\int_s^t H(\tau)d\tau)$ , is entirely determined by the n-point environment correlation functions  $C_{a_1,a_2...a_n}(t_1,t_2...t_n)$  [53–55]:

$$C_{a_1,a_2...a_n}(t_1,t_2...t_n) = \operatorname{Tr}_E\left[\left(\prod_{i=1}^n A_{a_i}(t_i)\right)\gamma_E\right].$$

We will make two physically reasonable assumptions on these environment correlation functions which are reasonable in several leading quantum information processing platforms, such as superconducting systems, [56–60], trapped ion systems as well as quantum optical systems [61–64]. First, Stationarity, i.e., the correlation functions  $C_{a_1,a_2...a_n}(t_1,t_2...t_n)$  depend only on time differences  $t_2-t_1,t_3-t_1...t_n-t_1$  i.e.

$$C_{a_1,a_2...a_n}(t_1,t_2,...t_n) = C_{a_1,a_2...a_n}(0,t_2-t_1,...t_n-t_1).$$
 (2)

Second, Gaussianity, i.e., the correlation functions  $C_{a_1,a_2...a_n}(t_1,t_2...t_n)$  satisfy the Wick's theorem i.e.,

$$C_{a_1,a_2...a_n}(t_1,t_2...t_n) = \sum_{\mathcal{S}} \prod_{(i,j)\in\mathcal{S}} C_{a_i,a_j}(t_i,t_j) \prod_{k\in\mathcal{S}^c} C_{a_k}(t_k),$$
(3)

where S is a subset of  $\{1, 2 \dots n\}$  with even number of elements that are divided into pairs (i, j) with i < j. Thus, a stationary Gaussian environment is described entirely by

$$\lambda_a = \mathcal{C}_a(0) = \text{Tr}(\gamma_E A_a(0)) \text{ and}$$
 (4)

$$K_{ab}(t) = \mathcal{C}_{a,b}(t,0) = \text{Tr}(\gamma_E A_a(t) A_b(0)). \tag{5}$$

Since we can always transform the environment operators  $A_a(t) \to A_a(t) - \lambda_a$  and the system Hamiltonian  $H_S \to H_S + \sum_{a \in \mathcal{P}_{SE}} \lambda_a P_a$  without changing the coupling Hamiltonian, without loss of generality we will assume that  $\lambda_a = 0$ .

A special class of such systems are non-dissipative systems, in which the environment operators,  $A_b(t)$ , commute with one another:  $[A_b(t), A_{b'}(s)] = 0$ . In this case, the evolution of the system qubits can be alternately described by a Hamiltonian ensemble i.e.,

$$\rho_S(t) = \mathbb{E}_{\alpha} \big( U_{\alpha}(t,0) \rho_S(0) U_{\alpha}(0,t) \big),$$

where  $U_{\alpha}(t,s) = \mathcal{T} \exp(-i \int_{s}^{t} H_{\alpha}(\tau) d\tau)$  with

$$H_{\alpha}(t) = \sum_{a \in \mathcal{P}_S} \lambda_a P_a + \sum_{b \in \mathcal{P}_{SE}} \alpha_b(t) P_b, \tag{6}$$

with  $\alpha_b(t)$  being a classical stationary real-valued Gaussian stochastic process with  $\mathbb{E}(\alpha_b(t)) = 0$  and  $\mathbb{E}(\alpha_a(t)\alpha_b(s)) = K_{ab}(t-s)$ . Thus, non-Markovian non-dissipative noise can equivalently be considered to be classical random noise in Hamiltonian parameters.

## B. The learning problem

Learning the quantum simulator model with either dissipative or non-dissipative noise, under the stationary Gaussian assumption, requires learning the Hamiltonian parameters  $\lambda_a$  as well as the kernels  $K_{a,b}(t)$ . Since, in the most general setting, the kernels can be almost arbitrary functions of time, learning them could require learning an infinite number of parameters and is thus not a well-posed problem. However, in most physical situations, the kernel is parameterized by a small number of parameters. Under the additional physically reasonable assumption that the kernels  $K_{a,b}(t)$  are smooth functions of time, we can then aim to learn its derivatives  $K_{a,b}^{(m)}(0)$  for  $m \in \{0, 1, 2 ... M\}$  upto a pre-specified order M, and then use these derivatives to infer the parameters that  $K_{a,b}(t)$  depends on.

As an example of a physically relevant non-Markovian noise model, consider the setting where the environment itself consists of a set of discrete bosonic modes undergoing Markovian particle loss. This family of models, referred to as the pseudomode model in open-system theory [65, 66], is a well-studied model for non-Markovian open systems and can also approximate the dynamics of any non-Markovian models with smooth kernels if a sufficiently large number of discrete modes are used [67]. For such models, it can be shown that the kernels  $K_{a,b}(t)$  are given by linear combinations of decaying exponentials [65]:

$$K_{a,b}(t) = \sum_{l} v_{a,l}^* v_{b,l} e^{(i\epsilon_l - \gamma_l/2)|t|}.$$
 (7)

Here the sum is over environment modes l that are coupled to  $P_a, P_b$  and  $\epsilon_l, \gamma_l$  are the resonant frequency and dissipation rate of the modes. In Section V A we simulate this kind of non-Markovian dynamics in the fermionic case and show that we can estimate the kernel derivatives at t=0 for m=0,1,...,M. With an ansatz for the kernel as in Eq.(7) this yields the system of equations relating the kernel derivatives  $K_{a,b}^{(m)}(0)$  to the parameters  $v_{a,l}, \epsilon_l, \gamma_l$ :

$$K_{a,b}^{(m)}(0) = \sum_{l} v_{a,l}^* v_{b,l} \left( i\epsilon_l - \frac{\gamma_l}{2} \right)^m.$$
 (8)

Inverting either this system of non-linear equations or by using a filter diagonalization algorithm [68, 69], we can then obtain the parameters  $v_{a,l}, \epsilon_l, \gamma_l$  from the learned derivative  $K_{a,b}^{(m)}(0)$ .

Note that this differs from previous work on characterizing many-body non-Markovian processes [18, 19] that could also be applied to our setting. Their general method of process tensor tomography requires a number of samples that grows exponentially with the system size and Markov order — their measure of non-Markovianity. Our work focuses on a particular non-Markovian model with geometrically-local kernels, which are relevant in many experimental platforms. We expect our learning problem to directly provide experimentally-relevant information, since kernel ansatzs such as Eq.7 provide resonant frequencies and dissipation rates of the environment modes.

In the next section, we summarize the main results of this paper showing that this learning problem can be solved with a number of copies of  $\rho_S(t)$  that scales at most logarithmically with the system size and outline the measurement protocols that attain this scaling.

#### III. RESULTS

## A. Non-Markovian models

We will consider the model of non-Markovian evolution given by a system S of N spin- $\frac{1}{2}$  particles interacting with stationary Gaussian environment E. We assume that the system-environment Hamiltonian H(t) is a sum of O(N) geometrically local terms — more specifically, we assume that the Pauli strings in  $H_S$  and  $V_{SE}(t)$  are supported on at most  $k_S$ ,  $k_{SE} = O(1)$  sites, respectively, and their support diameter is also upper bounded by a constant  $a_0 = O(1)$ . Note that this ensures that each Pauli string in the Hamiltonian H(t) overlaps with at most  $\mathfrak{d} = O(1)$  other Pauli strings in H(t). Additionally, we assume that the environment does not introduce nonlocal interactions in H(t) by assuming that each term  $P_a A_a(t)$  in the coupling Hamiltonian [Eq. (1c)] is noncommuting with at most  $\mathfrak{d} = O(1)$  other terms  $P_b A_b(t)$ and that for a fixed  $P_a$ , there's at most s = O(1) kernels  $K_{a,b}(t)$  that are nonzero. Finally, we will assume that the non-Markovian environment has "finite memory" as formalized by the total variation of the kernels  $K_{a,b}(t)$  in

Ref. [70] i.e., we will assume that

$$\sup_{a} \sum_{b} \int_{-\infty}^{\infty} |K_{a,b}(s)| \, ds \le O(1). \tag{9}$$

As established in Ref. [70], this condition is sufficient to ensure that the system has a finite velocity of information propagation, thus making it a reasonable assumption for an experimentally realistic model of a noisy quantum simulator.

Our first result shows that there is an efficient protocol that allows us to estimate both the parameters  $\lambda = \{\lambda_a\}_a$  of the system Hamiltonian as well as the Kernel derivatives

$$K_{a,b}^{(m)}(0) := \partial_t^m K_{a,b}(t)|_{t=0}, \quad K^{(m)} = \{K_{a,b}^{(m)}(0)\}_{(a,b)}$$
(10)

by only initializing and measuring the system.

**Proposition 1.** There is a protocol which uses only initial product states, single qubit gates and Pauli measurements and with probability  $\geq 1 - \delta$  obtains estimates  $\hat{\lambda}, \hat{K}^{(m)}(0)$  satisfying  $||\hat{\lambda} - \lambda||_{\infty}, ||\hat{K}^{(m)}(0) - K^{(m)}(0)||_{\infty} < \epsilon$  for every  $m \in \{0, 1..., M\}$  with  $N_S$  samples, where:

$$N_S = O\left(e^{O(M^2 \log M)} \frac{1}{\epsilon^2} \log\left(\frac{N}{\delta}\right)\right).$$

This protocol requires evolving initial states up to time t = O(1) and the classical postprocessing is  $O(N \cdot N_S)$ .

Note that the provable sample complexity in Proposition 1 grows super-exponentially with M, which is the degree of the highest derivative of the kernels  $K_{a,b}(t)$  that we want to learn. This indicates that this protocol would perform poorly in accurately learning noise models with very rapidly varying kernels — however in many physically relevant settings, these kernels are expected to be a sum of a small number of exponentials in t, as in Eq.(7), [65, 66] and can thus be specified by only low-order derivatives at t = 0.

Our protocol builds on a strategy recently developed for many-body Lindbladian learning [34], which is based on measuring system observables after a short-time evolution of an initial controllable system state. More specifically, we start with an initial system-environment state

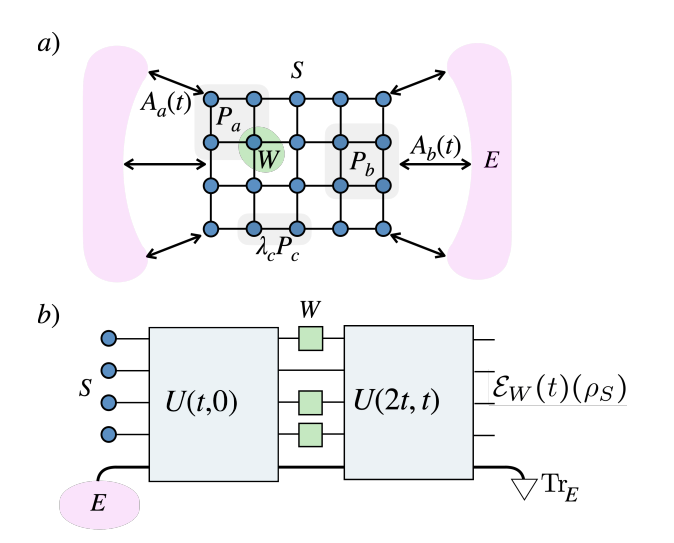


FIG. 2. a) Single-qubit gate W applied on the support of  $P_a$  when trying to estimate kernel  $K_{a,b}(t)$ . b) Quantum channel used to prepare the state: an initial state  $\rho(0) = \rho_S \otimes \gamma_E$  is prepared, where  $\rho_S$  is a product state chosen depending on the kernels we are trying to learn while  $\gamma_E$  is a Gaussian state. The state is time evolved under U(t,0) and a unitary W, consisting of single-qubit Clifford gates on certain sites, is applied. The state is further evolved under U(2t,t) and the environment is traced out.

 $\rho(0) = \rho_S \otimes \gamma_E$ , where  $\rho_S$  is a product state of our choice, and then prepare a state  $\mathcal{E}_W(t)(\rho_S)$  by performing the evolution shown in Figure 2:

$$\mathcal{E}_W(t)(\rho_S) = \text{Tr}_E(V_W(t)\rho_S \otimes \gamma_E V_W^{\dagger}(t)), \qquad (11)$$

where  $V_W(t) = U(2t,t)WU(t,0)$ , with W being a layer of single qubit gates applied on the system qubits and  $U(t,s) = \mathcal{T} \exp(-i \int_s^t H(\tau) d\tau)$ . For small enough t,  $\mathcal{E}_W(t)(\rho_S)$  can be well approximated by a second order Dyson series expansion of the system-environment evolution U(t,0) and U(2t,t):

$$\mathcal{E}_W(t)(\rho_S) \approx W \rho_S W^{\dagger} + \mathcal{F}_W^{(1)}(t)(\rho_S) + \mathcal{F}_W^{(2)}(t)(\rho_S),$$
(12a)

where  $\mathcal{F}_W^{(j)}(t)$  are system super-operators that correspond to the  $j^{\text{th}}$  order term in the Dyson series expansion.

sion:

$$\mathcal{F}_{W}^{(2)}(t)(\rho_{S}) = -\left(\int_{0}^{t} \int_{0}^{s_{1}} \operatorname{Tr}_{E}(W[H(s_{1}), [H(s_{2}), \rho_{S} \otimes \gamma_{E}]]W^{\dagger})d^{2}s + \int_{t}^{2t} \int_{0}^{t} \operatorname{Tr}_{E}([H(s_{1}), W[H(s_{2}), \rho_{S} \otimes \gamma_{E}]W^{\dagger}])d^{2}s + \int_{t}^{2t} \int_{t}^{s_{1}} \operatorname{Tr}_{E}([H(s_{1}), [H(s_{2}), W\rho_{S}W^{\dagger} \otimes \gamma_{E}]])d^{2}s\right).$$
(12a)

 $\mathcal{F}_W^{(1)}(t)(\rho_S) = -it(W[H_S, \rho_S]W^{\dagger} + [H_S, W\rho_S W^{\dagger}]),$ 

where in Eq. (12a) we have used that, by assumption,  $\operatorname{Tr}_E(A_a(t)\gamma_E)=0$ . From Eq. 12, it is clear that  $\mathcal{F}_W^{(1)}(t)$  is linear in the system Hamiltonian coefficients  $\lambda_a$ . Furthermore, since  $\mathcal{F}_W^{(2)}(t)$  is quadratic in the environment operators  $A_a(t)$  and the environment is traced out, it is linear in  $K_{a,b}(t)$ . Consequently, it follows from Eq. 11 that the first derivative of  $\mathcal{E}_W(t)$  at t=0 carries information about the system Hamiltonian coefficients  $\lambda_a$ , while second and higher derivatives carry information about  $K_{a,b}^{(m)}(0)$ . The problem of learning  $\lambda_a, K_{a,b}^{(m)}(0)$  thus reduces to finding an informationally complete set of initial states  $\rho_S$ , observables O and unitaries W for which the derivatives of  $\operatorname{Tr}_S[O\mathcal{E}_W(t)(\rho_S)]$  at t=0 can be used to uniquely determine  $\lambda_a, K_{a,b}^{(m)}(0)$ .

For learning system Hamiltonian parameters from first derivative information, it was shown in Ref. [33] that we can always choose  $W = \mathbb{1}^{\otimes N}$ , and for every  $\lambda_a$ , there is a unique choice of an initial state  $\rho_S$  as well as an observable O such that  $\partial_t \operatorname{Tr}_S[O\mathcal{E}_{W=1\otimes N}(t)(\rho_S)]|_{t=0} = -8\lambda_a$ , as shown in Eq. (13). In order to learn  $K_{a,b}^{(m)}(0)$ , we need to use higher-order derivative information and the nested commutator structure of  $\mathcal{F}_{W}^{(2)}(t)(\rho_{S})$  makes it more complicated to develop an explicit tomography protocol. One of the main contributions of our work, detailed in Section IV, is to determine a set of initial product states  $\rho_S$ , product observables O and single qubit unitaries W such that  $K_{a,b}^{(m)}(0)$  can be learned from the derivatives of  $\operatorname{Tr}_S[O\mathcal{E}_W(t)(\rho_S)]$  at t=0. In contrast to the case of Hamiltonian learning, where a single observable and initial state can be used to directly infer a given Hamiltonian parameter, we need to use several initial-state and

observable pairs  $(\rho_S, O)$  to learn a particular  $K_{a,b}^{(m)}(0)$ . Nevertheless, we show that it is sufficient to use product states and measure observables on a region that is slightly larger than the supports  $P_a$ ,  $P_b$  to learn  $K_{a,b}^{(m)}(0)$ . Furthermore, unlike Hamiltonian or Lindbladian learning [34], where the learning strategy involve preparing an initial state and measuring an observable after short time evolution (thus setting  $W = \mathbb{1}^{\otimes N}$ ), we show in Section IV that the short-time evolution of observables as described by a second-order Dyson series expansion does not depend on the kernels  $\operatorname{Im}[K_{c,c}^{(m)}(0)]$ . Nevertheless, we find that by applying a layer of single qubit gates W in the middle of the time-evolution allows us to also learn these Kernel parameters — we provide an explicit procedure to pick these gates W in addition to the initial state  $\rho_S$  and observables O that allows us to learn all the Kernel parameters in Section IV.

While our construction of the required measurement settings  $(\rho_S, O, W)$  is based on analyzing a second order Dyson series expansion, we rigorously account for the higher order terms in establishing the sample complexity result in Proposition 1. First, while the first and second order derivatives of the measured observable  $\operatorname{Tr}_S(O\mathcal{E}_W(t)(\rho_S))$ , at t=0, is entirely determined by the first and second order term in the Dyson series expansion of  $\mathcal{E}_W(t)$ , the third and higher order derivatives of  $\operatorname{Tr}_S(O\mathcal{E}_W(t)(\rho_S))$ , needed to obtain the higher derivatives of  $K_{a,b}(t)$ , in general have a contribution from higher order terms in the Dyson series for  $\mathcal{E}_W(t)$ . Furthermore, the third and higher order terms in the Dyson series of  $\mathcal{E}_W(t)$  would be non-linear in the parameters  $\lambda_a, K_{a,b}^{(m)}(0)$  — consequently, the derivatives of  $\operatorname{Tr}_S(O\mathcal{E}_W(t)(\rho_S))$  at t=0 depend nonlinearly on  $\lambda_a, K_{a,b}^{(m)}(0)$ . Despite this, we show that with the choice of  $(\rho_S, O, W)$  made on the basis of a second order Dyson series expansion of  $\mathcal{E}_W(t)$ , the resulting nonlinear equations relating  $\lambda_a, K_{a,b}^{(m)}(0)$  to the derivatives of  $\operatorname{Tr}_S(O\mathcal{E}_W(t)(\rho_S))$  at t=0 can be uniquely and efficiently solved to obtain  $\lambda_a, K_{a,b}^{(m)}(0)$ . Furthermore, in an actual experiment we can only measure the timetraces  $\operatorname{Tr}_S(O\mathcal{E}_W(t)(\rho_S))$  to an accuracy determined by the number of measurement shots and its derivatives have to be obtained by fitting a polynomial to the measured data — to obtain rigorous sample complexity bounds for the tomography protocol, following a strategy laid out in [34, 71] for Lindbladian learning, we use Lieb-Robinson bounds [70] to show that for evolution times  $t \leq t_{\text{max}} = O(1)$ , these time traces can be well approximated by polynomials of degree  $d = O(\text{poly}(t_{\text{max}}, \log(\epsilon^{-1})))$ , where  $\epsilon$  is the target precision desired in the parameters  $\lambda_a, K_{a,b}^{(m)}(0)$ , and with the observables measured only at times  $n\tau$  where  $n \in \{1, 2, 3...\}$  and  $\tau = \Theta(1/d^2)$ . These fitted polynomials are then used for extracting the derivatives of  $\text{Tr}_S(O\mathcal{E}_W(t)(\rho_S))$  which are the subsequently used for learning  $\lambda_a, K_{a,b}^{(m)}(0)$ .

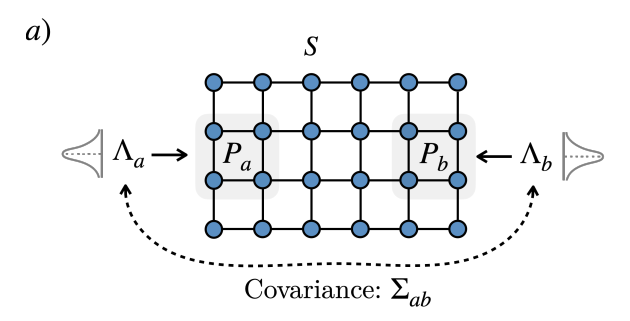
#### B. Ensemble Hamiltonian model

The second class of models that we address in this paper are Hamiltonians with noisy parameters — we consider the simulator to be described by

$$H_{\Lambda} = \sum_{a \in \mathcal{P}_S} \Lambda_a P_a,$$

where, again,  $P_a$  are geometrically local Paulis which are supported on at most O(1) sites and with diameter upper bounded by an O(1) constant and  $\Lambda_a$  are jointly Gaussian random variables with mean  $\lambda_a = \mathbb{E}(\Lambda_a)$  and covariances  $\Sigma_{a,b} = \mathbb{E}(\Lambda_a \Lambda_b) - \lambda_a \lambda_b$ . We assume the Hamiltonian contains  $|\mathcal{P}_S| = O(N)$  terms and allow the covariance matrix to be dense (i.e., allow for all-to-all correlations between the coefficients  $\Lambda_a$ ) and only assume that  $|\lambda_a| \leq 1$  and  $\operatorname{var}(\Lambda_a) = \Sigma_{aa} \leq 1$ . We remark that, as described in Section II, this model is equivalent to a non-dissipative open system model with system Hamiltonian  $\sum_a \lambda_a P_a$  and a time-independent kernel  $K_{a,b}(t) = \mathbb{E}_{\Lambda}(\Lambda_a \Lambda_b)$ . However, since the kernels  $K_{a,b}(t)$  are not necessarily sparse and do not satisfy the total variation condition in Eq. (9), Proposition 1 cannot be directly applied to this setting. Nevertheless, we show that both the means  $\lambda = {\lambda_a}_a$ and covariances  $\Sigma_{a,b}$  can be learned efficiently for this model following a strategy similar to the one used for the more general non-Markovian model.

**Proposition 2.** There is a protocol which uses only initial product states and Pauli measurements and with probability  $\geq 1 - \delta$  obtains estimates  $\hat{\lambda}, \hat{\Sigma}$  satisfying



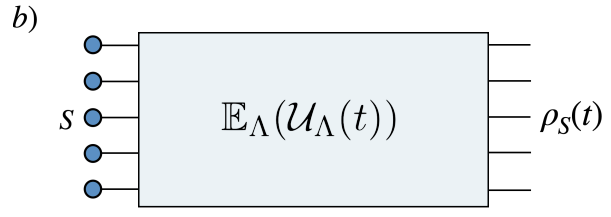


FIG. 3. a) In the ensemble Hamiltonian model, while the Pauli strings are geometrically local, the correlations between their coefficients can be all-to-all:  $\Lambda_a, \Lambda_b$  can have covariance  $\Sigma_{ab} = \Omega(1)$  even if the supports of  $P_a, P_b$  are far away. b) Quantum channel used to prepare the sate: a state  $\rho(0) = \rho_S \otimes \gamma_E$  is prepared, where  $\rho_S$  is a product state chosen depending on the kernel we are trying to learn while  $\gamma_E$  is a Gaussian state. The state is time evolved under  $\mathcal{U}_{\Lambda}(t)(\rho_S) = U_{\Lambda}(2t,0)\rho_S U_{\Lambda}(2t,0)^{\dagger}$  with  $U_{\Lambda}(t,0) = e^{-itH_{\Lambda}}$ , without introducing any intermediate gate W. We take the expectation value with respect to the jointly Gaussian random variables  $\Lambda$ .

 $||\hat{\lambda} - \lambda||_{\infty}, ||\hat{\Sigma} - \Sigma||_{\max} < \epsilon \text{ for an s-sparse } \Sigma \text{ with } N_S$  samples, where:

$$N_S = O\left(\frac{s}{\epsilon^2} \log\left(\frac{N}{\delta}\right)\right).$$

This protocol requires evolving initial states up to time  $t = O((\log(N)\log(1/\epsilon))^{-\frac{1}{2}})$  and the classical postprocessing is  $O(sN \cdot N_S)$ .

The learning protocol for this model is considerably simpler than that for the non-Markovian model. *First*, we do not need an intermediate layer of single qubit gates shown in Fig. 3. *Second*, we only need to extract the first and second derivatives of the measured observables — the mean  $\lambda_a$  are estimated from the first derivative, as in Hamiltonian learning [33, 39] and  $\mathbb{E}_{\Lambda}(\Lambda_a\Lambda_b)$  from the second derivatives. We describe the precise choice of initial product states as well as observables in the next section.

To obtain rigorous sample complexity bounds for this tomography protocol, we again use the Lieb-Robinson bounds [72] to show that the measured observables are well approximated by low degree polynomials — while the Lieb-Robinson bounds derived for non-Markovian lattice models [70] does not apply to this model directly (since  $\Lambda_a$  might have all-to-all correlations), we use the fact that since each  $\Lambda_a$  is Gaussian with mean and variance  $\leq 1$ , it is going to be  $\leq O(1)$  with high probability and consequently the  $H_{\Lambda}$  will have an O(1) Lieb-Robinson velocity with high probability. By controlling the tail contribution of the low probability event where  $H_{\Lambda}$  has a large Lieb-Robinson velocity, in Appendix B we show that the time trace up to  $t_{\text{max}} = O((\log(N)\log(1/\epsilon))^{-1/2})$ can be well-approximated by a polynomial of degree  $d = O(\text{poly}(t_{\text{max}}, \log(\epsilon^{-1})))$ , where  $\epsilon$  is the target precision in the means and covariances. The first and second time-derivatives of the observable at t = 0 can be extracted by evolving it from 0 to  $t_{\text{max}}$ , measuring it at times  $n\tau$  where  $n \in \{1, 2, 3...\}$  and  $\tau = \Theta(1/d^2)$ , and obtaining the polynomial fit.

#### IV. MEASUREMENT STRATEGY

We now present the details on the measurement protocols that have been outlined in Section III and achieve the sample complexities in propositions 1 and 2 — we focus on describing the measurement protocol for the non-Markovian setting since the same protocol also works for the ensemble Hamiltonian setting. We first briefly review the measurement protocol for learning the system Hamiltonian parameters  $\lambda_a$  which have been provided in [33] and then describe the more complex measurement protocol needed for measuring the kernel derivatives  $K_{a,b}^{(m)}(0)$ .

# A. Learning the system Hamiltonian parameters $\lambda_a$ (Review of Ref. [33])

To learn the system Hamiltonian parameter  $\lambda_a$ , we choose the intermediate unitary  $W=\mathbb{1}^{\otimes N}$ . For every Pauli string  $P_a, a \in \mathcal{P}_S$  in the system Hamiltonian

nian, we can always find a single-qubit Pauli  $P_I$  such that  $\{P_I, P_a\} = 0$  — suppose we choose the initial state  $\rho_S = (I^{\otimes N} + P_I)/2^N$  and the observable  $O = i[P_a, P_I] = 2iP_aP_I$ , then from Eqs. 11 and 12 it follows that the first derivative of the expected observable  $\text{Tr}[O\mathcal{E}_{W=1^{\otimes N}}(t)(\rho_S)]$  at t=0 is given by

$$\begin{split} \partial_t \mathrm{Tr}[O\mathcal{E}_{W=1^{\otimes N}}(t)(\rho_S)]|_{t=0} \\ &= \frac{4}{2^N} \sum_{b \in \mathcal{P}_S} \lambda_b \mathrm{Tr}(P_a P_I[P_b, P_I]). \end{split}$$

Noting that since  $P_I$  and  $P_a$  anticommute by construction,  $\text{Tr}(P_aP_I[P_b,P_I]) = -2\text{Tr}(P_aP_b) = -2^{N+1}\delta_{a,b}$ , and consequently

$$\partial_t \text{Tr}[O\mathcal{E}_{W=1 \otimes N}(t, \rho_S)]|_{t=0} = -8\lambda_a. \tag{13}$$

This shows that using  $W = \mathbb{1}^{\otimes N}$ ,  $\rho_S = (I + P_I)/2^N$  and  $O = 2iP_aP_I$  is enough to learn  $\lambda_a$  from the first derivative of the expected observable at t = 0.

In practice, it is more convenient to prepare initial product states instead of states of the form  $\rho_S = (I + P_I)/2^N$  for a Pauli string  $P_I$ . In particular, we can recognize that  $\rho_S$  has product states as its eigenvectors, so it can be expressed as

$$\rho_{S} = \frac{1}{2^{N}} \sum_{r_{1}, r_{2} \dots r_{|\mathcal{S}|} = \pm 1} (1 + r_{1} r_{2} \dots r_{|\mathcal{S}|}) \bigotimes_{i \in \mathcal{S}} |r_{i}\rangle_{i} \langle r_{i}|,$$

$$(14)$$

where we assume that  $P_I$  is supported on qubits in S with  $|S| \leq O(1)$  and  $|\pm 1\rangle_i$  is the  $\pm 1$  eigenstate of the pauli at the  $i^{\text{th}}$  qubit in  $P_I$ . Therefore, if we measure the expected value of an observable, and its derivatives, with  $2^{|S|}$  states of the form  $\bigotimes_{i \in S} |r_i\rangle_i \langle r_i| \bigotimes_{i \in S^c} I/2$ , then they can be classically postprocessed as per Eq. (14) to obtain its expected value in the state  $(I+P_I)/2^N$  in  $O(2^{|S|}) \leq O(1)$  time.

# B. Learning the Kernel parameters $K_{a,b}^{(m)}(0)$

#### 1. Notation and preliminaries

Next, we consider learning the derivatives  $K_{a,b}^{(m)}(0)$  of  $K_{a,b}(t)$  at t=0. To explicitly construct initial states and observables that would be needed to learn  $K_{a,b}^{(m)}(0)$ ,

it will be instructive to consider the action of the channel  $\mathcal{E}_W(t)$  defined in Eq. 11 and depicted schematically in Fig. 4 on an "input" Pauli  $P_I$  and take its overlap with an "output" Pauli  $P_O$  i.e.,

$$B_{W,(O,I)}(t) = \frac{1}{2^N} \text{Tr}[P_O \mathcal{E}_W(t)(P_I)]. \tag{15}$$

Even though  $P_I/2^N$  is not a valid initial state of the system qubits, as long as  $P_I$  is supported on O(1) qubits, we can follow the strategy outlined in the previous Section to efficiently obtain  $B_{W,(O,I)}(t)$  — first initialize the system qubits in the eigenstates of  $P_I$ , measuring the observable  $P_O$  and then classically postprocess the resulting measurements to obtain  $B_{W,(O,I)}(t)$ .

Performing a Dyson series expansion of  $\mathcal{E}_W(t)$ , we can express

$$B_{W,(O,I)}(t) = \frac{1}{2^N} \sum_{n=1}^{\infty} \text{Tr}[P_O \mathcal{F}_W^{(n)}(t)(P_I)],$$
 (16)

where  $\mathcal{F}_W^{(n)}(t)(P_I)$  is the  $n^{\text{th}}$  order term in the Dyson series expansion of  $\mathcal{E}_W(t)(P_I)$  as introduced in Eq. 12. We remark that  $\mathcal{F}_W^{(n)}(t)(\rho_S)$  will have n commutators with the full system-environment Hamiltonian H(t) and n integrals over time. Furthermore, the Taylor expansion of  $\mathcal{F}_W^{(n)}(t)$  as a function of t around t=0 will have the form

$$\mathcal{F}_{W}^{(n)}(t) = \sum_{m>n} \frac{t^{m}}{m!} [\partial_{s}^{m} \mathcal{F}_{W}^{(n)}(s)]_{s=0},$$

i.e., due to the n time integrals in  $\mathcal{F}_W^{(n)}(t)$ , the leading order of its Taylor expansion will be  $t^n$  and hence the summation in the above equation starts from n. We emphasize that if the system-environment Hamiltonian is time-independent (for e.g., for the ensemble Hamiltonian model with the trace over the environment replaced with a classical ensemble average), then  $\mathcal{F}_W^{(n)}(t)$  will only have a term proportional to  $t^n$  in its Taylor expansion.

The first order term  $\mathcal{F}_W^{(1)}(t)$  [Eq. (12b)] would depend only on the system Hamiltonian coefficients  $\lambda_a$ , which have already been learned. Since  $\text{Tr}(A_a(t)\gamma_E) = 0$ , the second order term  $\mathcal{F}_W^{(2)}(t)$  [Eq. (12c)] can further be expressed as:

$$\mathcal{F}_{W}^{(2)}(t) = \mathcal{F}_{WSE}^{(2)}(t) + \mathcal{F}_{WS}^{(2)}(t), \tag{17}$$

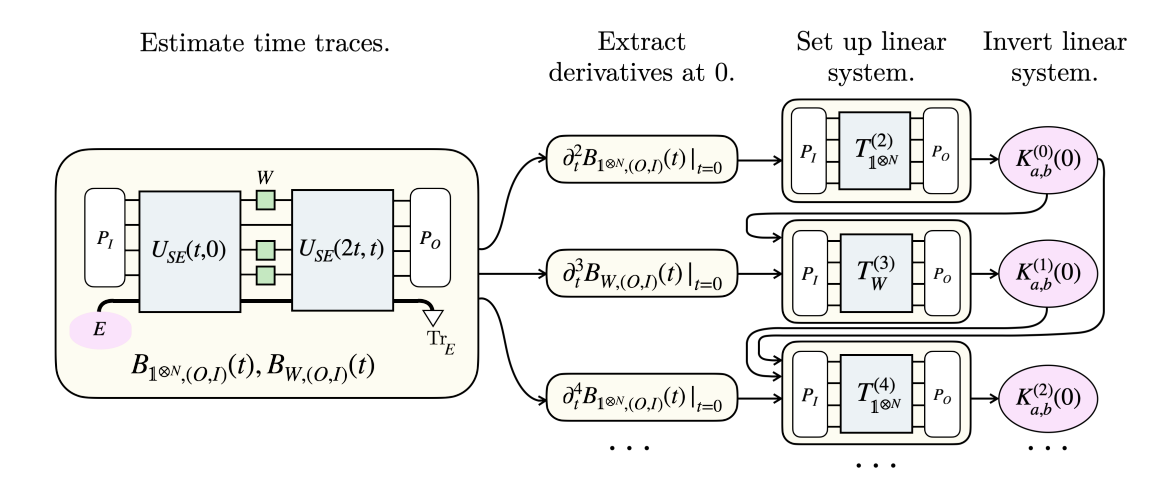


FIG. 4. Schematic for the procedure to learn the kernel derivatives  $K_{a,b}^{(0)}(0), K_{a,b}^{(1)}(0), \dots$  Given the Pauli strings  $P_a, P_b$  associated to the kernel  $K_{a,b}(t)$ , we perform tomography on a region  $\mathcal{I}_{a,b}$  slightly larger than the supports of  $P_a, P_b$ . We estimate  $\frac{1}{2^N} \operatorname{Tr}(P_O \mathcal{E}_W(t)(P_I))$  by sampling eigenstates of  $P_I$ , which is supported only on  $\mathcal{I}_{a,b}$ , evolving for time t, introducing a layer of single-qubit gates W, evolving further until time 2t and finally measuring  $P_O$ , which is only supported on  $\mathcal{I}_{a,b}$ . The intermediate W depends on  $P_a, P_b$  and can be chosen to be a single-qubit gate according to Table I. Repeating this procedure for several t yields a time trace  $B_{W,(O,I)}(t)$ . We similarly obtain the time trace  $B_{1\otimes N,(O,I)}(t)$ , this time without introducing any gate W. We estimate the m-th derivative at t=0 of these time traces using polynomial interpolation: these yield systems of equations  $T_{1\otimes N}^{(m)}$  (m even),  $T_W^{(m)}$  (m odd) that are linear in the (m-2)-th kernel derivative, using Eq. (18). In order to obtain  $T_{1\otimes N}^{(2)}$  from  $\partial_t^2 B_{1\otimes N,(O,I)}(t)|_{t=0}$  we need to use estimates  $\lambda_a$  for the system coefficients. Tomography allows us to obtain an estimate for  $K_{a,b}^{(0)}(0)$  from the linear map  $T_{1\otimes N}^{(2)}$  using Eq. (21). Similarly, we obtain  $T_W^{(3)}$  from  $\partial_t^3 B_{W,(O,I)}(t)|_{t=0}$  and recover  $K_{a,b}^{(1)}(0)$  using Eqs. (26),(31). The fourth derivative  $\partial_t^4 B_{1\otimes N,(O,I)}(t)|_{t=0}$  will depend nonlinearly on  $K_{a,b}^{(0)}(0)$ , as well as the system parameters  $\lambda_a$ . Thus, we use our estimates obtained in previous steps to obtain the linear map  $T_{1\otimes N}^{(4)}$ , which allows us to obtain an estimate for  $K_{a,b}^{(2)}(0)$ . Similarly, higher derivatives of the time trace depend linearly on the kernel derivatives not yet estimated, and nonlinearly on those kernel derivatives and system parameters already estimated.

with  $\mathcal{F}_{W,SE}^{(2)}(t)$  is given by Eq. (12c) with  $H(t) \to V_{SE}(t)$  and  $\mathcal{F}_{W,S}^{(2)}(t)$  is given by Eq. (12c) with  $H(t) \to H_S$ .  $\mathcal{F}_{W,S}^{(2)}(t)$  depends only on the system Hamiltonian coefficients  $\lambda_a$ , while  $\mathcal{F}_{W,SE}^{(2)}(t)$  depends on the kernels  $K_{a,b}(t)$ .

The second and higher derivatives of  $B_{W,(O,I)}(t)$  can then be expressed as

$$\partial_t^m B_{W,(O,I)}(t)\big|_{t=0} = \frac{1}{2^N} \text{Tr}[P_O T_W^{(m)}(P_I)] + f_{W,(O,I)}^{(m)},$$
(18a)

where  $m \geq 2$ ,

$$T_W^{(m)} := \partial_t^m \mathcal{F}_{W,SE}^{(2)}(t)|_{t=0},$$
 (18b)

and

$$f_{W,(O,I)}^{(m)} = \frac{1}{2^N} \partial_t^m \text{Tr} \left( P_O \left( \mathcal{F}_{W,S}^{(2)}(t)(P_I) + \sum_{2 < n \le m}^{\infty} \mathcal{F}_W^{(n)}(t)(P_I) \right) \right) \Big|_{t=0}.$$
(18c)

We note that  $T_W^{(m)}$  depends linearly on  $K_{a,b}^{(m-2)}(0)$ . On the other hand  $f_{W,(O,I)}^{(m)}$  is a non-linear function of  $K_{a,b}^{(m)}(0)$  — however,  $\mathcal{F}_{W,S}^{(2)}(t)$ , and consequently  $\partial_t^m \mathcal{F}_W^{(2)}(t)|_{t=0}$ , is independent of  $K_{a,b}^{(m)}(0)$ . Furthermore, since  $\mathcal{F}_W^{(n)}(t)$  is obtained from  $n^{\text{th}}$  term in the Dyson series expansion of the system-environment unitary,  $\partial_t^m \mathcal{F}_W^{(n)}(t)|_{t=0}$ , for  $2 < n \le m$ , depends only on  $K_{a,b}^{(0)}(0), K_{a,b}^{(1)}(0) \dots K_{a,b}^{(m-3)}(0)$ . We provide an explicit expression for  $f_{W,(O,I)}^{(m)}$  in Appendix A 3.

This structure in the dependence of  $T_W^{(m)}$  and  $f_{W,(O,I)}^{(m)}$  on the kernel derivatives  $K_{a,b}^{(m)}(0)$  allows us to build a strategy that allows us to learn  $K_{a,b}^{(m)}(0)$  from the experimentally measurable time-traces  $B_{W,(O,I)}(t)$  [Eq. (15)]: First, construct a set of measurements specified by the input Pauli string  $P_I$ , output Pauli string  $P_O$  as well as single-qubit unitaries W such that  $K_{a,b}^{(m-2)}(0)$  can be uniquely determined from  $\text{Tr}[P_O T_W^{(m)}(P_I)]/2^N$  — note

that this only involves analyzing the invertability of the linear map  $K_{a,b}^{(m-2)}(0) \to \text{Tr}[P_O T_W^{(m)}(P_I)]$ . Then, experimentally measure the time-traces  $B_{W,(O,I)}(t)$  — from the second derivative of this time-trace at t=0, using Eq. (18) for m=2 and the inverse of the map  $K_{a,b}^{(0)}(0) \to \text{Tr}[P_O T_W^{(2)}(P_I)]$ , we immediately obtain  $K_{a,b}^{(0)}(0)$ . Similarly, the third derivative of the time-trace  $B_{W,(O,I)}(t)$  at t=0 yields  $K_{a,b}^{(1)}(0)$  since  $f_{W,(O,I)}^{(3)}$  depends only on  $K_{a,b}^{(0)}(0)$ . Proceeding similarly, we can sequentially determine  $K_{a,b}^{(2)}(0), K_{a,b}^{(3)}(0) \dots$  from increasingly higher derivatives of  $B_{W,(O,I)}(t)$  at t=0.

It then remains to determine a set of measurements  $(P_I, P_O, W)$  such that the linear map  $K_{a,b}^{(m-2)}(0) \rightarrow \text{Tr}[P_O T_W^{(m)}(P_I)]$  is invertible — we do so in the next two subsections. We first provide a general local tomography procedure that works for any geometrically local open system model and then go onto optimize it for certain experimentally relevant settings.

#### 2. Local tomography procedure

Since the invertibility of the map

$$K_{a,b}^{(m-2)}(0) \to \text{Tr}[P_O T_W^{(m)}(P_I)]$$

determines the set of measurements (as specified by the input Pauli string  $P_I$ , output Pauli string  $P_O$  and single-qubit unitary W), it will be convenient to obtain an explicit expression for the superoperator  $T_W^{(m)}$ . Note that the kernels satisfy  $K_{a,b}(t) = K_{b,a}(-t)^*$  and consequently

$$\operatorname{Re}[K_{a,b}^{(m)}(0)] = (-1)^m \operatorname{Re}[K_{b,a}^{(m)}(0)] \text{ and,}$$
  
 $\operatorname{Im}[K_{a,b}^{(m)}(0)] = (-1)^{m+1} \operatorname{Im}[K_{b,a}^{(m)}(0)].$ 

In particular,  $K_{a,a}^{(m)}(0)$  is real for even m and imaginary for odd m. Using Eq. (18b), we then obtain

$$\begin{split} T_W^{(m)} &= \sum_{c \in \mathcal{P}_{SE}} \mathrm{Re}[K_{c,c}^{(m-2)}(0)] \tau_{W,c,c}^{(m),-} + \\ & \mathrm{Im}[K_{c,c}^{(m-2)}(0)] \tau_{W,c,c}^{(m),+} + \\ & \sum_{(c,d) \in \mathcal{P}_{SE}} \mathrm{Re}[K_{c,d}^{(m-2)}(0)] (\tau_{W,c,d}^{(m),-} + (-1)^m \tau_{W,d,c}^{(m),-}) + \\ & \mathrm{Im}[K_{c,d}^{(m-2)}(0)] (\tau_{W,c,d}^{(m),+} + (-1)^{m+1} \tau_{W,d,c}^{(m),+}), \end{split}$$

$$(19a)$$

where the sum over  $(c,d) \in \mathcal{P}_{SE}$  runs over all unordered pairs of Paulis  $c,d \in \mathcal{P}_{SE}$  appearing in the coupling Hamiltonian,  $V_{SE}(t)$ , and  $\tau_{W,c,d}^{(m),\pm}$  are superoperators given by:

$$\tau_{W,c,d}^{(m),\pm} := -(W[P_c, [P_d, (\cdot)]_{\pm}]W^{\dagger} + [P_c, W[P_d, (\cdot)]_{\pm}W^{\dagger}](2^m - 2) + [P_c, [P_d, W(\cdot)W^{\dagger}]_{\pm}])e^{i\frac{\pi}{4}(1\pm 1)}, \quad (19b)$$

with  $[\cdot,\cdot]_+:=\{\cdot,\cdot\},[\cdot,\cdot]_-:=[\cdot,\cdot]$  being the anticommutator and commutator, respectively. At this point, we remark that if  $W=\mathbbm{1}^{\otimes N}$ , then  $\tau_{\mathbbm{1}^{\otimes N},c,c}^{(m),-}=0$  since for any pauli string  $P,[P,\{P,\cdot\}]=0$ . Furthermore, the coefficients of  $\mathrm{Re}[K_{c,d}^{(m-2)}(0)],\mathrm{Im}[K_{c,d}^{(m-2)}(0)]$  in Eq. (19b) evaluate to

$$\tau_{\mathbb{1}\otimes N,c,d}^{(m),\pm} \mp (-1)^m \tau_{\mathbb{1}\otimes N,d,c}^{(m),\pm} = -2^m e^{i\frac{\pi}{4}(1\pm 1)} \times \begin{cases} [[P_c, P_d]_{\pm}, (\cdot)] &, m \text{ odd,} \\ \{[P_c, P_d]_{\mp}, (\cdot)\} + 2(\pm P_c(\cdot)P_d - P_d(\cdot)P_c) &, m \text{ even.} \end{cases}$$
(20)

Therefore, for m odd, from Eqs. (19b) and (20) it follows that  $T_{1^{\otimes N},c,d}^{(m+2)}$  depends only on the sums

$$\begin{split} \sum_{(c,d) \in \mathcal{P}_{SE}: [P_c, P_d] = Q} & \text{Re}[K_{c,d}^{(m)}(0)], \\ \sum_{(c,d) \in \mathcal{P}_{SE}: \{P_c, P_d\} = Q} & \text{Im}[K_{c,d}^{(m)}(0)], \end{split}$$

instead of individually on  $\operatorname{Re}[K_{c,d}^{(m)}(0)]$ ,  $\operatorname{Im}[K_{c,d}^{(m)}(0)]$ . Consequently, the usual measurement strategy involving short-time evolution of an initial product state and a Pauli measurement is not sufficient for learning  $K_{c,d}^{(m)}(0)$ . To overcome this issue, we need to additionally apply a non-identity intermediate layer of gates W — this is in contrast to the Hamiltonian or Lindbladian learning [33, 34], where no intermediate gates are required. The gate W that we introduce will depend on the kernel coefficient  $K_{a,b}^{(m)}(0)$  that we want to learn, as summarized in three cases in Table I. In the remainder of this section, we will analyze these cases one by one.

Case 1, m is even. For m even, we do not need the intermediate gate layer i.e., we can set  $W = \mathbb{1}^{\otimes N}$ . From Eq. (19a), it follows that

$$T_{1 \otimes N}^{(m)} = \sum_{P,Q} \xi_{P,Q}^{1 \otimes N,(m)} P(\cdot)Q,$$

Target coefficient	W	
Case 1:		
$\operatorname{Re}[K_{a,b}^{(m)}(0)], m \text{ even}$	$\mathbb{1}^{\otimes N}$	
$\operatorname{Im}[K_{a,b}^{(m)}(0)], m \text{ even}$		
$\operatorname{Re}[K_{a,a}^{(m)}(0)], m \text{ even}$		
Case 2:		
$\text{Re}[K_{a,b}^{(m)}(0)], m \text{ odd}$	$\operatorname{Re}[K_{a,b}^{(m)}(0)], m \text{ odd } $ Single-qubit Pauli $P_w$ :	
$Im[K^{(m)}(0)] m \text{ odd}   \{P_m, P_n P_k\} = 0$		

#### Case 3:

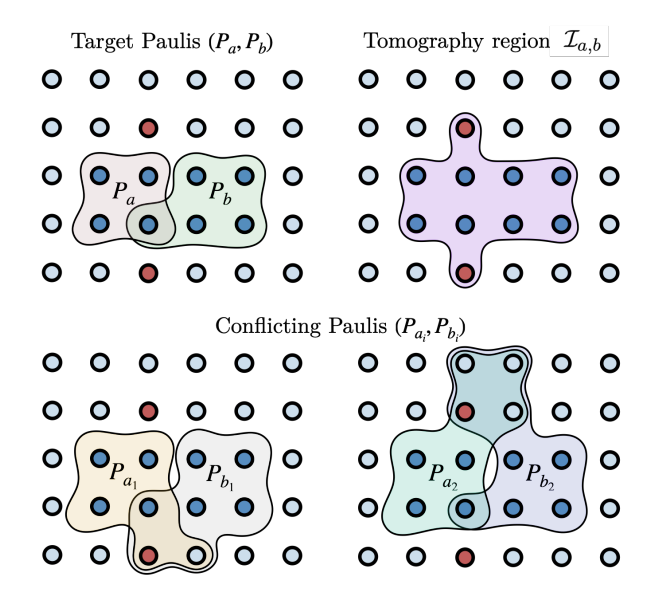
 $\operatorname{Im}[K_{a,a}^{(m)}(0)], m \text{ odd } \operatorname{Single-qubit gate } S \cdot H \text{ on } \mathcal{S}_a$ 

TABLE I. Intermediate W gate needed to learn  $K_{a,b}^{(m)}(0)$ . The choice of W gate depends on if a and b are the same, on whether the real and imaginary part is the target coefficient and on the parity of m. In case 2  $P_w$  needs to commute with one of  $P_a, P_b$  and anticommute with the other: since  $P_a \neq P_b$  there is a site where they differ. If both are non-identity at that site, let  $P_w$  be the Pauli of  $P_b$  at that site. If, say,  $P_b$  is identity at that site, let  $P_w$  be a Pauli different from  $P_a$  at that site. In case 3 the gate SH can be applied on any site in the support of  $P_a$ . Note that since  $K_{a,b}(t) = K_{b,a}^*(-t)$ ,  $\text{Re}[K_{a,a}^{(m)}(0)] = 0$  if m is odd and  $\text{Im}[K_{a,a}^{(m)}(0)] = 0$  if m is even, and thus do not appear in the cases listed above.

where either  $P, Q \in \mathcal{P}_{SE}$ ,  $P = Q = \mathbb{1}^{\otimes N}$  or  $(P, Q) = ([P_c, P_d]_{\pm}, \mathbb{1}^{\otimes N})$  or  $(\mathbb{1}^{\otimes N}, [P_c, P_d]_{\pm})$  for  $P_c, P_d \in \mathcal{P}_{SE}$ . Furthermore, for  $P_a, P_b \in \mathcal{P}_{SE}$ ,

$$\begin{split} \xi_{P_{a},P_{b}}^{\mathbb{1}^{\otimes N},(m)} &= 2^{m+1} (\text{Re}[K_{a,b}^{(m-2)}(0)] - i \text{Im}[K_{a,b}^{(m-2)}(0)]), \\ \xi_{P_{b},P_{a}}^{\mathbb{1}^{\otimes N},(m)} &= 2^{m+1} (\text{Re}[K_{a,b}^{(m-2)}(0)] + i \text{Im}[K_{a,b}^{(m-2)}(0)]), \end{split}$$

We can thus recover  $\operatorname{Re}[K_{a,b}^{(m-2)}(0)]$ ,  $\operatorname{Im}[K_{a,b}^{(m-2)}(0)]$  provided we can learn  $\xi_{P_a,P_b}^{\mathbb{I}^{\otimes N},(m)}$ ,  $\xi_{P_b,P_a}^{\mathbb{I}^{\otimes N},(m)}$ . To learn the latter from  $\operatorname{Tr}[P_O T_{\mathbb{I}^{\otimes N}}^{(m)}(P_I)]$ , a possible approach is to perform process tomography on  $T_{\mathbb{I}^{\otimes N}}^{(m)}$ . We remind the reader that performing full process tomography on an N-qubit hermiticity-preseving superoperator  $\mathcal{M}$  expressible as  $\mathcal{M}(X) = \sum_{P,Q \in \mathcal{P}_N} s_{P,Q} PXQ$  would allow us to unambiguously learn the coefficients  $s_{P,Q}$  [15]. However, since  $T_{\mathbb{I}^{\otimes N}}^{(m)}$  is a N-qubit superoperator, full process tomography will require  $\sim \exp(N)$  measurements as well as  $\sim \exp(N)$  classical postprocessing time [15]. Instead, by using the locality of the Pauli strings appearing in  $T_{\mathbb{I}^{\otimes N}}^{(m)}$  we can reduce both the number of measurements as well



• Joint support of  $(P_a, P_b)$  . • Qubits added to the tomography region.

FIG. 5. We show how to find a tomography support  $\mathcal{I}_{a,b}$  that allows us learn the derivatives  $K_{a,b}^{(m)}(0)$ . The target Pauli strings  $P_a$ ,  $P_b$ , shown in the top left panel, act on the joint support  $\mathcal{S}_{a,b}$  (dark blue). The conflicting pairs of Pauli strings  $(P_{a_1}, P_{b_1}), (P_{a_2}, P_{b_2})$ , depicted in the bottom panels, satisfy Eqs.(22),(23), so their kernel coefficients would mix with those of  $K_{a,b}^{(m)}(0)$  if we only performed tomography on  $\mathcal{S}_{a,b}$ . We add one extra qubit from the region  $\mathcal{S}_{a,b}^c$  that lies in the support of each pair (red), obtaining  $\mathcal{Q}_{a,b}$ . Our tomography region is  $\mathcal{I}_{a,b} = \mathcal{S}_{a,b} \cup \mathcal{Q}_{a,b}$ , the dark blue and red sites in the top right panel.

as the classical postprocessing time to O(N), as we discuss next.

Suppose we want to learn  $\xi_{P_a,P_b}^{\mathbb{1}^{\otimes N},(m)}$  for some distinct  $P_a, P_b \in \mathcal{P}_{SE}$  without performing process tomography on all the qubits — a first guess would be to perform process tomography on  $S_{a,b} = \text{supp}(P_a) \cup \text{supp}(P_b)$ . However, there could be Pauli strings  $P_c, P_d \in \mathcal{P}_{SE}$  such that

$$P_c|_{\mathcal{S}_{a,b}} = P_a|_{\mathcal{S}_{a,b}}, P_d|_{\mathcal{S}_{a,b}} = P_b|_{\mathcal{S}_{a,b}}, \tag{22}$$

i.e.,  $P_c$  and  $P_d$  are identical to  $P_a$  and  $P_b$  respectively on the region  $S_{a,b}$  and

$$P_c|_{\mathcal{S}_{a,b}^c} = P_d|_{\mathcal{S}_{a,b}^c},\tag{23}$$

i.e.,  $P_c$  and  $P_d$  are identical to each other outside  $S_{a,b}$ . Equivalently, these are the Pauli strings such that

 $\operatorname{Tr}(P_O P_c P_I P_d) = \operatorname{Tr}(P_O P_a P_I P_b)$  for any  $P_I, P_O$  supported only on  $\mathcal{S}_{a,b}$  and, consequently, we cannot distinguish the contribution of  $P_c, P_d$  in  $T_{1 \otimes N}^{(m)}$  from that of  $P_a, P_b$  by tomography on  $\mathcal{S}_{a,b}$ . We will denote by  $\mathcal{Y}_{\mathcal{S}_{a,b}}(a,b)$  the set of such pairs of Pauli strings i.e., Pauli strings in  $\mathcal{P}_{SE} \setminus \{a,b\}$  that can't be distinguished from  $P_a, P_b$  by tomography on  $\mathcal{S}_{a,b}$ . Indeed, performing process tomography on  $\mathcal{S}_{a,b}$  can only unambiguously yield

$$\xi_{P_a,P_b}^{\mathbb{I}^{\otimes N},(m)} + \sum_{(P_c,P_d) \in \mathcal{Y}_{\mathcal{S}_{a,b}}(a,b)} \xi_{P_c,P_d}^{\mathbb{I}^{\otimes N},(m)},$$

instead of  $\xi_{P_a,P_b}^{\mathbb{I}^{\otimes N},(m)}$ . Since pairs of Pauli strings satisfying Eqs.(22) and (23) prevent us from estimating the desired coefficient directly, we call them *conflicting* pairs of Pauli strings. Our strategy will be to slightly enlarge the support of the tomography region to  $\mathcal{I}_{a,b}$  such that  $|\mathcal{Y}_{\mathcal{I}_{a,b}}(a,b)| = \emptyset$ , i.e. there are no further conflicting Pauli strings. To construct  $\mathcal{I}_{a,b}$ , we pick the smallest set of qubits  $\mathcal{Q}_{a,b}$  outside  $\mathcal{S}_{a,b}$  such that for every pair of Paulis  $(P_c, P_d) \in \mathcal{Y}_{\mathcal{S}_{a,b}}(a,b)$ ,  $\mathcal{Q}_{a,b}$  contains a qubit in the support of  $P_c$  or  $P_d$  but outside  $\mathcal{S}_{a,b}$ . Performing tomography on

$$\mathcal{I}_{a,b} := \mathcal{S}_{a,b} \cup \mathcal{Q}_{a,b}, \tag{24}$$

then allows us to uniquely obtain  $\xi_{P_a,P_b}^{\mathbb{I}^{\otimes N},(m)}$  since the additional qubits in  $\mathcal{Q}_{a,b}$  allow us to distinguish the target Pauli pair  $(P_a,P_b)$  from the Pauli string pairs that originally were conflicting with it. An example of constructing  $\mathcal{I}_{a,b}$  is illustrated in Figure 5: here, the tomography region  $\mathcal{S}_{a,b}$  is enlarged with one site from each conflicting pair of Pauli strings. We show in Appendix A1 that the number of additional qubits  $|\mathcal{Q}_{a,b}| \leq |\mathcal{Y}_{\mathcal{S}_{a,b}}(a,b)|$  is upper bounded by  $\mathfrak{d}$ . Since  $|\mathcal{S}_{a,b}| = O(k_{SE})$  and we add one extra qubit from each pair in  $\mathcal{Y}_{\mathcal{S}_{a,b}}(a,b)$ , we get that the region  $\mathcal{I}_{a,b}$  has size  $|\mathcal{I}_{a,b}| = O(k_{SE}) + O(\mathfrak{d})$ .

Recall that for m even,  $K_{a,a}^{(m)}(0)$  is real, and we can learn it from  $\xi_{P_a,P_a}^{\mathbb{R}^{\otimes N},(m)} = 2^{m+1} \operatorname{Re}[K_{a,a}^{(m)}(0)]$ . In this case we only need to enlarge the support by  $|\mathcal{Q}_{a,a}| \leq \mathfrak{d}$  qubits.

Case 2, m is odd and  $a \neq b$ . For m odd, we will introduce an intermediate unitary W. We will consider W to be a single-site Pauli matrix, with the corresponding Pauli string  $P_w$  that is identity everywhere except at that site. Suppose we want to learn

 $\operatorname{Re}[K_{a,b}^{(m)}(0)], \operatorname{Im}[K_{a,b}^{(m)}(0)], a \neq b.$  Then we can pick  $P_w$  that anticommutes with  $P_a$  and commutes with  $P_b$ : if there is a site in  $P_a$  that does not overlap with  $P_b$ , let W be a Pauli matrix different from  $P_a$  at that site; if  $P_a, P_b$  overlap everywhere, since  $P_a \neq P_b$  there is a site where they differ, so let W be  $P_b$  at that site. We check whether two Pauli strings  $P_a, P_w$  commute or anticommute using the function  $\chi(a, w) = 0$  if  $[P_a, P_w] = 0$  and  $\chi(a, w) = 1$  if  $\{P_a, P_w\} = 0$ . Notice that conjugating by  $P_w$  only adds a phase:  $P_w P_a P_w^{\dagger} = (-1)^{\chi(a,w)} P_a$ . Then, if we use an input Pauli  $P_I$ , the coefficients of  $\operatorname{Re}[K_{a,b}^{(m)}(0)], \operatorname{Im}[K_{a,b}^{(m)}(0)]$  in Eq. (19b) evaluate to

$$(\tau_{P_{w}a,b}^{(m),\pm} \mp (-1)^{m} \tau_{P_{w},b,a}^{(m),\pm})(P_{I}) = (-1)^{\chi(w,I) + \chi(w,b)} \times \frac{2^{m} - 2}{2^{m-1}} (\tau_{\mathbb{1}^{\otimes N},a,b}^{(m-1),\pm} \mp (-1)^{m-1} \tau_{\mathbb{1}^{\otimes N},b,a}^{(m-1),\pm})(P_{I}).$$

$$(25)$$

Thus, introducing such a W reduces the problem to case 1, up to phases that can be corrected in postprocessing. From Eq. (19a), it follows that

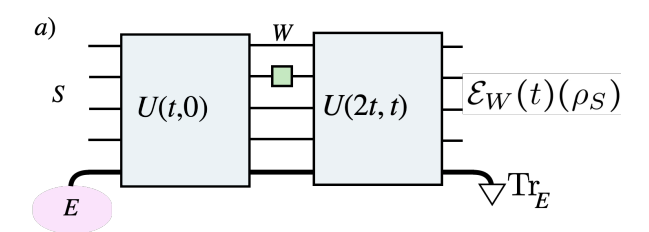
$$T_{P_w}^{(m)}(P_I) = (-1)^{\chi(w,I)} \sum_{P,Q} \xi_{P,Q}^{P_w,(m)} P P_I Q,$$

where either  $P,Q \in \mathcal{P}_{SE}$ ,  $P = Q = \mathbb{1}^{\otimes N}$  or  $(P,Q) = ([P_c,P_d]_{\pm},\mathbb{1}^{\otimes N})$  or  $(\mathbb{1}^{\otimes N},[P_c,P_d]_{\pm})$  for  $P_c,P_d \in \mathcal{P}_{SE}$ . In this case, notice that before we invert this system of equations we need to correct the samples  $\frac{1}{2^N} \text{Tr}(P_O T_{P_w}^{(m)}(P_I)) \mapsto \frac{1}{2^N} \text{Tr}(P_O T_{P_w}^{(m)}(P_I))(-1)^{\chi(w,I)}$ . Then we can obtain the coefficients for  $P_a,P_b \in \mathcal{P}_{SE}$ ,

$$\xi_{P_a,P_b}^{P_w,(m)} = (2^{m+1} - 4)(-1)^{\chi(w,b)} \times (\text{Re}[K_{a,b}^{(m-2)}(0)] - i\text{Im}[K_{a,b}^{(m-2)}(0)]), \quad (26)$$

and  $\xi_{P_b,P_a}^{P_w,(m)} = \xi_{P_a,P_b}^{P_w,(m),*}$ . We can thus recover  $\operatorname{Re}[K_{a,b}^{(m-2)}(0)], \operatorname{Im}[K_{a,b}^{(m-2)}(0)],$  for  $a \neq b$  and m odd, from  $\xi_{P_a,P_b}^{P_w,(m)}, \xi_{P_b,P_a}^{P_w,(m)}$ . From Eq.(IV B 2) one can see that the same analysis of the region of tomography carried out in case 1 holds, so it suffices to do tomography on  $\mathcal{I}_{a,b}$ .

Case 3, m is odd and a = b. For m odd,  $\text{Im}[K_{a,a}^{(m)}(0)]$  vanishes from  $T_{P_w}^{(m)}$  for the same reason as in  $T_{1\otimes N}^{(m)}$ . Instead, we will pick a site on the support of  $P_a$  and choose W to be a single-qubit Clifford gate on that site of the form  $S \cdot H$ , a product of the phase gate S and the Hadamard H. This has the nice property of cycling



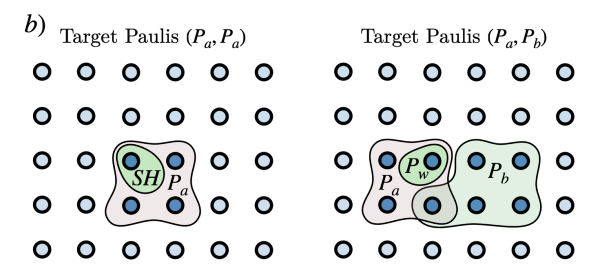


FIG. 6. a) A single-qubit gate W is applied in the middle of the time evolution. b) (Left) If  $P_a = P_b$ , W can be chosen to be  $S \cdot H$  on any site in the support of  $P_a$ . (Right) If  $P_a \neq P_b$ , W can be chosen to be a Pauli string  $P_w$  that is non-identity only on one site of  $P_a$  or  $P_b$ , such that it commutes with one and anticommutes with the other.

through non-identity Pauli matrices upon conjugation:

$$\sigma^x \to \sigma^z \to \sigma^y \to \sigma^x,$$
 (27)

where  $\to$  applies  $SH(\cdot)(SH)^{\dagger}$ . The coefficient of  $Im[K_{a,a}^{(m)}(0)]$  in Eq.(19) evaluates to

$$\tau_{SH,a,a}^{(m),+}(P_I) = -i(2^m - 2) \times (\{P_a\tilde{P}_a, \tilde{P}_I\} + P_a\tilde{P}_I\tilde{P}_a - \tilde{P}_a\tilde{P}_IP_a),$$
 (28)

where we introduced the notation  $\tilde{P}_a = W P_a W^{\dagger}$ , which is a Pauli string, since W is a Clifford gate. Our particular choice of W means  $\tilde{P}_a$  has no global phase: it is equal to  $P_a$  except at one site, where the Pauli is shifted as above. We want to obtain  $\text{Im}[K_{a,a}^{(m)}(0)]$  from the coefficient of  $P_a \tilde{P}_I \tilde{P}_a$ , but there might be other terms of this form in  $T_{SH}^{(m)}(P_I)$ . The rest of coefficients in Eq.(19) evaluate to

$$(\tau_{SH,c,d}^{(m),\pm} \pm \tau_{SH,d,c}^{(m),\pm})(P_I) = -e^{i\frac{\pi}{4}(1\pm 1)} \times ([[\tilde{P}_c, \tilde{P}_d]_{\pm}, \tilde{P}_I] + [[P_c, P_d]_{\pm}, \tilde{P}_I] + (2^m - 2)([P_c, [\tilde{P}_d, \tilde{P}_I]_{\pm}] \pm [P_d, [\tilde{P}_c, \tilde{P}_I]_{\pm}])),$$
(29)

so the terms  $P_c\tilde{P}_I\tilde{P}_d$ ,  $\tilde{P}_d\tilde{P}_IP_c$ ,  $P_d\tilde{P}_I\tilde{P}_c$ ,  $\tilde{P}_c\tilde{P}_IP_d$  might mix with  $P_a\tilde{P}_I\tilde{P}_a$ . The first and third term require  $P_c=P_a$ ,  $P_d=P_a$ , but  $P_c\neq P_d$ , so this term does not

appear. The second and third are satisfied for  $P_c = WP_aW^{\dagger}$ ,  $P_d = W^{\dagger}P_aW$  and vice versa (recall that the pair  $P_c$ ,  $P_d$  is unordered). From Eq.(19), it follows that

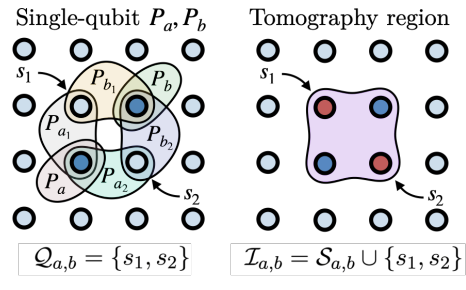
$$T_{SH}^{(m)}(P_I) = \sum_{P,Q} \xi_{P,Q}^{SH,(m)} P \tilde{P}_I Q,$$
 (30)

where either  $P, W^{\dagger}QW \in \mathcal{P}_{SE}$ ,  $W^{\dagger}PW, Q \in \mathcal{P}_{SE}$   $P = Q = \mathbb{1}^{\otimes N}$  or  $(P,Q) = (RS, \mathbb{1}^{\otimes N})$  or  $(\mathbb{1}^{\otimes N}, RS)$ where either  $R, W^{\dagger}RW, S, W^{\dagger}SW$  are in  $\mathcal{P}_{SE}$ . Note that  $\tilde{P}_I$  on the right hand side requires that either we modify the inversion procedure to include the extra map  $W(\cdot)W^{\dagger}$  or we can simply prepare  $W^{\dagger}P_IW$  instead of  $P_I$ . We recover  $\text{Im}[K_{a,a}^{(m)}(0)]$  from the coefficients

$$\xi_{P_a,\tilde{P}_a}^{SH,(m)} = (2^m - 2)(-\text{Re}[K_{c,d}^{(m)}(0)] + i(\text{Im}[K_{c,d}^{(m)}(0)] - \text{Im}[K_{a,a}^{(m)}(0)])),$$
(31)

and  $\xi_{P_a,\tilde{P}_a}^{SH,(m)} = \xi_{\tilde{P}_a,P_a}^{SH,(m),*}$ , where we let  $(P_c,P_d) = (WP_aW^{\dagger},W^{\dagger}P_aW)$ . While we can remove  $\text{Re}[K_{c,d}^{(m)}(0)]$  using the conjugate coefficient, we need to manually remove  $\text{Im}[K_{c,d}^{(m)}(0)]$  in classical postprocessing. Since  $P_c \neq P_d$ , we will already have learned this coefficient from case 2. The tomography region to learn  $\xi_{P_a,\tilde{P}_a}^{SH,(m)}$  is  $\mathcal{I}_{a,\tilde{a}}$ , where  $\tilde{a}$  indicates Pauli string  $\tilde{P}_a$ . This, again, satisfies  $|\mathcal{I}_{a,\tilde{a}}| \leq O(k_{SE}) + O(\mathfrak{d})$ , as detailed in Appendix A 1.

We have seen that, in order to learn the derivatives of  $K_{a,b}(t)$  at t=0 we need to introduce a gate W halfway through time evolution and perform tomography on a region  $\mathcal{I}_{a,b}$ . While *process* tomography on  $\mathcal{I}_{a,b}$  allows us to learn the Hermiticity-preserving maps  $T_W^{(m)}[15]$ , it is sufficient to use a procedure with the sample requirement of state tomography, as shown in Lemma 4. The key is that we do not need to learn all the coefficients in  $T_W^{(m)}$  because we are only interested in  $\xi_{P,Q}^{W,(m)}, \xi_{Q,P}^{W,(m)}$ , for P,Q as described in Eqs.(21),(26),(31). Thus, we only perform the necessary measurements to learn these coefficients, so the number of configurations  $(\rho, O, W)$  that we need to prepare to learn the derivatives of  $K_{a,b}(t)$  is at most  $3^{|\mathcal{I}_{a,b}|} \cdot 2$ , where  $|\mathcal{I}_{a,b}| \leq O(k_{SE}) + O(\mathfrak{d})$ . In particular, this does not depend on the locality of the system Hamiltonian,  $k_S$ , which could be much larger.



- O Joint support of  $(P_a, P_b)$ :  $S_{a,b}$ .
- Qubits added to the tomography region.

FIG. 7. Measurement supports to learn the derivatives of a kernel  $K_{a,b}(t)$  with  $P_a, P_b$  single-qubit Paulis when  $\mathcal{P}_{SE}$  have at most 2-qubit jump operators. The pairs  $(P_{a_1}, P_{b_1}), (P_{a_2}, P_{b_2})$  consist of 2-qubit jump operators satisfying Eqs.(22), (23). The extra qubits that need to be added to the tomography region are  $\mathcal{Q}_{a,b} = \{s_1, s_2\}$ , so the tomography region is  $\mathcal{I}_{a,b} = \mathcal{S}_{a,b} \cup \mathcal{Q}_{a,b}$ .

#### 3. One- and two-qubit jump operators

It is common for dissipation in experimental settings to be given by few-body interaction terms, so we consider now the case that  $\mathcal{P}_{SE}$  contained at most two-qubit Pauli strings. Then, if either  $P_a$  or  $P_b$  was at least 2-local, there would be no pairs of Pauli strings in  $\mathcal{P}_{SE}$  satisfying Eqs.(22)(23), since they would need to be at least 3-local, so it would suffice to measure on  $\mathcal{S}_{a,b}$ . If  $P_a, P_b$  are both single-qubit it is possible to have such pairs, as illustrated in Figure 7.

#### 4. Parallelizing the measurements

For tomography on a region  $\mathcal{I}_{a,b}$  we only need to prepare states, introduce W and measure observables all within the support  $\mathcal{I}_{a,b}$ . If we have several regions  $\mathcal{I}_{a,b}, \mathcal{I}_{c,d}, \mathcal{I}_{e,f}, \dots$  that don't overlap we can estimate their observables simultaneously, as they act on different supports and, thus, commute. As shown in Figure 8 for the 1D case we can perform several rounds of measurement, measuring several non-overlapping regions at each round, until we have performed tomography on all necessary regions.

a) Dissipative case with geometrically local kernel.

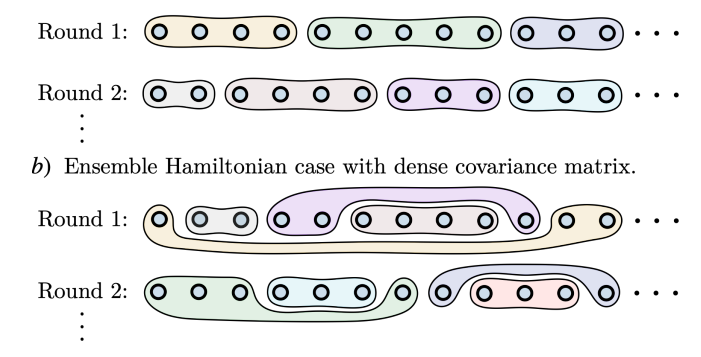


FIG. 8. Parallelized measurements in a 1D system. a) Dissipative case, with geometrically-local kernels. Tomography on regions  $\mathcal{I}_{a,b}, \mathcal{I}_{c,d}, ...$  that do not overlap can be performed simultaneously. In order to perform tomography on all required regions, several rounds of measurement with different regions will be necessary. By geometric locality, each  $\mathcal{I}_{a,b}$  only overlaps with a constant number of regions, so the total number of rounds is independent on the system size. b) Ensemble Hamiltonian case, with dense covariance matrix. Since the covariance between terms acting on far away regions of the lattice is nonzero, the resulting tomography regions within each round will not be geometrically local. Instead of a sparse kernel we now have a dense covariance matrix with  $O(N^2)$  parameters, so the number of rounds we need to perform in this case grows like O(N).

In the dissipative case, with geometrically-local kernels, we know that each Pauli string  $P_a, P_b \in \mathcal{P}_{SE}$  is supported on at most  $k_{SE}$  sites and kernels with Pauli strings that are far away vanish, so we get an effective diameter  $a_0 = O(k_{SE})$  for  $\mathcal{S}_{a,b}$  and for  $\mathcal{I}_{a,b}$ . Each  $\mathcal{I}_{a,b}$  then overlaps with only a constant number of regions, so the number of necessary rounds of measurment is independent of N, as detailed in Appendix A 2.

In the ensemble Hamiltonian case, while the Pauli strings  $P_a, P_b \in \mathcal{P}_{SE}$  are geometrically local, we consider the case where there might be all-to-all correlated errors, i.e. the covariance matrix  $\Sigma$  is dense. This means that even if  $P_a, P_b$  act on distant regions of the lattice,  $\Sigma_{a,b} \neq 0$ , so each row of  $\Sigma$  has O(N) nonzero terms. Then each  $\mathcal{I}_{a,b}$  overlaps with O(N) other  $\mathcal{I}_{c,d}$ , so we need to perform O(N) measurement rounds.

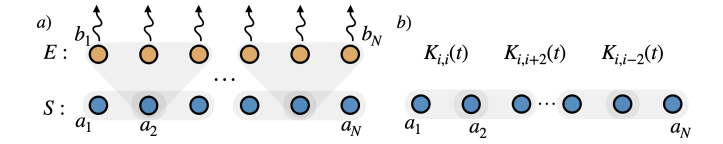


FIG. 9. Fermionic model leading to non-Markovian dynamics on the system S. a) The fermionic modes of the system interact locally among themselves and with the environment modes E. The environment modes undergo dissipation. This leads to effective non-Markovian dynamics on the system, i.e. upon tracing out the environment. b) The environment modes have been traced out and their data is equivalently specified by the kernels  $K_{ij}(t)$ .

#### V. NUMERICAL STUDY

## A. Free fermions coupled to a bath with memory

We consider a system S of N fermionic modes with annihilation operators  $a_1, ..., a_N$ :

$$H_S = -J \sum_{i=1}^{N-1} (a_i^{\dagger} a_{i+1} + a_i^{\dagger} a_{i+1}^{\dagger}) + h.c. + 2h \sum_{i=1}^{N} a_i^{\dagger} a_i.$$
(32)

The system is bilinearly coupled to an environment E consisting of N fermionic modes with annihilation operators  $b_1, ..., b_N$  through a Hamiltonian  $V_{SE}$  and the environment dynamics is given by on-site dissipation  $\mathcal{D}$ :

$$V_{SE} = \sum_{i,j=1}^{N} v_{ij} a_i (b_j^{\dagger} + b_j) + h.c.,$$
 (33)

$$\mathcal{D}(\rho) = \sum_{i=1}^{N} \gamma_i (b_i \rho b_i^{\dagger} - \frac{1}{2} \{ b_i^{\dagger} b_i, \rho \}). \tag{34}$$

The bath is initially assumed to be in the vacuum,  $\gamma = |0\rangle\langle 0|$ . After tracing out the bath, the system dynamics follows a non-Markovian evolution [65], resulting in the memory kernels:

$$K_{ij}(t) = \sum_{l=1}^{N} v_{il}^* v_{jl} \operatorname{Tr}(a_l^{\dagger}(t) a_l(0) \gamma)$$
 (35)

We will choose  $v_{ij} = \delta_{i+1,j} - \delta_{i,j+1}$ . Thus, we obtain interactions between the system and the environment as given in Figure 9 (left) and if we trace the environment, we can equivalently describe it by the kernels (right). Since the Hamiltonian is free-fermionic and the jump operators are linear in the creation/annihilation operators,

time traces of observables can be simulated efficiently [73].

Following the learning algorithm outlined in the main text, we recover the coefficients of the system and kernel derivatives at t = 0. We measure the observable for 10 evenly-spaced timesteps between  $t_{\rm min}=10^{-3}$  and  $t_{\rm max} = 10^{-1}$  for a certain number of shots S, fit a polynomial of degree 3 and estimate the desired parameters. The absolute error in the estimated parameters decreases like  $1/\sqrt{S}$  with the number of shots per timestep S in Figure 10 b). Since the scaling with  $1/\sqrt{S}$  is the same regardless of the system size, as seen in Figure 10 c), the absolute error in the estimate parameters does not increase with system size, as expected. The logarithmic scaling with the system size in Proposition 1 arises from the estimation of O(N) parameters to a desired precision. In this numerical example we assume translational invariance for the system parameters and the kernels, so we only estimate one instance of each. The scaling we obtain predicts comparable accuracies in h, J as obtained for Lindbladian learning [34], as both Hamiltonian learning and Lindbladian learning are based on estimating the first derivative of the observable time trace. The constant term of the kernel and its first deriative at t=0 are obtained by estimating the second and third derivative of the observable time trace at t = 0, which are harder to estimate with the same number of samples [34], so we obtain coarser estimates. From these derivatives of the kernels we can estimate the environment bandwidth  $\gamma$ and the system-environment coupling v using Eq. (8). As we can see in Figure 11, the errors in the recovered coefficients do not scale with the system size N.

#### B. Transverse field Ising model

We consider a system S of N spin- $\frac{1}{2}$  particles in 1D evolving under the transverse-field Ising Hamiltonian:

$$H_S = -J \sum_{i=1}^{N-1} \sigma_i^x \sigma_{i+1}^x - h \sum_{i=1}^N \sigma_i^z,$$
 (36)

where h, J are given by jointly Gaussian random variables:

$$(h, J)^T = B \cdot (Z_1, Z_2)^T + \mu^T, \tag{37}$$

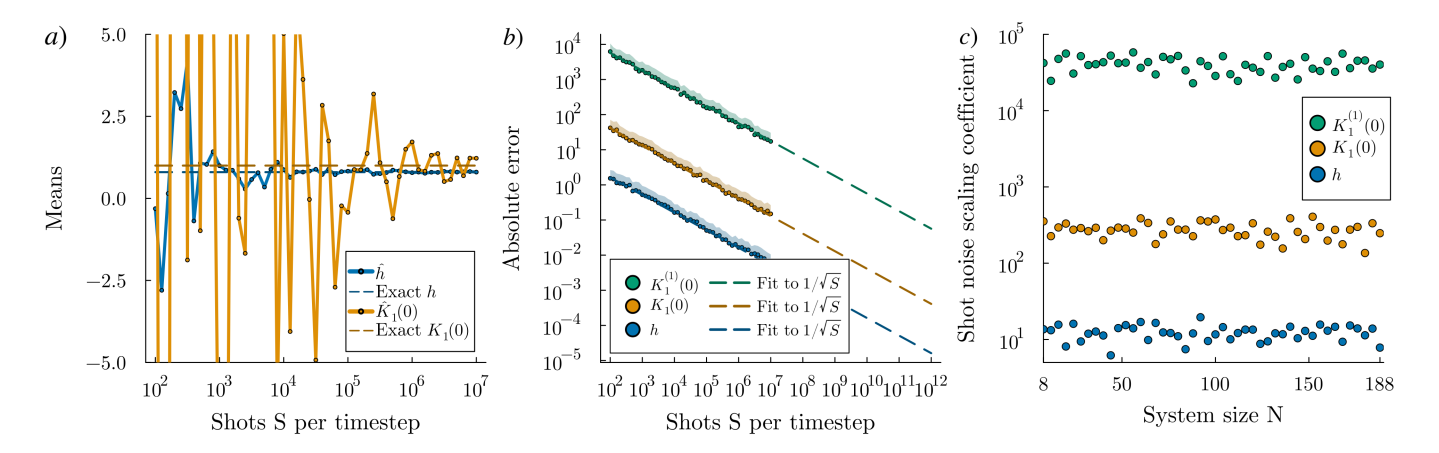


FIG. 10. Error in the recovered coefficients for the transverse-field Ising model coupled to a non-Markovian bath, with coefficients  $J=0.2, h=0.8, v_i=1, \gamma_i=0.9$ . The values of the time traces are computed exactly for 10 evenly spaced timesteps between  $t_{\min}=10^{-3}$  and  $t_{\max}=10^{-1}$ . Then, for each timestep S shots are drawn from the Bernoulli distribution, obtaining a noisy time trace with projection noise that is fit to a polynomial to estimate the desired parameter. The shaded regions indicate the variance in the absolute error for a fixed S, obtained by estimating the error in each parameter for 100 different batches. a) Convergence of the estimate for h and for the constant term of a kernel,  $K_1(0)$ , with the number of shots per timestep S. We fixed N=120. b) Absolute error in h (|h|=0.8), the constant term,  $K_1(0)$  ( $|K_1(0)|=1$ ), and the first derivative of a kernel at t=0,  $K_1^{(1)}(0)$  ( $|K_1^{(1)}(0)|=0.45$ ) using S shots per timestep and fixing N=120. The dashed lines represent fits to  $1/\sqrt{S}$ , as expected from Hoeffding's inequality. c) More precisely, from plot b) we expect that the absolute error will scale like  $\sigma/\sqrt{S}$ , where the standard deviation  $\sigma$  is the shot noise scaling coefficient. We plot it for the magnetic field, h, the constant term,  $K_1(0)$ , and the first derivative of the kernel  $K_1^{(1)}(0)$  and see that it does not depend on the system size. Note that, since we assume translational invariance, we only need to estimate one instance of each desired parameter. In Proposition 1 we see a logarithmic scaling with N because we want to estimate all O(N) parameters correctly.

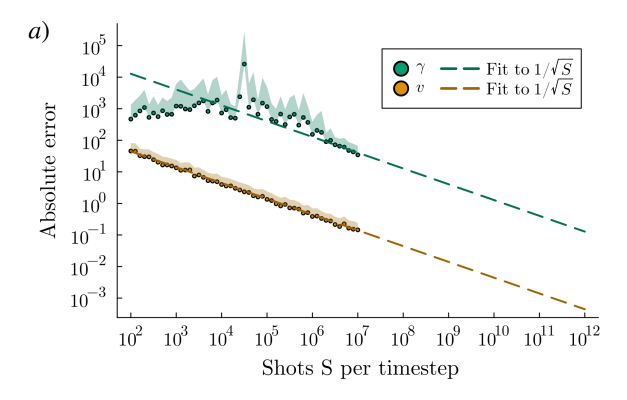
where  $Z_i \sim \mathcal{N}(0,1)$ , the covariance matrix is  $\Sigma = BB^T$  and the means are  $\mu = (\mathbb{E}(h), ..., \mathbb{E}(J))$ .

Following the measurement strategy outlined in Section V A for the constant term of the kernel, we obtain estimates for the covariance matrix. We evolve each observable for 10 evenly-spaced timesteps between  $t_{\rm min}=10^{-3}$ and  $t_{\text{max}} = 10^{-1}$ , each time drawing a new set of random parameters for the transverse field Ising model and obtaining a projective measurement outcome. We repeat this for S shots per timestep and fit a polynomial of degree 2 to obtain the required derivatives. The absolute error in estimating the system parameters and covariances decreases with  $1/\sqrt{S}$  in Figure 12 b). In Figure 12 c) we see that this scaling does not increase with N, so the absolute error does not increase with system size. Recall that Proposition 2 is only valid for time  $t = O((\log(N)\log(1/\epsilon))^{-1/2})$ . In practice this is sufficient for system sizes accessible to current devices: using the same  $t_{\text{max}} = 10^{-1}$  for all N we do not see an increase

in the shot noise scaling coefficient. The scaling we obtain predicts comparable accuracies in h,J is similar to that obtained in the dissipative case. The covariance matrix is obtained from the second derivative of the observable, so we obtain similar precision to the constant term in the kernel for the dissipative case, as expected.

#### VI. SAMPLE COMPLEXITY ANALYSIS

From the measurement procedure we obtain samples for the time traces  $B_{W,(O,I)}(t) = \frac{1}{2^N} \mathrm{Tr}(P_O \mathcal{E}_W(t)(P_I))$  for t in an interval  $[t_0,t_{\mathrm{max}}]$ , which we determine below. We will use the robust interpolation method from [34] to obtain a polynomial fit to each time trace. They use a Lieb-Robinson bound for the Heisenberg evolution of local observables. In Appendix A 6 we explain how it can be adapted to the non-Markovian case to obtain the following result.



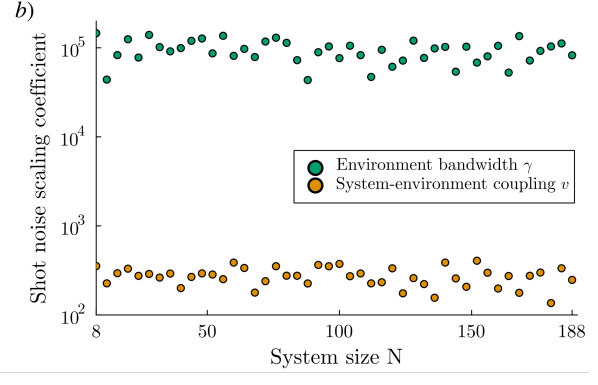


FIG. 11. a) Error in the estimates of the coupling strength between system and environment, v = 1, and the decay rate,  $\gamma = 0.9$ . The estimates are obtained from the translationallyinvariant system in Figure 10 using Eq. (8): v is obtained from  $K_1(0)$ , while  $\gamma$  is obtained from  $K_1^{(1)}(0)$  using the estimate for v. The dashed lines represent fits to  $1/\sqrt{S}$ : while the error in v decreases as expected, the error in  $\gamma$  only decreases once we have an estimate for v that is commensurate with its exact value. We thus fit the error for  $\gamma$  once the error in vgoes below  $\frac{v}{2}$ , in this case  $S \in [10^6, 10^7]$ , and see the expected decrease. The system size is N = 120. b) The offset in the graphs of a), i.e. the scaling coefficients of the fit  $1/\sqrt{S}$ , for the bandwidth  $\gamma$  and system-environment coupling v, does not depend on the system size. Although reducing the error in the bandwidth, as seen in a), requires a larger number of samples, the errors do not scale with the system size, consistent with Proposition 1.

**Lemma 1** (Adapted Theorem D.2, [34]). Let  $\mathcal{H}_{\Gamma}(t)$  be a geometrically local Hamiltonian acting on a system with a D-dimensional regular lattice  $\Gamma$  with constant g and a free bosonic environment with finite memory. Moreover, let  $t_{\max}, \epsilon > 0$  be given and  $O_Y$  an observable such that  $||O_Y|| \leq 1$  and  $O_Y$  is supported on a constant number

of qubits on the system. Then there is a polynomial p of degree

$$d = \tilde{O}\left(\log^{D}\left(\frac{\exp(vt_{\max}) - 1}{\epsilon}\right)t_{\max}\log\left(\frac{1}{\epsilon}\right)\right), \quad (38)$$

such that for all  $0 \le t \le t_{\max}$ :

$$|\text{Tr}(U^{\dagger}(t)O_YU(t)\rho_S\otimes\gamma_E)-p(t)|\leq\epsilon,$$
 (39)

and

$$p^{(m)}(0) = \text{Tr}(U^{\dagger}(t)O_Y U(t)\rho_S \otimes \gamma_E)^{(m)}|_{t=0}, m = 1, ..., d,$$
(40)

where 
$$U(t) = \mathcal{T} \exp(-it \int_0^t H(s) ds)$$
.

This shows that time traces of local observables can be approximated by a polynomial of controlled degree for constant time. For  $W \neq \mathbb{1}^{\otimes N}$ , since  $W(\cdot)W^{\dagger}$  is a tensor product of single-qubit unitary changes of basis, it does not change the support of local observables. Therefore,  $B_{W,(O,I)}(t)$ , can be approximated by a polynomial of controlled degree,  $p_{W,(O,I)}(t)$ , for constant time t = O(1). Moreover, the derivatives of the truncation  $p_{W,(O,I)}(t)$  at 0 match those of the time trace  $B_{W,(O,I)}(t)$ . In order to estimate this polynomial from measurement samples we follow the robust interpolation method described in Appendix E of [34], obtaining an estimate  $\hat{p}_{W,(O,I)}(t)$  for  $p_{W,(O,I)}(t)$  such that  $|\hat{p}_{W,(O,I)}(t) - p_{W,(O,I)}(t)| < \epsilon$  for all  $t_0 \leq t \leq t_{\text{max}}$ . Similarly, the higher derivatives of the estimate  $\hat{p}_{W,(O,I)}(t)$  at 0 are close to those of  $p_{W,(O,I)}(t)$ in the following sense.

**Lemma 2** (Adapted Theorem E.1, Proposition E.1, Corollary E.1 [34], Theorem 1.2 [71]). Let p(t) be a polynomial of degree d defined on an interval [a,b] with  $a = d^{-2}$  and b = 2 + a,  $\epsilon_{S,M} > 0$  a desired precision in the M-th derivative at 0. Then for  $\delta > 0$ , sampling

$$O\left(d\log\left(\frac{d}{\delta}\right)\right),$$
 (41)

i.i.d. points  $(x_i, y_i)$  from the Chebyshev measure on [a, b] satisfying

$$p(x_i) = y_i + w_i, |w_i| \le \epsilon_S = \epsilon_{S,M} \frac{(2M-1)!!}{3d^{2M}},$$
 (42)

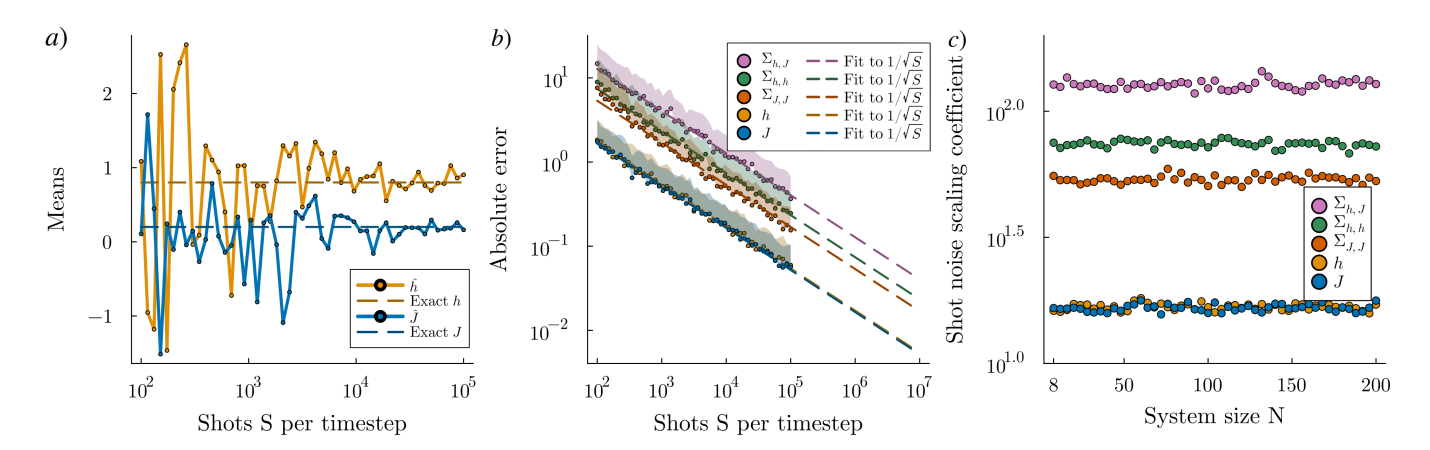


FIG. 12. Recovery of the mean and covariance of the Hamiltonian coefficients for ensemble transverse field Ising Hamiltonians with dense  $\Sigma$ . We fix  $J=0.2, h=0.8, \Sigma_{hh}=0.6, \Sigma_{hJ}=0.3, \Sigma_{JJ}=0.7$ . a) Convergence of h,J towards the exact values in terms of the number of shots per timestep S, with fixed N=200. For each observable we measure 10 timesteps between  $t_{\min}=10^{-3}$  and  $t_{\max}=10^{-1}$  to obtain the polynomial fit. b) Absolute error in h,J and the entries of the covariance matrix in terms of the number of shots per timestep S, with fixed N=200. The dashed lines are fits to  $1/\sqrt{S}$ , and we see the expected scaling from Hoeffding's inequality. c) More precisely, from plot b) we expect that the absolute error will scale like  $\sigma/\sqrt{S}$ , where the standard deviation  $\sigma$  is the shot noise scaling coefficient. We plot it for h,J and their covariances and see that it does not depend on the system size. Note that, since we assume translational invariance, we only need to estimate one instance of each desired parameter. In this case the covariance matrix is dense (with many parameters being equal, by translational invariance), so in Proposition 2 we see a scaling with  $N \log(N)$  because we want to estimate all  $O(N^2)$  parameters correctly.

for at least a fraction  $\alpha > \frac{1}{2}$  of the points is sufficient to obtain a polynomial  $\hat{p}$  satisfying

$$|p^{(m)}(0) - \hat{p}^{(m)}(0)| = \epsilon_{S,m} \le \epsilon_{S,M} \frac{(2M-1)!!}{d^{2M}} \frac{d^{2m}}{(2m-1)!!}, m = 0, 1, ..., M. \quad (43)$$

Note that, since  $m \leq M \leq d$ , all derivative estimates are at least as precise as the highest derivative:  $\epsilon_{S,0} \leq \epsilon_{S,1} \leq \ldots \leq \epsilon_{S,M}$ . Sampling from the uniform measure  $t \in [\frac{1}{d^2}, 2 + \frac{1}{d^2}]$  instead requires  $O(d^2 \log(\frac{1}{\delta}))$  samples [34], where at least half the samples are estimated to precision  $\epsilon_S$ .

We show in Appendix A 4 that, after taking into account the required precision to estimate the offsets  $f_{W,(O,I)}^{(m)}$  accurately, the precision in learning the kernel derivatives  $K_{a,b}^{(m)}(0), m=0,...,M$  to precision at least  $\epsilon_{K,M}$  is bounded by the precision in the sampling and polynomial fit as follows:

$$\epsilon_{K,M} \le e^{O(M^2 \log M)} \epsilon_{S,M+2}. \tag{44}$$

While this is independent of the system size, it is prohibitive for large M. The recursive structure of the

linear systems of equations required to estimate the kernel derivatives up to order M, see Figure 4, leads to a large overhead due to errors compounding from lower-order estimates.

In Appendix A 2 we estimate the number of samples required to estimate all the time traces to precision  $\epsilon_S$  using a parallelized measurement scheme. Plugging in the bounds above means that the total number of samples is upper bounded by:

$$O\left(\frac{((\mathfrak{d}+2)(s+\mathfrak{d})\mathfrak{d}^2+1)e^{O(M^2\log M)}}{\epsilon_{K,M}^2} \times \log\left(\frac{sN\cdot 3^{2k_{SE}+\mathfrak{d}}}{\delta}\right)\right). \tag{45}$$

## VII. CONCLUSION AND OUTLOOK

We formulate the problem of learning open system models beyond the Born-Markov approximation. We work within the assumption of a Gaussian environment, where the memory effects can be captured by the environment memory kernels, i.e. the two-point correlators of the environment operators coupling to the system. The Gaussian-environment assumption is physically reasonable for both free-space and cavity-based quantum simulators with atomic or molecular systems [74–77], as well as for describing non-Markovian noise in superconducting devices [59, 78, 79]. Under this assumption, we show that the derivatives of these memory kernels at t=0 can be systematically learnt from the time evolution of local observables. Our proposed protocol has a favorable sample-complexity scaling with system size, although learning higher-order derivatives of the memory kernel still requires a substantially large amount of samples. While this makes it difficult to learn certain non-Markovian models – either because the memory kernel contains many unknown parameters or because it exhibits sharply different short- and long-time behavior, both of which require very high-order derivatives to capture accurately – in most experimentally relevant settings, a Gaussian non-Markovian environment can be well described by only a few lossy bosonic modes [65]. In such systems, we expect our protocol to perform comparably to established Hamiltonian or Lindbladian learning methods.

Furthermore, we also consider an ensemble Hamiltonian model where the noisy simulator is described by a geometrically local Hamiltonian with the coefficients of the local Hamiltonian terms being Gaussian random variables. Here, we allowed for possible all-to-all correlations between the coefficients of the different Hamiltonian terms. This model would capture noise in global controls applied in a quantum simulator which would introduce all-to-all correlated errors in the Hamiltonian. For instance, in Rydberg-atom arrays [11] and trapped-ion simulators [80], both laser and microwave fields drive entire qubit arrays and lead to correlated frequency and intensity fluctuations that affect all qubits simultaneously [81]. We establish that, despite this all-to-all correlation, the mean and covariance matrix of the Hamiltonian coefficients can also be efficiently learnt by measuring the time-evolution of local observables in the model.

Our work opens up several interesting questions the first and most immediate open question is to develop learning protocols that would be efficient for more complex memory kernels i.e., memory kernels whose parameters cannot be deduced from just a few derivatives. Furthermore, while experimental setups might be aware of their predominant source of noise and thus have prior information of the Paulis appearing in noise operators, it could also be useful to relax this assumption. For example, assuming that Pauli strings of weight larger than k are 0, in the Lindbladian setting one can learn all terms with Pauli strings less than k using classical shadows [34]. Furthermore, for Hamiltonian learning, recently developed protocols require no prior assumption on the structure of the Hamiltonian [82]. Developing similar results for the non-Markovian regime would increase their experimental applicability and minimize modeling errors. Furthermore, while an emphasis of our work has been on developing rigorous protocols with provable sample complexity bounds, it would be important to develop more heuristic but practically efficient methods that can operate with a relatively small sample-budget. Finally, as quantum simulators scale up to  $\gtrsim 500 - 1000$  qubits, even employing protocols with linear sample-complexity to learn a detailed noise-model for the simulator would also become inefficient. In this regime, it is likely that we would need protocols that simply estimate an upper-bound on the noise rate with a much smaller number of samples and bypass the task of learning a full-blown noise model.

#### VIII. ACKNOWLEDGEMENTS

We acknowledge useful discussions with Jeongwan Haah, Hsin-Yuan (Robert) Huang and Daniel Stilck França. R.T. acknowledges support from Center for Integration of Modern Optoelectronic Materials on Demand (IMOD) seed grant (DMR-2019444), from QuPIDC, an Energy Frontier Research Center, funded by the US Department of Energy (DOE), Office of Science, Basic Energy Sciences (BES), under the award number DE-SC0025620 and from the European Union's Horizon Europe research and innovation program under grant agreement number 101221560 (ToNQS). J.A.M.L and R.T. acknowledge funding from the Munich Center for

Quantum Science and Technology (MCQST), funded by the Deutsche Forschungsgemeinschaft (DFG) under Germany's Excellence Strategy (EXC2111-390814868). The research is part of the Munich Quantum Valley, which is supported by the Bavarian State Government with funds from the High tech Agenda Bayern Plus. J.C. acknowledges support from AFOSR (YIP No. FA9550-25-1-0147) and the Terman Faculty Fellowship at Stanford University.

- [1] D. Bluvstein, S. J. Evered, A. A. Geim, S. H. Li, H. Zhou, T. Manovitz, S. Ebadi, M. Cain, M. Kalinowski, D. Hangleiter, et al., Logical quantum processor based on reconfigurable atom arrays, Nature 626, 58 (2024).
- [2] G. Q. AI *et al.*, Quantum error correction below the surface code threshold, Nature **638**, 920 (2024).
- [3] D. Main, P. Drmota, D. Nadlinger, E. Ainley, A. Agrawal, B. Nichol, R. Srinivas, G. Araneda, and D. Lucas, Distributed quantum computing across an optical network link, Nature, 1 (2025).
- [4] B. W. Reichardt, D. Aasen, R. Chao, A. Chernoguzov, W. van Dam, J. P. Gaebler, D. Gresh, D. Lucchetti, M. Mills, S. A. Moses, et al., Demonstration of quantum computation and error correction with a tesseract code, arXiv preprint arXiv:2409.04628 (2024).
- [5] Quantum error correction below the surface code threshold, Nature 638, 920 (2025).
- [6] Suppressing quantum errors by scaling a surface code logical qubit, Nature **614**, 676 (2023).
- [7] X. Zhang, E. Kim, D. K. Mark, S. Choi, and O. Painter, A superconducting quantum simulator based on a photonic-bandgap metamaterial, Science 379, 278 (2023).
- [8] D. K. Mark, J. Choi, A. L. Shaw, M. Endres, and S. Choi, Benchmarking quantum simulators using ergodic quantum dynamics, Physical Review Letters 131, 110601 (2023).
- [9] A. Miessen, D. J. Egger, I. Tavernelli, and G. Mazzola, Benchmarking digital quantum simulations above hundreds of qubits using quantum critical dynamics, PRX Quantum 5, 040320 (2024).
- [10] J. Eisert, D. Hangleiter, N. Walk, I. Roth, D. Markham, R. Parekh, U. Chabaud, and E. Kashefi, Quantum certification and benchmarking, Nature Reviews Physics 2, 382 (2020).
- [11] A. L. Shaw, Z. Chen, J. Choi, D. K. Mark, P. Scholl, R. Finkelstein, A. Elben, S. Choi, and M. Endres, Benchmarking highly entangled states on a 60-atom

- analogue quantum simulator, Nature 628, 71 (2024).
- [12] Z. Cai, R. Babbush, S. C. Benjamin, S. Endo, W. J. Huggins, Y. Li, J. R. McClean, and T. E. O'Brien, Quantum error mitigation, Reviews of Modern Physics 95, 045005 (2023).
- [13] R. Takagi, S. Endo, S. Minagawa, and M. Gu, Fundamental limits of quantum error mitigation, npj Quantum Information 8, 114 (2022).
- [14] Y. Quek, D. Stilck França, S. Khatri, J. J. Meyer, and J. Eisert, Exponentially tighter bounds on limitations of quantum error mitigation, Nature Physics 20, 1648 (2024).
- [15] I. L. Chuang and M. A. Nielsen, Prescription for experimental determination of the dynamics of a quantum black box, Journal of Modern Optics 44, 2455 (1997).
- [16] M. Mohseni, A. T. Rezakhani, and D. A. Lidar, Quantum-process tomography: Resource analysis of different strategies, Physical Review A—Atomic, Molecular, and Optical Physics 77, 032322 (2008).
- [17] F. A. Pollock, C. Rodríguez-Rosario, T. Frauenheim, M. Paternostro, and K. Modi, Non-markovian quantum processes: Complete framework and efficient characterization, Physical Review A 97, 012127 (2018).
- [18] G. A. White, C. D. Hill, F. A. Pollock, L. C. Hollenberg, and K. Modi, Demonstration of non-markovian process characterisation and control on a quantum processor, Nature Communications 11, 6301 (2020).
- [19] G. A. White, F. A. Pollock, L. C. Hollenberg, K. Modi, and C. D. Hill, Non-markovian quantum process tomography, PRX Quantum 3, 020344 (2022).
- [20] S. Mangini, M. Cattaneo, D. Cavalcanti, S. Filippov, M. A. Rossi, and G. García-Pérez, Tensor network noise characterization for near-term quantum computers, Physical Review Research 6, 033217 (2024).
- [21] C. Guo, K. Modi, and D. Poletti, Tensor-network-based machine learning of non-markovian quantum processes, Physical Review A 102, 062414 (2020).
- [22] I. A. Luchnikov, M. Sonner, and D. A. Abanin, Scalable tomography of many-body quantum environ-

- ments with low temporal entanglement, arXiv preprint arXiv:2406.18458 (2024).
- [23] E. Knill, D. Leibfried, R. Reichle, J. Britton, R. B. Blakestad, J. D. Jost, C. Langer, R. Ozeri, S. Seidelin, and D. J. Wineland, Randomized benchmarking of quantum gates, Physical Review A—Atomic, Molecular, and Optical Physics 77, 012307 (2008).
- [24] J. J. Wallman and S. T. Flammia, Randomized benchmarking with confidence, New Journal of Physics 16, 103032 (2014).
- [25] J. Emerson, R. Alicki, and K. Życzkowski, Scalable noise estimation with random unitary operators, Journal of Optics B: Quantum and Semiclassical Optics 7, S347 (2005).
- [26] C. Dankert, R. Cleve, J. Emerson, and E. Livine, Exact and approximate unitary 2-designs and their application to fidelity estimation, Physical Review A—Atomic, Molecular, and Optical Physics 80, 012304 (2009).
- [27] J. Kelly, R. Barends, B. Campbell, Y. Chen, Z. Chen, B. Chiaro, A. Dunsworth, A. G. Fowler, I.-C. Hoi, E. Jeffrey, et al., Optimal quantum control using randomized benchmarking, Physical review letters 112, 240504 (2014).
- [28] M. Veldhorst, J. Hwang, C. Yang, A. Leenstra, B. de Ronde, J. Dehollain, J. Muhonen, F. Hudson, K. M. Itoh, A. t. Morello, et al., An addressable quantum dot qubit with fault-tolerant control-fidelity, Nature nanotechnology 9, 981 (2014).
- [29] J. Helsen, I. Roth, E. Onorati, A. H. Werner, and J. Eisert, General framework for randomized benchmarking, PRX Quantum 3, 020357 (2022).
- [30] T. Proctor, K. Rudinger, K. Young, M. Sarovar, and R. Blume-Kohout, What randomized benchmarking actually measures, Physical review letters 119, 130502 (2017).
- [31] S. Gandhari and M. J. Gullans, Quantum nonmarkovian noise in randomized benchmarking of spinboson models, arXiv preprint arXiv:2502.14702 (2025).
- [32] A. Brillant, P. Groszkowski, A. Seif, J. Koch, and A. A. Clerk, Randomized benchmarking with non-markovian noise and realistic finite-time gates, Physical Review Letters 135, 070601 (2025).
- [33] J. Haah, R. Kothari, and E. Tang, Learning quantum hamiltonians from high-temperature gibbs states and real-time evolutions, Nature Physics, 1 (2024).
- [34] D. Stilck França, L. A. Markovich, V. Dobrovitski, A. H. Werner, and J. Borregaard, Efficient and robust estima-

- tion of many-qubit hamiltonians, Nature Communications **15**, 311 (2024).
- [35] T. Möbus, A. Bluhm, M. C. Caro, A. H. Werner, and C. Rouzé, Dissipation-enabled bosonic hamiltonian learning via new information-propagation bounds, arXiv preprint arXiv:2307.15026 (2023).
- [36] T. Möbus, A. Bluhm, T. Gefen, Y. Tong, A. H. Werner, and C. Rouzé, Heisenberg-limited hamiltonian learning continuous variable systems via engineered dissipation, arXiv preprint arXiv:2506.00606 (2025).
- [37] D. Hangleiter, I. Roth, J. Fuksa, J. Eisert, and P. Roushan, Robustly learning the hamiltonian dynamics of a superconducting quantum processor, Nature Communications 15, 9595 (2024).
- [38] Y. Wu, Y. Zhang, C. Wang, and X. Yuan, Hamiltonian dynamics learning: A scalable approach to quantum process characterization, arXiv preprint arXiv:2503.24171 (2025).
- [39] A. Gu, L. Cincio, and P. J. Coles, Practical hamiltonian learning with unitary dynamics and gibbs states, Nature Communications 15, 312 (2024).
- [40] M. Ma, S. T. Flammia, J. Preskill, and Y. Tong, Learning k-body hamiltonians via compressed sensing, arXiv preprint arXiv:2410.18928 (2024).
- [41] T. Olsacher, T. Kraft, C. Kokail, B. Kraus, and P. Zoller, Hamiltonian and liouvillian learning in weakly-dissipative quantum many-body systems, Quantum Science and Technology 10, 015065 (2025).
- [42] D. S. França, T. Möbus, C. Rouzé, and A. H. Werner, Learning and certification of local time-dependent quantum dynamics and noise, arXiv preprint arXiv:2510.08500 (2025).
- [43] H.-Y. Huang, Y. Tong, D. Fang, and Y. Su, Learning many-body hamiltonians with heisenberg-limited scaling, Physical Review Letters 130, 200403 (2023).
- [44] H. Zhang, B. Pokharel, E. Levenson-Falk, and D. Lidar, Predicting non-markovian superconducting-qubit dynamics from tomographic reconstruction, Physical Review Applied 17, 054018 (2022).
- [45] F. Ivander, L. P. Lindoy, and J. Lee, Unified framework for open quantum dynamics with memory, Nature Communications 15, 8087 (2024).
- [46] A. Vezvaee, N. Shitara, S. Sun, and A. Montoya-Castillo, Fourier transform noise spectroscopy, npj Quantum Information 10, 52 (2024).
- [47] D. Aguiar, K. Wold, S. Denisov, and P. Ribeiro, Quantum liouvillian tomography, arXiv preprint

- arXiv:2504.10393 (2025).
- [48] X. Yang, X. Long, R. Liu, K. Tang, Y. Zhai, X. Nie, T. Xin, J. Li, and D. Lu, Control-enhanced non-markovian quantum metrology, Communications Physics 7, 282 (2024).
- [49] M. Gullans, M. Caranti, A. Mills, and J. Petta, Compressed gate characterization for quantum devices with time-correlated noise, PRX Quantum 5, 010306 (2024).
- [50] W. Dong and Y. Wang, Efficient learning and optimizing non-gaussian correlated noise in digitally controlled qubit systems, arXiv preprint arXiv:2502.05408 (2025).
- [51] S. Varona, M. Müller, and A. Bermudez, Lindblad-like quantum tomography for non-markovian quantum dynamical maps, npj Quantum Information 11, 96 (2025).
- [52] R. Trivedi, Description and complexity of non-markovian open quantum dynamics, arXiv preprint arXiv:2204.06936 (2022).
- [53] R. P. Feynman and F. L. Vernon Jr, The theory of a general quantum system interacting with a linear dissipative system, Annals of physics **281**, 547 (2000).
- [54] Z. Huang, L. Lin, G. Park, and Y. Zhu, Unified analysis of non-markovian open quantum systems in gaussian environment using superoperator formalism, arXiv preprint arXiv:2411.08741 (2024).
- [55] M. Cirio, N. Lambert, P. Liang, P.-C. Kuo, Y.-N. Chen, P. Menczel, K. Funo, and F. Nori, Pseudofermion method for the exact description of fermionic environments: From single-molecule electronics to the kondo resonance, Physical Review Research 5, 033011 (2023).
- [56] L. Chirolli and G. Burkard, Decoherence in solid-state qubits, Advances in Physics 57, 225 (2008).
- [57] J.-S. Zhang, J.-B. Xu, and Q. Lin, Controlling entanglement sudden death in cavity qed by classical driving fields, The European Physical Journal D 51, 283 (2009).
- [58] J.-S. Tang, C.-F. Li, Y.-L. Li, X.-B. Zou, G.-C. Guo, H.-P. Breuer, E.-M. Laine, and J. Piilo, Measuring non-markovianity of processes with controllable systemenvironment interaction, Europhysics Letters 97, 10002 (2012).
- [59] M. Malekakhlagh, A. Petrescu, and H. E. Türeci, Nonmarkovian dynamics of a superconducting qubit in an open multimode resonator, Physical Review A 94, 063848 (2016).
- [60] P. Heidler, C. M. Schneider, K. Kustura, C. Gonzalez-Ballestero, O. Romero-Isart, and G. Kirchmair, Nonmarkovian effects of two-level systems in a niobium coaxial resonator with a single-photon lifetime of 10 mil-

- liseconds, Physical Review Applied 16, 034024 (2021).
- [61] C. Gardiner and P. Zoller, Quantum noise: a handbook of Markovian and non-Markovian quantum stochastic methods with applications to quantum optics (Springer Science & Business Media, 2004).
- [62] B.-H. Liu, L. Li, Y.-F. Huang, C.-F. Li, G.-C. Guo, E.-M. Laine, H.-P. Breuer, and J. Piilo, Experimental control of the transition from markovian to non-markovian dynamics of open quantum systems, Nature Physics 7, 931 (2011).
- [63] A. Chiuri, C. Greganti, L. Mazzola, M. Paternostro, and P. Mataloni, Linear optics simulation of quantum nonmarkovian dynamics, Scientific reports 2, 968 (2012).
- [64] I. de Vega, D. Porras, and J. Ignacio Cirac, Matter-wave emission in optical lattices: Single particle and collective effects, Physical review letters 101, 260404 (2008).
- [65] D. Tamascelli, A. Smirne, S. F. Huelga, and M. B. Plenio, Nonperturbative treatment of non-markovian dynamics of open quantum systems, Physical review letters 120, 030402 (2018).
- [66] D. Ferracin, A. Smirne, S. F. Huelga, M. B. Plenio, and D. Tamascelli, Spectral density modulation and universal markovian closure of fermionic environments, The Journal of Chemical Physics 161 (2024).
- [67] R. Trivedi, D. Malz, and J. I. Cirac, Convergence guarantees for discrete mode approximations to nonmarkovian quantum baths, Physical review letters 127, 250404 (2021).
- [68] V. A. Mandelshtam and H. S. Taylor, Multidimensional harmonic inversion by filter-diagonalization, The Journal of chemical physics 108, 9970 (1998).
- [69] V. A. Mandelshtam, The multidimensional filter diagonalization method: I. theory and numerical implementation, Journal of Magnetic Resonance 144, 343 (2000).
- [70] R. Trivedi and M. Rudner, A lieb-robinson bound for open quantum systems with memory, arXiv preprint arXiv:2410.15481 (2024).
- [71] V. Arora, A. Bhattacharyya, M. Boban, V. Guruswami, and E. Kelman, Outlier robust multivariate polynomial regression, arXiv preprint arXiv:2403.09465 (2024).
- [72] M. B. Hastings and T. Koma, Spectral gap and exponential decay of correlations, Communications in mathematical physics 265, 781 (2006).
- [73] S. Bravyi and R. König, Classical simulation of dissipative fermionic linear optics, arXiv preprint arXiv:1112.2184 (2011).

- [74] C. W. Gardiner and M. J. Collett, Input and output in damped quantum systems: Quantum stochastic differential equations and the master equation, Physical Review A 31, 3761 (1985).
- [75] K. H. Madsen, S. Ates, T. Lund-Hansen, A. Löffler, S. Reitzenstein, A. Forchel, and P. Lodahl, Observation of non-markovian dynamics of a single quantum dot in a micropillar cavity, Physical review letters 106, 233601 (2011).
- [76] M. K. Svendsen, S. Ali, N. Stenger, K. S. Thygesen, and J. Iles-Smith, Signatures of non-markovianity in cavity qed with color centers in two-dimensional materials, Physical Review Research 5, L032037 (2023).
- [77] L. Krinner, M. Stewart, A. Pazmiño, J. Kwon, and D. Schneble, Spontaneous emission of matter waves from a tunable open quantum system, Nature 559, 589 (2018).
- [78] A. O. Caldeira and A. J. Leggett, Path integral approach to quantum brownian motion, Physica A: Statistical mechanics and its Applications **121**, 587 (1983).
- [79] K. Nakamura and J. Ankerhold, Gate operations for superconducting qubits and non-markovianity, Physical Review Research 6, 033215 (2024).
- [80] S.-A. Guo, Y.-K. Wu, J. Ye, L. Zhang, Y. Wang, W.-Q. Lian, R. Yao, Y.-L. Xu, C. Zhang, Y.-Z. Xu, et al., Hamiltonian learning for 300 trapped ion qubits with long-range couplings, Science Advances 11, eadt4713 (2025).
- [81] X. Jiang, J. Scott, M. Friesen, and M. Saffman, Sensitivity of quantum gate fidelity to laser phase and intensity noise, Physical Review A 107, 042611 (2023).
- [82] A. Bakshi, A. Liu, A. Moitra, and E. Tang, Structure learning of hamiltonians from real-time evolution, arXiv preprint arXiv:2405.00082 (2024).
- [83] This is just the multinomial theorem:  $a^b = (\sum_{j=1}^a 1)^b = \sum_{z_1 + \dots + z_a = b} \frac{b!}{z_1! \dots z_a!}$ .
- [84] S. Aaronson and D. Gottesman, Improved simulation of stabilizer circuits, Physical Review A—Atomic, Molecular, and Optical Physics 70, 052328 (2004).
- [85] A. Jena, Partitioning Pauli operators: in theory and in practice, Master's thesis, University of Waterloo (2019).
- [86] R. Harper, S. T. Flammia, and J. J. Wallman, Efficient learning of quantum noise, Nature Physics 16, 1184 (2020).
- [87] J. Kelly, R. Barends, A. G. Fowler, A. Megrant, E. Jeffrey, T. C. White, D. Sank, J. Y. Mutus, B. Campbell, Y. Chen, et al., State preservation by repetitive error

- detection in a superconducting quantum circuit, Nature **519**, 66 (2015).
- [88] N. Khaneja, B. Luy, and S. J. Glaser, Boundary of quantum evolution under decoherence, Proceedings of the National Academy of Sciences 100, 13162 (2003).
- [89] U. Hoeppe, C. Wolff, J. Küchenmeister, J. Niegemann, M. Drescher, H. Benner, and K. Busch, Direct observation of non-markovian radiation dynamics in 3d bulk photonic crystals, Physical review letters 108, 043603 (2012).
- [90] B. M. Terhal and G. Burkard, Fault-tolerant quantum computation for local non-markovian noise, Physical Review A—Atomic, Molecular, and Optical Physics 71, 012336 (2005).
- [91] D. Aharonov, A. Kitaev, and J. Preskill, Fault-tolerant quantum computation with long-range correlated noise, Physical review letters **96**, 050504 (2006).
- [92] D. Aharonov and M. Ben-Or, Fault-tolerant quantum computation with constant error, in *Proceedings of the* twenty-ninth annual ACM symposium on Theory of computing (1997) pp. 176–188.
- [93] A. Y. Kitaev, Quantum computations: algorithms and error correction, Russian Mathematical Surveys 52, 1191 (1997).
- [94] E. Knill, R. Laflamme, and W. H. Zurek, Resilient quantum computation: error models and thresholds, Proceedings of the Royal Society of London. Series A: Mathematical, Physical and Engineering Sciences 454, 365 (1998).
- [95] P. Aliferis, D. Gottesman, and J. Preskill, Quantum accuracy threshold for concatenated distance-3 codes, arXiv preprint quant-ph/0504218 (2005).
- [96] A. Raza, M. C. Caro, J. Eisert, and S. Khatri, Online learning of quantum processes, arXiv preprint arXiv:2406.04250 (2024).
- [97] J. A. Barandes, The stochastic-quantum correspondence, arXiv preprint arXiv:2302.10778 (2023).
- [98] D. Bluvstein, H. Levine, G. Semeghini, T. T. Wang, S. Ebadi, M. Kalinowski, A. Keesling, N. Maskara, H. Pichler, M. Greiner, et al., A quantum processor based on coherent transport of entangled atom arrays, Nature 604, 451 (2022).
- [99] H. Ammann, R. Gray, I. Shvarchuck, and N. Christensen, Quantum delta-kicked rotor: Experimental observation of decoherence, Physical review letters 80, 4111 (1998).

- [100] M. A. Ali Ahmed, G. A. Álvarez, and D. Suter, Robustness of dynamical decoupling sequences, Physical Review A—Atomic, Molecular, and Optical Physics 87, 042309 (2013).
- [101] B. Reggio, N. Butt, A. Lytle, and P. Draper, Fast partitioning of pauli strings into commuting families for optimal expectation value measurements of dense operators, Physical Review A 110, 022606 (2024).
- [102] V. Kashyap, G. Styliaris, S. Mouradian, J. I. Cirac, and R. Trivedi, Accuracy guarantees and quantum advantage in analogue open quantum simulation with and without noise, arXiv preprint arXiv:2404.11081 (2024).
- [103] D. Kane, S. Karmalkar, and E. Price, Robust polynomial regression up to the information theoretic limit, in 2017 IEEE 58th Annual Symposium on Foundations of Computer Science (FOCS) (IEEE, 2017) pp. 391–402.
- [104] F. E. Gutiérrez, Simple algorithms to test and learn local hamiltonians, arXiv preprint arXiv:2404.06282 (2024).
- [105] C. Benedetti, A. P. Shurupov, M. G. Paris, G. Brida, and M. Genovese, Experimental estimation of quantum discord for a polarization qubit and the use of fidelity to assess quantum correlations, Physical Review A—Atomic, Molecular, and Optical Physics 87, 052136 (2013).
- [106] W. H. Zurek, Decoherence, einselection, and the quantum origins of the classical, Reviews of modern physics 75, 715 (2003).
- [107] D. I. Tsomokos, M. J. Hartmann, S. F. Huelga, and M. B. Plenio, Entanglement dynamics in chains of qubits with noise and disorder, New Journal of Physics 9, 79 (2007).
- [108] M. C. Caro, Learning quantum processes and hamiltonians via the pauli transfer matrix, ACM Transactions on Quantum Computing 5, 1 (2024).
- [109] W. Yu, J. Sun, Z. Han, and X. Yuan, Robust and efficient hamiltonian learning, Quantum 7, 1045 (2023).
- [110] A. M. Souza, G. A. Alvarez, and D. Suter, Experimental protection of quantum gates against decoherence and control errors, Physical Review A—Atomic, Molecular, and Optical Physics 86, 050301 (2012).
- [111] A. Bakshi, A. Liu, A. Moitra, and E. Tang, Learning quantum hamiltonians at any temperature in polynomial time, in *Proceedings of the 56th Annual ACM Sym*posium on Theory of Computing (2024) pp. 1470–1477.
- [112] F. G. Tricomi, Sulla funzione gamma incompleta, Annali di Matematica Pura ed Applicata 31, 263 (1950).

- [113] H.-Y. Huang, R. Kueng, and J. Preskill, Predicting many properties of a quantum system from very few measurements, Nature Physics 16, 1050 (2020).
- [114] M. J. Biercuk, H. Uys, A. P. VanDevender, N. Shiga, W. M. Itano, and J. J. Bollinger, Optimized dynamical decoupling in a model quantum memory, Nature 458, 996 (2009).
- [115] D. S. Wild and Á. M. Alhambra, Classical simulation of short-time quantum dynamics, PRX Quantum 4, 020340 (2023).
- [116] G. B. Mbeng, A. Russomanno, and G. E. Santoro, The quantum ising chain for beginners, arXiv preprint arXiv:2009.09208 59 (2020).

## Appendix A: Non-Markovian learning

## 1. Tomography on a support of bounded size $\mathcal{I}_{a,b}$

We now show which measurements need to be performed in order to invert the linear map:

$$K_{a,b}^{(m-2)}(0) \to \text{Tr}[P_O T_W^{(m)}(P_I)].$$
 (A1)

In Section IV B 2 we proposed to perform tomography on  $\mathcal{I}_{a,b}$ , which is an enlargement of the joint support of  $P_a, P_b$ ,  $\mathcal{S}_{a,b}$ , by at most a constant number of qubits. Here, we formally define the tomography region  $\mathcal{I}_{a,b}$ , provide bounds on its size and prove that it is sufficient to perform tomography on it to learn  $K_{a,b}^{(m-2)}(0)$ . Recall the decomposition of the linear map  $T_W^{(m)}$ :

$$T_W^{(m)}(X) = \sum_{P,Q} \xi_{P,Q}^{W,(m)} P X Q.$$
 (A2)

We recall from Eqs. (22) and (23) that for given Pauli strings  $P_a$ ,  $P_b$  and a support  $\mathcal{V}$  we defined  $\mathcal{Y}_{\mathcal{V}}(a,b)$  via:

$$(P_c, P_d) \in \mathcal{Y}_{\mathcal{V}}(a, b)$$
 if and only if  $P_c|_{\mathcal{V}} = P_a|_{\mathcal{V}}, P_d|_{\mathcal{V}} = P_b|_{\mathcal{V}}$  and  $P_c|_{\mathcal{V}^c} = P_d|_{\mathcal{V}^c} \neq \mathbb{1}_{\mathcal{V}^c}$ . (A3)

As discussed in the main text,  $\mathcal{Y}_{\mathcal{V}}(a,b)$  can be interpreted as the set of Pauli string pairs whose contribution to  $T_W^{(m)}$  cannot be distinguished from that of  $P_a, P_b$  by performing tomography on only  $\mathcal{V}$ . Indeed, if we restrict our measurements to a support  $\mathcal{V}$  we obtain a map whose coefficients are sums of various  $\xi_{c,d}^{(m)}$ :

$$\frac{1}{2^{|\mathcal{V}^c|}} \text{Tr}_{\mathcal{V}^c}(T_W^{(m)}(X)) = \sum_{P,Q \in \mathcal{P}_{|\mathcal{V}|}} \Xi_{P,Q}^{W,\mathcal{V},(m)} P X Q, \quad \Xi_{P_c,P_d}^{W,\mathcal{V},(m)} = \xi_{P_c,P_d}^{W,(m)} + \sum_{(P_e,P_f) \in \mathcal{Y}_{\mathcal{V}}(c,d)} \xi_{P_e,P_f}^{W,(m)}$$
(A4)

Our general strategy is to find a support  $\mathcal{I}_{a,b}$  such that  $\mathcal{Y}_{\mathcal{I}_{a,b}}(a,b) = \emptyset$ , yielding:

$$\Xi_{P_c, P_d}^{W, \mathcal{I}_{a,b}, (m)} = \xi_{P_c, P_d}^{W, (m)}. \tag{A5}$$

We can obtain the kernel derivatives by estimating  $\xi_{P,Q}^{W,(m)}$ ,  $\xi_{Q,P}^{W,(m)}$ , for P,Q as described in Eqs.(21),(26) and (31). Since we only need to learn particular coefficients of the super-operator  $T_W^{(m)}$ , we don't need to perform process tomography [15]. In Lemma 4 we outline the procedure to obtain the desired coefficients, which has the cost of state tomography.

**Lemma 3** (Enlarged support). Let  $P_a, P_b \in \mathcal{P}_{SE}$  be Pauli strings with nonzero kernel,  $K_{a,b} \neq 0$ . The derivative  $K_{a,b}^{(m)}(0)$  can be recovered with the following procedure:

If 
$$a \neq b$$
: 
$$\begin{cases} Tomography \ on \ \mathcal{I}_{a,b} \ using \ W = \mathbb{1}^{\otimes N}, & m \ even. \\ Tomography \ on \ \mathcal{I}_{a,b} \ using \ W = P_w, & m \ odd. \end{cases}$$
(A6)

If 
$$a = b : \begin{cases} Tomography \ on \ \mathcal{I}_{a,a} \ using \ W = \mathbb{1}^{\otimes N}, & m \ even. \\ Tomography \ on \ \mathcal{I}_{a,\tilde{a}} \ using \ W = (S \cdot H)_s \otimes \mathbb{1}^{\otimes N-1}, & m \ odd. \end{cases}$$
 (A7)

where  $P_w$  is a single-qubit Pauli string that anticommutes with  $P_a \cdot P_b$  and  $(S \cdot H)_s \otimes \mathbb{1}^{\otimes N-1}$  is identity everywhere except at site s, which can be any site in the support of  $P_a$ . These supports have bounded size:

$$|\mathcal{I}_{a,b}| \le 2k_{SE} + \mathfrak{d}_0 - 2, \quad |\mathcal{I}_{a,\bar{a}}| \le k_{SE} + \mathfrak{d}_0 - 1, \quad \text{with } \mathfrak{d}_0 := \max_{K_{a,b} \ne 0} |\mathcal{Y}_{\mathcal{S}_{a,b}}(a,b)| \le \mathfrak{d}. \tag{A8}$$

Symbol	Defined in	Informal description
$\mathcal{P}_S$	Eq.(1)	Index set for the Pauli strings in the system Hamiltonian $H_S$ .
$\mathcal{P}_{SE}$	Eq.(1)	Index set for the Pauli strings in the coupling Hamiltonian $V_{SE}(t)$ .
$P_a$	Below Eq.(1)	Pauli string acting on the system.
$A_a(t)$	Below Eq.(1)	Hermitian operator linear in the bosonic creation and annihilation operators.
$K_{a,b}(t)$	Eq.(5)	Non-Markovian kernel: two-point correlation function of environment modes.
$K_{a,b}^{(m)}(0)$	Eq.(10)	$m$ -th derivative of $K_{a,b}(t)$ at $t=0$ .
$k_S, k_{SE}$	Above Eq.(9)	Size of the support of Pauli strings in $\mathcal{P}_S$ and $\mathcal{P}_{SE}$ , respectively.
ð	Above Eq.(9)	Counts how many terms in $H(t)$ might not commute with a given term in $H(t)$ .
$\mathcal{Y}_{\mathcal{V}}(a,b)$	Eq.(A3)	Set of pairs of Pauli strings whose coefficients would mix with those of $K_{a,b}(t)$ if we were to only measure on the support $\mathcal{V}$ .
$\mathcal{S}_{a,b}$	Above Eq.(22)	Joint support of Pauli strings $P_a, P_b$ . Satisfies $ S_{a,b}  \leq O(k_{SE})$
$\mathfrak{d}_0$	Eq. (A8)	Upper bound on $ \mathcal{Y}_{\mathcal{S}_{a,b}}(a,b) $ for every $a,b\in\mathcal{P}_{SE}$ . Satisfies $\mathfrak{d}_0\leq\mathfrak{d}$ .
$\mathcal{Q}_{a,b}$	Above Eq.(24)	Extra sites that need to be added to $S_{a,b}$ to recover the coefficients of $K_{a,b}(t)$ . Satisfies $ Q_{a,b}  \leq \mathfrak{d}_0$ .
$\mathcal{I}_{a,b}$	Eq.(24)	Tomography on support $\mathcal{I}_{a,b}$ is sufficient to learn $K_{a,b}(t)$ . Satisfies $ \mathcal{I}_{a,b}  \leq O(k_{SE}) + \mathfrak{d}_0$ .
8	Above Eq.9	Sparsity of the kernel: for each $P_a$ there are at most $s$ Pauli strings $P_b$ such that $K_{a,b}(t) \neq 0$ . In the ensemble Hamiltonian case, sparsity of the covariance matrix $\Sigma$ .
$a_0$	Appendix A 2	Diameter of Pauli strings in $\mathcal{P}_{SE}$ .
M	Proposition 1	Highest derivative $\partial_t^M K_{a,b}(t) _{t=0}$ that we estimate.
$\mathcal{E}_W(t)$	Eq. 11	State preparation channel with an intermediate gate $W$ .
$\mathcal{F}_{W}^{(m)}(t)$	Eq. A28	$m$ -th term in the Dyson series of the channel $\mathcal{E}_W(t)$ .
$\mathcal{F}_{W,S}^{(2)}(t), \mathcal{F}_{W,SE}^{(2)}$	$_{\rm E}(t)$ Eq. 17	Terms in $\mathcal{F}_W^{(2)}(t)$ that only involve $H_S$ and $V_{SE}(t)$ , respectively.
$T_W^{(m)}$	Eq. 18b	Certain entries of this linear map yield the derivatives $K_{a,b}^{(m-2)}(0)$ .
$B_{W,(O,I)}(t)$	Eq. 15	Time trace for initial Pauli string $P_I$ , observable $P_O$ and intermediate gate $W$ .
$f_{W,(O,I)}^{(m)}$	Eq. 18c	Offset containing terms in $H_S$ and kernel derivatives of order $\leq m-3$ .
$B_a(t)$	Above Eq. A34	Variable that can be $\lambda_a$ , $A_a(t)$ , $\lambda_a + A_a(t)$ when $a$ is in $\mathcal{P}_S$ , $\mathcal{P}_{SE}$ , or both.
$\hat{x}$		The hat indicates an estimate for a variable $x$ .
d	Lemma 1	Degree of the polynomial fit.
Σ	Section III B	Covariance matrix of the ensemble Hamiltonian model.

 $TABLE\ II.\ Table\ of\ the\ symbols\ used\ in\ the\ non-Markovian\ and\ ensemble\ Hamiltonian\ models.$ 

Proof. Recall that we want to find  $\mathcal{I}_{a,b}$  such that  $\mathcal{Y}_{\mathcal{I}_{a,b}}(a,b) = \emptyset$  to learn the derivatives of the kernel from Eq. (A5). We will construct  $\mathcal{I}_{a,b}$  as an enlargement of  $\mathcal{S}_{a,b}$  that sequentially resolves the conflicting pairs in  $\mathcal{Y}_{\mathcal{S}_{a,b}}(a,b)$ . We begin by bounding this set. Consider a pair of Pauli strings  $(P_c, P_d) \in \mathcal{Y}_{\mathcal{S}_{a,b}}(a,b)$ . Since  $P_c|_{\mathcal{S}_{a,b}} = P_a|_{\mathcal{S}_{a,b}}$ , we know that  $P_c$  overlaps with  $P_a$ . But  $P_a$  can overlap with at most  $\mathfrak{d}$  terms in  $\mathcal{P}_{SE}$ , so there are at most  $\mathfrak{d}$  options for  $P_c$ . Since  $(P_c, P_d) \in \mathcal{Y}_{\mathcal{S}_{a,b}}(a,b)$ ,  $P_d$  is fixed by  $P_a, P_b, P_c$  per Eq.(A3). Therefore, the number of pairs in  $\mathcal{Y}_{\mathcal{S}_{a,b}}(a,b)$  is at most  $\mathfrak{d}$ , so  $\mathfrak{d}_0 \leq \mathfrak{d}$ .

The pairs  $(P_c, P_d) \in \mathcal{Y}_{\mathcal{S}_{a,b}}(a, b)$  can also be written as  $P_c = Q \cdot P_a, P_d = Q \cdot P_b$ , where Q is a non-identity Pauli string that does not overlap with  $\mathcal{S}_{a,b}$ . We label the pairs in  $\mathcal{Y}_{\mathcal{S}_{a,b}}(a, b)$  from 1 to  $\mathfrak{d}_0$ , and consider the corresponding  $Q_1, ..., Q_{\mathfrak{d}_0}$ . Pick one site  $s_i$  from the support of each  $Q_i$  and define the enlarged support  $\mathcal{I}_{a,b}$  as follows:

$$Q_{a,b} := \{s_1, ..., s_{\mathfrak{d}_0}\}, \quad \mathcal{I}_{a,b} := S_{a,b} \cup Q_{a,b}.$$
 (A9)

If two  $Q_i, Q_j$  overlap, we can pick  $s_i = s_j$  to minimize the number of extra sites we need to do tomography on. Since  $S_{a,b} \subseteq \mathcal{I}_{a,b}$ , we have  $\mathcal{Y}_{\mathcal{I}_{a,b}}(a,b) \subseteq \mathcal{Y}_{\mathcal{S}_{a,b}}(a,b)$ . But for each pair  $(P_c, P_d) \in \mathcal{Y}_{\mathcal{S}_{a,b}}(a,b)$ , there is a site in  $s \in \mathcal{Q}_{a,b}$  where  $P_c|_s = P_d|_s \neq 1$ . Therefore,  $P_c|_{\mathcal{I}_{a,b}} \neq P_a|_{\mathcal{I}_{a,b}}$  so  $(P_c, P_d) \notin \mathcal{Y}_{\mathcal{I}_{a,b}}(a,b)$ , yielding  $\mathcal{Y}_{\mathcal{I}_{a,b}}(a,b) = \emptyset$ .

We now bound  $|\mathcal{I}_{a,b}|$ . If  $|\mathcal{S}_{a,b}| = 2k_{SE}$  or  $2k_{SE} - 1$ , then one of the Pauli strings in each pair  $(P_c, P_d) \in \mathcal{Y}_{\mathcal{S}_a \cup \mathcal{S}_b}(a, b)$  would need to be at least  $(k_{SE} + 1)$ -local, since  $(P_c, P_d) = (Q \cdot P_a, Q \cdot P_b)$  and Q is non-identity and supported outside of  $\mathcal{S}_{a,b}$ . Since Pauli strings in  $\mathcal{P}_{SE}$  are at most  $k_{SE}$ -local, if  $|\mathcal{S}_{a,b}| = 2k_{SE}$  or  $2k_{SE} - 1$  we have  $\mathcal{Y}_{\mathcal{S}_{a,b}}(a, b) = \emptyset$ . Thus  $\mathcal{I}_{a,b}$  is a support of at most  $2k_{SE} - \mathfrak{d}_0 + 2$  qubits:  $|\mathcal{I}_{a,b}| \le 2k_{SE} - \mathfrak{d}_0 + 2$ . Similarly we obtain  $|\mathcal{I}_{a,\tilde{a}}| \le k_{SE} + \mathfrak{d}_0 - 1$ .

If we perform process tomography on  $\mathcal{I}_{a,b}$  or, as we will see in Lemma 4, a tomography procedure with the sample requirement of state tomography, by Eq. (A5) we can recover the coefficients  $\Xi_{P,Q}^{W,\mathcal{I}_{a,b},(m+2)} = \xi_{P,Q}^{W,(m+2)}$ , for P,Q as described in Eqs.(21),(26) and (31). Note that since  $\mathcal{I}_{b,a} = \mathcal{I}_{a,b}$ , tomography on this region also recovers  $\xi_{Q,P}^{W,(m+2)}$ , which allows us to recover the real and imaginary parts of  $K_{a,b}^{(m)}(0)$ .

**Lemma 4.** Let  $T(\cdot) = \sum_{c,d} \xi_{c,d} P_c \cdot P_d$  be a Hermiticity-preserving linear map acting on N-qubit states. Suppose we can estimate  $O_{a,b} = \frac{1}{2^N} \text{Tr}(P_a T(P_b))$  to precision  $\epsilon$ , where  $P_a, P_b$  are phaseless Pauli strings of length N, satisfying  $\text{Tr}(P_a P_b) = 2^N \delta_{a,b}$ . Estimating all  $4^N \times 4^N$  observables  $O_{a,b}$  allows us to obtain estimates for every complex  $\xi_{c,d}$  to precision  $\epsilon$ . Collecting the coefficients in vectors and using hats for the estimates, this is stated as:

$$\|\hat{\vec{O}} - \vec{O}\|_{\infty} \le \epsilon \Rightarrow \|\hat{\vec{\xi}} - \vec{\xi}\|_{\infty} \le \epsilon. \tag{A10}$$

Moreover, if we only want to obtain estimates for one particular  $\xi_{ef}$  we only need estimates for  $4^N$  different  $O_{a,b}$ . Proof. The vector  $\vec{O}$  for which we have good estimates is related to  $\vec{\xi}$  by a linear equation:

$$O_{a,b} = \frac{1}{2^N} \text{Tr}(P_a T(P_b)) = \sum_{c,d} \frac{1}{2^N} \text{Tr}(P_a P_c P_b P_d) \xi_{c,d} \Rightarrow \vec{O} = G \cdot \vec{\xi}, \text{ where } G_{(a,b),(c,d)} = \frac{1}{2^N} \text{Tr}(P_a P_c P_b P_d)$$
(A11)

Introducing a SWAP operator and writing the vectorized superoperator as  $\tilde{T} = \sum_{c,d} P_c \otimes P_d \xi_{c,d}$  we can invert G:

$$G_{(a,b),(c,d)} = \frac{1}{2^N} \operatorname{Tr}(P_a P_c P_b P_d) = \frac{1}{2^N} \operatorname{Tr}((P_a \otimes P_b)(P_c \otimes P_d) \operatorname{SWAP}) \Rightarrow$$
(A12)

$$O_{a,b} = \frac{1}{2^N} \text{Tr}(P_a \otimes P_b \cdot \tilde{T} \cdot \text{SWAP}) \Rightarrow \tilde{T} \cdot \text{SWAP} = \frac{1}{2^N} \sum_{a,b} P_a \otimes P_b O_{a,b} \Rightarrow \tilde{T} = \frac{1}{2^N} \sum_{a,b} (P_a \otimes P_b) \text{SWAP} \cdot O_{a,b} \Rightarrow \tilde{T} = \frac{1}{2^N} \sum_{a,b} (P_a \otimes P_b) \hat{T} \cdot \hat{T}$$

(A13)

$$\xi_{c,d} = \sum_{a,b} \frac{1}{2^{3N}} \operatorname{Tr}((P_c \otimes P_d)(P_a \otimes P_b) \operatorname{SWAP}) O_{a,b} \Rightarrow G_{(c,d),(a,b)}^{-1} = \frac{1}{2^{3N}} \operatorname{Tr}(P_c P_a P_d P_b). \tag{A14}$$

We used the fact that the Pauli strings form a basis and  $\text{Tr}(P_a P_b) = 2^N \delta_{a,b}$  to write  $\tilde{T} \cdot \text{SWAP}$  in terms of  $O_{a,b}$  in the second line. In the third line we apply  $P_c \otimes P_d$  on the left and take the trace. This means that we can obtain  $\vec{\xi}$  from  $\vec{O}$  as:

$$\vec{\xi} = G^{-1} \cdot \vec{O}. \tag{A15}$$

Notice that  $\vec{O}$  is a vector of  $4^N$  real entries, while  $\vec{\xi}$  is a vector of  $4^N$  complex entries. However, since T is a Hermiticity-preserving map we have that  $\xi_{c,d}^* = \xi_{c,d}$ , so the number of independent real entries is  $4^N$ . Suppose we want to estimate a particular  $\xi_{ef}$ . The row  $G_{(e,f),(\cdot,\cdot)}^{-1}$  is largely filled with 0: for each  $P_a$  there is only one phaseless Pauli string  $P_b$  such that  $G_{(e,f),(a,b)}^{-1} \neq 0$ , the one satisfying  $P_b \propto (P_e P_a P_f)^{\dagger}$ . Therefore, let  $R_a^{e,f} := G_{(e,f),(a,b)}^{-1}$  be the row entry corresponding to  $P_b$  being fixed to the (phaseless) Pauli string satisfying  $P_b \propto (P_e P_a P_f)^{\dagger}$  and similarly  $O_a^{ef} := O_{a,b}$ . Thus from each row of the equation above we obtain:

$$\xi_{ef} = \vec{R}^{ef} \cdot \vec{O}^{ef},\tag{A16}$$

where the dot product is between two vectors of length  $4^N$ . Since  $|R_a^{ef}| = \frac{1}{4^N}$ , by the triangle inequality we obtain the bound on the precision:

$$|\hat{\xi}_{ef} - \xi_{ef}| = |\vec{R}^{ef} \cdot (\hat{\vec{O}}^{ef} - \vec{O}^{ef})| \le 4^N \cdot \frac{1}{4^N} ||\hat{\vec{O}}^{ef} - \vec{O}^{ef}||_{\infty} \le \epsilon.$$
(A17)

Notice that if we are only interested in estimating one particular  $\xi_{ef}$ , it suffices to have estimates for only  $4^N$  observables,  $\vec{O}^{ef}$ , instead of  $4^N \times 4^N$  required for process tomography. If we initialize Pauli eigenstates and measure in the Pauli basis, we can estimate  $\vec{O}^{ef}$  by preparing initial states in all  $3^N$  distinct bases, measuring in the corresponding basis of  $P_b$  and reconstructing each observable with the correct eigenvalue signs.

This Lemma means that in order to estimate  $\xi_{a,b}^{W,\mathcal{I}_{a,b}}$  we only need to prepare  $3^{|\mathcal{I}_{a,b}|}$  experimental configurations and measure to the desired precision. We summarize this Section in the following Lemma.

**Lemma 5.** Given a geometrically local  $V_{SE}(t)$  with each term supported on at most  $k_{SE}$  sites and not commuting with at most  $\mathfrak{d}$  other terms in  $\mathcal{P}_{SE}$ , the derivatives at t=0 of kernel  $K_{a,b}(t)$  can be learned by doing state tomography on  $\mathcal{I}_{a,b} := \mathcal{S}_{a,b} \cup \{s_1,...,s_{\mathfrak{d}_0}\}$ , a region of size at most  $O(k_{SE}) + O(\mathfrak{d}_0)$ , where  $\mathfrak{d}_0 \leq \mathfrak{d}$ .

In order to learn all  $\mathfrak{d}N$  kernels it suffices to estimate the  $3^{2k_{SE}+\mathfrak{d}_0-2} \cdot \mathfrak{d}N$  configurations required for tomography on each  $\mathcal{I}_{a,b}$ . In the next Appendix we show that, since many  $\mathcal{I}_{a,b}$  don't overlap, we can estimate them simultaneously.

# 2. Initial states and measurements for parallelization

We now show how to minimize the number of measurement rounds by measuring a large number of regions  $\mathcal{I}_{a,b}, \mathcal{I}_{c,d},...$  simultaneously in each round of measurements. Since we can only measure simultaneously those regions that don't overlap, we first characterize how many regions each  $\mathcal{I}_{a,b}$  overlaps with. In the main text we argued that geometric locality yields a maximum diameter  $a_0 = O(k_{SE})$  for Pauli strings  $P_a, P_b$ , which bounds the regions that  $\mathcal{I}_{a,b}$  can overlap with. Here we provide a more detailed counting in terms of  $\mathfrak{d}$  directly.

**Lemma 6.** Let  $\{\mathcal{I}_{a,b}\}_{(a,b)}$  be a collection of supports satisfying that  $P_a, P_b \in \mathcal{P}_{SE}$  wach overlap with at most  $\mathfrak{d}$  other terms in  $\mathcal{P}_{SE}$  and that for a fixed  $P_a$  there's at most s terms  $P_b \in \mathcal{P}_{SE}$  such that  $K_{a,b}(t) \neq 0$ . Then each  $\mathcal{I}_{a,b}$  overlaps with at most  $(\mathfrak{d}_0 + 2)(s + \mathfrak{d})\mathfrak{d}^2$  other  $\mathcal{I}_{c,d}$ 

Proof. Recall that  $\mathcal{I}_{a,b} = \mathcal{S}_{a,b} \cup \mathcal{Q}_{a,b}$ , where  $|\mathcal{Q}_{a,b}| \leq \mathfrak{d}_0$ . We first show that each  $\mathcal{I}_{a,b}$  can overlap with  $(\mathfrak{d}_0 + 2)\mathfrak{d}_0$  Pauli strings  $P_c \in \mathcal{P}_{SE}$ :  $P_a, P_b$  each overlap with at most  $\mathfrak{d}$  Paulis in  $\mathcal{P}_{SE}$  and since each of the  $\mathfrak{d}_0$  sites in  $\mathcal{Q}_{a,b}$  is in the support of a pair of Paulis in  $\mathcal{P}_{SE}$ , that site can overlap with at most  $\mathfrak{d}$  other Paulis. We now show that each  $P_c \in \mathcal{P}_{SE}$  can overlap with at most  $(s+\mathfrak{d})\mathfrak{d}$  regions  $\mathcal{I}_{e,f}$ : suppose  $P_c$  overlaps with  $P_e$ , then there's s choices of  $P_f$  such that  $P_c$  overlaps with  $\mathcal{S}_{e,f}$  and  $K_{e,f}(t) \neq 0$ . Since  $P_c$  overlaps with at most  $\mathfrak{d}$  Paulis in  $\mathcal{P}_{SE}$ , we get that it overlaps with at most  $s\mathfrak{d}$  supports  $\mathcal{S}_{e,f}$  corresponding to nonzero kernels, each yielding one region  $\mathcal{I}_{e,f}$ . Now suppose that  $P_c$  overlaps with  $\mathcal{Q}_{e,f}$  but not with  $P_e, P_f$ , i.e.  $P_c$  overlaps with some pair  $(P_{e_1}, P_{f_1}) \in \mathcal{Y}_{S_{e,f}}(e,f)$ . For a fixed  $(P_{e_1}, P_{f_1})$ , there's at most  $\frac{1}{2}\mathfrak{d}$  regions  $\mathcal{Q}_{g,h}$  that  $(P_{e_1}, P_{f_1})$  could be a part of:  $P_{e_1}, P_{f_1}$  overlap with  $P_e, P_f$  and every other  $(P_{e_i}, P_{f_i}) \in \mathcal{Y}_{S_{e,f}}(e,f)$ , respectively, and since  $P_{e_j} \neq P_{e_i} \neq P_{f_i}$  having  $\frac{1}{2}\mathfrak{d}$  pairs means that  $P_e$  would overlap with  $\mathfrak{d}$  distinct Pauli strings. Therefore,  $P_c$  can overlap with at most  $\mathfrak{d}^2$  regions  $\mathcal{Q}_{e,f}$ . We thus see that  $P_c$  can overlap with at most  $(\mathfrak{d}_0 + \mathfrak{d}_0)\mathfrak{d}^2$ .

In order to minimize the required number of rounds of measurements we need to maximize the number of supports  $\mathcal{I}_{a,b}$  that we measure simultaneously. In the Hamiltonian learning setting this has been solved using a graph coloring algorithm [33], which we adapt here. Let  $\mathfrak{G}$  be a graph with a vertex  $v_{a,b} = (a,b)$  for every nonzero kernel  $K_{a,b}(t)$  and an edge between  $v_{a,b}, v_{c,d}$  if the regions  $\mathcal{I}_{a,b}, \mathcal{I}_{c,d}$  overlap. The degree d of the graph  $\mathfrak{G}$  is the number of neighbors that each vertex has, i.e. the number of edges connecting this vertex to others. By Lemma 6, each vertex has edges with at most  $(\mathfrak{d}_0 + 2)(s + \mathfrak{d})\mathfrak{d}^2$  of their neighbors. Therefore, the degree of graph  $\mathfrak{G}$  satisfies  $d \leq (\mathfrak{d}_0 + 2)(s + \mathfrak{d})\mathfrak{d}^2$ . A graph of degree d can be colored by a standard greedy algorithm using d + 1 colors,  $\mathcal{C}_1, ..., \mathcal{C}_{d+1}$ . Those vertices assigned to the same color  $\mathcal{C}_i$  will not have any edges between them, i.e. they are not neighbors, so the corresponding regions don't overlap. For example, in Figure 8 we see that for color  $\mathcal{C}_1 = \{v_{a,b}, v_{c,d}, v_{e,f}\}$ , the regions  $\mathcal{I}_{a,b}, \mathcal{I}_{c,d}, \mathcal{I}_{e,f}$  don't overlap, so they can be measured simultaneously in the same round. Since each round of measurements corresponds to a color, there are  $(\mathfrak{d}_0 + 2)(s + \mathfrak{d})\mathfrak{d}^2 + 1$  different rounds.

Thus, for the round of measurement corresponding to color  $C_i$ , we will prepare an initial state of the form:

$$\rho_S = \bigotimes_{(a,b)\in\mathcal{C}_i} \rho_{S,a,b} \bigotimes_{s\in\mathcal{C}_i^c} \frac{1}{2},\tag{A18}$$

where  $\rho_{S,a,b}$  is a state supported only on  $\mathcal{I}_{a,b}$  and  $\mathcal{C}_i^c$  is the complement of the supports of all regions of the same color. Similarly, we will measure in each region in  $\mathcal{C}_i$  and trace our the rest. In the main text we have reduced our problem to estimating expectation values of the form  $B_{W,(O,I)}(t) = \frac{1}{2^N} \text{Tr}(P_O \mathcal{E}_W(t,P_I))$ , for several t, with  $P_O, P_I$  being Pauli strings that implement tomography on  $\mathcal{I}_{a,b}$  following Lemma 4. We can estimate many of these simultaneously by preparing  $\rho_{S,a,b}$  according to Lemma 7 and measuring on that support, for all the supports in  $\rho_S$ . This Lemma also tells us that, we can estimate one  $B_{W,(O,I)}(t)$  to precision  $\epsilon_S$  with success probability at least  $1-\delta$  using a number of samples  $2/\epsilon_S^2 \log(2/\delta)$ . However, we want to estimate all expectation values correctly with probability at least  $1-\delta'$ . Recall that, since  $|\mathcal{P}_{SE}| = O(N)$ , there are at most  $s \cdot O(N)$  kernels. For each kernel we need to prepare at most  $3^{2k_{SE}+\mathfrak{d}_0-2}$  different basis pairs  $(\rho,O)$  (Lemma 4) and 2 choices of W, as well as some O(1) number of timesteps t, so we obtain  $\delta'$  by dividing  $\delta$  by all these cases. Since there are  $(\mathfrak{d}_0+2)(s+\mathfrak{d})\mathfrak{d}^2+1$  colors, in order to estimate all necessary  $B_{W,(O,I)}(t)$  to precision  $\epsilon_S$ , we use a number of samples:

$$O\left(\frac{2((\mathfrak{d}_0+2)(s+\mathfrak{d})\mathfrak{d}^2+1)}{\epsilon_S^2} \cdot \log\left(\frac{sN \cdot 2^2 \cdot 3^{2k_{SE}+\mathfrak{d}_0-2}}{\delta}\right)\right). \tag{A19}$$

**Lemma 7.** Let P,Q be Pauli strings on N qubits and  $\Phi$  a quantum channel on N-qubit states. Suppose we prepare an intial state  $\rho$  drawn uniformly from the eigenstates of P and perform a projective measurement in the basis of Q,

obtaining a measurement sample. In order to estimate  $\frac{1}{2^N} \text{Tr}(Q\Phi(P))$  to additive precision  $\epsilon$  with probability at least  $1-\delta$  it suffices to use

$$\frac{2}{\epsilon^2} \log \left( \frac{2}{\delta} \right) \tag{A20}$$

samples.

Proof. Consider a Pauli string  $P = \bigotimes_{i=1}^N \sigma^{\alpha_i}$  and let  $|r_i, \alpha_i\rangle$  be the  $r_i$ -eigenstate of  $\sigma^{\alpha_i}$ , with  $r_i \in \{\pm 1\}$ ,  $\alpha_i \in \{x, y, z\}$ . Then if we consider initial states of the form  $|r, \alpha\rangle := \bigotimes_{i=1}^N |r_i, \alpha_i\rangle$  we can write the expectation value as:

$$\frac{1}{2^N} \operatorname{Tr}(Q\Phi(P)) = \frac{1}{2^N} \sum_{r \in \{\pm 1\}^N} \left( \prod_{i=1}^N r_i \right) \operatorname{Tr}(P_O\Phi(|r,\alpha\rangle\langle r,\alpha|)). \tag{A21}$$

We now produce i.i.d. samples  $Z_j \in \{\pm 1\}$ , for j = 1, ..., m, by:

- 1. Drawing  $r_j$  uniformly at random from  $\{\pm 1\}^N$ .
- 2. Preparing the initial state  $\rho_j = |r_j, \alpha\rangle\langle r_j, \alpha|$ .
- 3. Applying the quantum channel  $\Phi$ .
- 4. Performing a projective measurement in the basis of Q, obtaining  $X_j \in \{\pm 1\}$ , which follows Born's rule:

$$\mathbb{E}(X_j|r_j) = \text{Tr}(P_O\Phi(\rho_j)). \tag{A22}$$

5. Letting  $Z_j = X_j \cdot \prod_{i=1}^N r_i$ .

These are random variables with the following mean and variance:

$$\mathbb{E}(Z_j) = \frac{1}{2^N} \sum_{r \in \{\pm 1\}^N} \left( \prod_{i=1}^N r_i \right) \mathbb{E}(X_j | r) = \frac{1}{2^N} \operatorname{Tr}(Q\Phi(P)), \tag{A23}$$

$$Var(Z_j) = 1 - \mathbb{E}(Z_j)^2 \le 1, \tag{A24}$$

where in the last line we used that  $\left|\frac{1}{2^N}\text{Tr}(Q\Phi(P))\right| \leq 1$ . Therefore, the sample mean  $\hat{\mu} = \frac{1}{m}\sum_{j=1}^m Z_j$  satisfies:

$$\mathbb{E}(\hat{\mu}) = \frac{1}{2^N} \text{Tr}(Q\Phi(P)), \quad \text{Var}(\hat{\mu}) = \frac{\text{Var}(Z_j)}{m} \le \frac{1}{m}.$$
 (A25)

Use Hoeffding's inequality to get sufficient number of samples to estimate  $\mathbb{E}(\hat{\mu})$  to precision  $\epsilon$  with success probability at least  $1 - \delta$ . Recall that  $Z_j \in [a, b] = [-1, 1]$ :

$$\Pr(|\hat{\mu} - \mathbb{E}(\hat{\mu})| \ge \epsilon) \le 2e^{-\frac{2m\epsilon^2}{(b-a)^2}} \le \delta \Rightarrow m \ge \frac{2}{\epsilon^2} \log\left(\frac{2}{\delta}\right). \tag{A26}$$

3. Computing  $f_{W,(O,I)}^{(m)}$ 

We first show that the offset function only involves at most m orders in the Dyson series:

 $f_{W,(O,I)}^{(m)} = \frac{1}{2^N} \text{Tr}\left(P_O\left(\partial_t^m \mathcal{F}_{W,S}^{(2)}(t)(P_I)|_{t=0} + \sum_{\substack{n=0\\n\neq 2}}^{\infty} \partial_t^m \mathcal{F}_W^{(n)}(t)(P_I)|_{t=0}\right)\right), \tag{A27}$ 

where the n-th term in the Dyson series is:

$$\mathcal{F}_{W}^{(n)}(t)(P_{I}) = (-i)^{n} \sum_{l=0}^{n} \int_{t}^{2t} dt_{1} \int_{t}^{t_{1}} dt_{2} \dots \int_{t}^{t_{l-1}} dt_{l} \int_{0}^{t} dt_{l+1} \dots \int_{0}^{t_{n-1}} dt_{n} \cdot \operatorname{Tr}_{E}([H(t_{1}), \dots [H(t_{l}), W[H(t_{l+1}), \dots [H(t_{n}), P_{I} \otimes \gamma_{E}]]W^{\dagger}]]). \tag{A28}$$

The integrand will be a sum of terms, each of which is a product of kernels and system variables. We assume that each kernel  $K_{a,b}(t)$  is analytic at t=0. In particular there is no Markovian component given by a Lindbladian, whose kernel is  $\delta(t)$ . Then, for small enough t we have a Taylor series for each kernel, so we can write each product of kernels as a Taylor series. Consider the coefficients of order 0, i.e. the constants. After performing the integrals above they will have a time term  $t^n$ , so if n < m this term is killed by the derivatives, while if n > m the term  $t^{n-m}|_{t=0} = 0$  makes it vanish. Thus, only the coefficients with time power n = m after integration remain in  $f_{W,(O,I)}^{(m)}$ . In particular:

$$\partial_t^m \mathcal{F}_W^{(n)}(t)(P_I)|_{t=0} = 0 \quad \text{if} \quad n > m. \tag{A29}$$

Since  $m \ge 2$ , the n = 0, 1 terms vanish upon taking the derivatives and we get the simpler expressions:

$$f_{W,(O,I)}^{(2)} = \frac{1}{2^N} \text{Tr}\left(P_O\left(\partial_t^m \mathcal{F}_{W,S}^{(2)}(t)(P_I)|_{t=0}\right)\right) = \frac{-4}{2^N} \text{Tr}(P_O[H_S, [H_S, P_I]]),\tag{A30}$$

$$f_{W,(O,I)}^{(m)} = \frac{1}{2^N} \text{Tr}\left(P_O \sum_{n=3}^m \partial_t^m \mathcal{F}_W^{(n)}(t)(P_I)|_{t=0}\right), \quad \text{for } m \ge 3.$$
(A31)

The m=2 case only involves system Hamiltonian terms, so the integral can be evaluate easily. We now show how to compute the  $m \geq 3$  case. We will compute it for the case  $W = \mathbb{1}^{\otimes N}$  for notational clarity:

$$\mathcal{F}_{1\otimes N}^{(n)}(t)(P_I) = (-i)^n \int_0^{2t} dt_1 \dots \int_0^{t_{n-1}} dt_n \operatorname{Tr}_E([H(t_1), \dots [H(t_n), P_I \otimes \gamma_E]]). \tag{A32}$$

Note that for general W we only need to carry out the same computation for each term l = 0, ..., n in the sum above, each with different Pauli strings being conjugated by W. The expectation value with  $P_O$  then yields:

$$\frac{1}{2^N} \text{Tr}_E(P_O \partial_t^m \mathcal{F}_{1 \otimes N}^{(n)}(t)(P_I)|_{t=0}) = \frac{(-i)^n}{2^N} \partial_t^m \int_0^{2t} dt_1 \dots \int_0^{t_{n-1}} dt_n \text{Tr}([[P_O, H(t_1)] \dots H(t_n)] P_I \otimes \gamma_E) \Big|_{t=0}, \tag{A33}$$

where we used  $\operatorname{Tr}(A[B,C]) = \operatorname{Tr}([A,B]C)$  repeatedly. We rewrite the trace over nested commutators in the cluster expansion formalism to obtain a better bound on the number of nonvanishing terms: while a naive bound is  $O(\mathfrak{d}^{\frac{n(n+1)}{2}})$ , using the cluster expansion in Lemma 8 we obtain the estimate  $O((\mathfrak{d}_0+2)(\mathfrak{d}+1)(e\mathfrak{d})^n) \cdot e^{O(n\log n)}$ . Define a cluster  $\mathbf{V}$  as a set of tuples  $\{(a,\mu(a))|a\in\mathcal{P}_S\cup\mathcal{P}_{SE}\}$ , where  $\mu(a)$  is the multiplicity of a in cluster  $\mathbf{V}$ . The weight of the cluster is  $|\mathbf{V}| := \sum_a \mu(a)$  and its support is  $\operatorname{Supp} \mathbf{V} = \{a\in\mathcal{P}_S\cup\mathcal{P}_{SE}: \mu(a)\geq 1\}$ . We write  $a\in\mathbf{V}$  if  $\mu(a)\neq 0$  and let  $\mathbf{V}! := \prod_a \mu(a)!$ . While  $\mathbf{V}$  is a multiset, we can also fix an ordering and label its elements  $\{\mathbf{V}_1,\mathbf{V}_2,...,\mathbf{V}_{|\mathbf{V}|}\}$ . Using  $B_a(t)$  for a variable that can be either  $\lambda_a$ ,  $A_a(t)$  or  $\lambda_a+B_a(t)$ , depending on whether a is in  $\mathcal{P}_S,\mathcal{P}_{SE}$  or both, Lemma 8 tells us we can rewrite the trace as:

$$\operatorname{Tr}([[P_O, H(t_1)], ... H(t_n)] P_I \otimes \gamma_E) = \sum_{\mathbf{V} \in \mathcal{G}_{\circ}^{O}} \frac{1}{\mathbf{V}!} \sum_{\sigma \in S_n} \operatorname{Tr}(P_O, [P_{\mathbf{V}_{\sigma(1)}} B_{\mathbf{V}_{\sigma(1)}}(t_1), ..., [P_{\mathbf{V}_{\sigma(n)}} B_{\mathbf{V}_{\sigma(n)}}(t_n), P_I \otimes \gamma_E]]), (A34)$$

where  $\mathcal{G}_n^O$  is a set of at most  $|\mathcal{G}_n^O| \leq O((\mathfrak{d}_0 + 2)(\mathfrak{d} + 1)(e\mathfrak{d})^n)$  clusters. We now expand each commutator. In the resulting terms, there will be l choices to the left of  $P_I \otimes \gamma_E$  and n - l to its right, for l = 0, ..., n. Thus let  $Q(n, l) = \{(q_1, ..., q_l) | q_1 < q_2 < ... < q_l; q_j \in \{1, ..., n\}\}$  be the set all of choices of l indices among a set of length n, arranging them in increasing order. Given  $(q_1, ..., q_l) \in Q(n, l)$ , we fix  $q_{l+1}, ..., q_n$  to be the indices in  $\{1, ..., n\}$  not chosen in  $q_1, ..., q_l$ , in decreasing order: they are fixed by the conditions  $\bigcup_{i=1}^n \{q_i\} = \{1, ..., n\}$  and  $q_{l+1} > ... > q_n$ . We

abuse notation slightly and write  $q = (q_1, ..., q_n) \in Q(n, l)$  to say that the first l indices are chosen and the rest are fixed by this choice. We can now expand the commutators as follows:

$$\operatorname{Tr}(P_{O}, [P_{\mathbf{V}_{\sigma(1)}}B_{\mathbf{V}_{\sigma(1)}}(t_{1}), ..., [P_{\mathbf{V}_{\sigma(n)}}B_{\mathbf{V}_{\sigma(n)}}(t_{n}), P_{I} \otimes \gamma_{E}]]) = \sum_{l=0}^{n} (-1)^{n-l} \times \sum_{q \in Q(n,l)} \operatorname{Tr}(P_{O}P_{\mathbf{V}_{\sigma(q_{1})}}B_{\mathbf{V}_{\sigma(q_{1})}}(t_{q_{1}}) ... P_{\mathbf{V}_{\sigma(q_{l})}}B_{\mathbf{V}_{\sigma(q_{l})}}(t_{q_{l}}) (P_{I} \otimes \gamma_{E}) P_{\mathbf{V}_{\sigma(q_{l+1})}}B_{\mathbf{V}_{\sigma(q_{l+1})}}(t_{q_{l+1}}) ... P_{\mathbf{V}_{\sigma(q_{n})}}B_{\mathbf{V}_{\sigma(q_{n})}}(t_{q_{n}})).$$
(A35)

We will now study each of these traces term by term. For ease of notation we will use the indices  $c = (c_1, ..., c_n)$ , where  $c_i := \mathbf{V}_{\sigma(i)}$ . Let  $c_S = \{a \in c | B_a(t) = \lambda_a, \lambda_a + A_a(t)\}$  be the set of indices that involve system parameters,  $\lambda_a$ , and  $c_E = \{a \in c | B_a(t) = A_a(t), \lambda_a + A_a(t)\}$  the set of indices that involve bath operators,  $A_a(t)$ . The trace in each of the terms above can be decomposed into a trace over the system and a trace over the environment:

$$\operatorname{Tr}(P_{O}P_{c_{q_{1}}}B_{c_{q_{1}}}(t_{q_{1}})...P_{c_{q_{l}}}B_{c_{q_{l}}}(t_{q_{l}})(P_{I}\otimes\gamma_{E})P_{c_{q_{l+1}}}B_{c_{q_{l+1}}}(t_{q_{l+1}})...P_{c_{q_{n}}}B_{c_{q_{n}}}(t_{q_{n}})) = \prod_{i|c_{q_{i}}\in c_{S}}\lambda_{c_{q_{i}}}\operatorname{Tr}(P_{O}\prod_{i=1}^{l}P_{c_{q_{i}}}P_{I}\prod_{i=l+1}^{n}P_{c_{q_{i}}})\operatorname{Tr}(\prod_{i=1|c_{q_{i}}\in c_{E}}A_{c_{q_{i}}}(t_{q_{i}})\gamma_{E}\prod_{i=l+1|c_{q_{i}}\in c_{E}}A_{c_{q_{i}}}(t_{q_{i}}))$$
(A36)

Here we used the notation that the products are ordered from left to right with increasing i. In the trace over the environment, we use the ciclicity of the trace to move those bath operators to the right of  $\gamma_E$  to its left. Note that in the general case with  $W \neq \mathbb{1}^{\otimes N}$  we obtain the same trace over the environment, and the trace over the system will have  $W(\cdot)W^{\dagger}$  applied to some product of Pauli strings, i.e. a Pauli string with a phase, which is mapped to a different Pauli string with the same support under W. Introducing the rolled over indices  $q' = (q_{l+1}, q_{l+2}, ..., q_n, q_1, q_2, ..., q_l)$  we can write the trace over the environment in terms of the kernels using Wick's theorem:

$$\operatorname{Tr}(\prod_{i=1|c_{q_{i}} \in c_{E}}^{l} A_{c_{q_{i}}}(t_{q_{i}}) \gamma_{E} \prod_{i=l+1|c_{q_{i}} \in c_{E}}^{n} A_{c_{q_{i}}}(t_{q_{i}})) = \operatorname{Tr}(\prod_{i=l+1|c_{q_{i}} \in c_{E}}^{n} A_{c_{q_{i}}}(t_{q_{i}}) \prod_{i=1|c_{q_{i}} \in c_{E}}^{l} A_{c_{q_{i}}}(t_{q_{i}}) \gamma_{E}),$$

$$= \operatorname{Tr}(\prod_{i=1|c_{q'_{i}} \in c_{E}}^{n} A_{c_{q'_{i}}}(t_{q'_{i}}) \gamma_{E}),$$

$$= \sum_{p \in \mathcal{P}_{2u_{c}}^{2}} \prod_{i=1,i_{2} \in c_{E}}^{n} K_{c_{q'_{i_{1}}} c_{q'_{i_{2}}}}(t_{q'_{i_{1}}} - t_{q'_{i_{2}}}).$$
(A38)

An odd number of bath operators makes the trace vanish, so we let  $2u_c = |c_E|$  be the number of bath operators, and thus  $u_c$  is the number of kernels. We introduce  $\mathcal{P}^2_{2u_c}$ , which consists of all partitions of  $\{1, ..., 2u_c\}$  into pairs  $p = \{p_1, p_2\}$ . For numerical computations it is better to use Gaussian integration by parts:

$$\operatorname{Tr}(A_{c_1}(t_1)...A_{c_{2u_c}}(t_{2u_c})\gamma_E) = \sum_{i=2}^{2u_c} \operatorname{Tr}(A_{c_1}(t_1)A_{c_i}(t_i)\gamma_E)\operatorname{Tr}(A_{c_2}(t_2)...\widehat{A_{c_i}(t_i)}...A_{c_{2u_c}}(t_{2u_c})\gamma_E), \tag{A39}$$

where the hat indicates that the term is missing. Since we know that for fixed  $P_{c_1}$  there's at most s  $P_{c_i}$  such that  $K_{c_1,c_i}(t_1-t_i) \neq 0$ , the sum involves only s terms. Applying this recursively we see that the total number of terms is  $s^{u_c} << |\mathcal{P}^2_{2u_c}| = \frac{(2u_c)!}{2^{u_c}u_c!}$ . Since we take n integrals, m derivatives of this expression, with  $1 \leq m \leq m$ , and then set m = 1 we obtain an expression of the form:

$$\partial_{t}^{m} \int_{0}^{2t} dt_{1} \dots \int_{0}^{t_{n-1}} dt_{n} \sum_{p \in \mathcal{P}_{2u_{c}}^{2}} \prod_{\substack{\{i_{1}, i_{2}\} \in p \\ i_{1} < i_{2}}} K_{c_{q'_{1}} c_{q'_{2}}} (t_{q'_{1}} - t_{q'_{12}}) \Big|_{t=0} = \sum_{p \in \mathcal{P}_{2u_{c}}^{2}} \sum_{z_{1} + \dots + z_{u_{c}} = m-n} \tilde{v}_{c,q}^{z,p} \prod_{j=1}^{u_{c}} \frac{1}{z_{j}!} K_{c_{q'_{p_{j,1}}} c_{q'_{p_{j,2}}}}^{(0)} (0).$$
(A40)

We ordered the partition p into ordered pairs of indices  $(p_{j,1}, p_{j,2})$  labeled by  $1 \le j \le u$ , with  $p_{j,1} < p_{j,2}$ . We collect combinatorial factors and signs arising from the integrals and derivatives into  $\tilde{v}_{c,q}^{z,p}$  and write  $v_{c,q}^{z,p} = \tilde{v}_{c,q}^{z,p} \prod_{j=1}^{u_c} (z_j!)^{-1}$ . Therefore, for  $m \ge 3$  the offset can be computed to be:

$$f_{1\otimes N,(O,I)}^{(m)} = \frac{1}{2^N} \sum_{n=3}^m (-i)^m \sum_{\mathbf{V} \in \mathcal{G}_n^O} \frac{1}{\mathbf{V}!} \sum_{\sigma \in S_n} \sum_{l=0}^n (-1)^{n-l} \sum_{q \in Q(n,l)} \prod_{i \mid c_{q_i} \in c_S} \lambda_{c_{q_i}} \operatorname{Tr}(P_O \prod_{i=1}^l P_{c_{q_i}} P_I \prod_{i=l+1}^n P_{c_{q_i}}) \times$$

$$\sum_{p \in \mathcal{P}_{2u,z_1}^2} \sum_{z_1 + \dots + z_{u_c} = m-n} v_{c,q}^{z,p} \prod_{j=1}^{u_c} K_{c_{q'_{p_{j,1}}}^{(z_j)} c_{q'_{p_{j,2}}}}^{(0)}(0),$$
(A41)

where recall that  $c_i := \mathbf{V}_{\sigma(i)}$ . Since  $n \ge 3$  we see that for the m-th derivative, the offset only contains kernel coefficients up to order m-3.

**Lemma 8.** Let  $H(t) = \sum_{a \in \mathcal{P}_S \cup \mathcal{P}_{SE}} B_a(t)$ , where  $B_a(t)$  can be  $\lambda_a, A_a(t)$ , or their sum, be a Hamiltonian such that each  $P_a B_a(t)$  might not commute with at most  $\mathfrak{d}$  other terms  $P_b B_b(s)$  with  $b \in \mathcal{P}_S \cup \mathcal{P}_{SE}$ . Then if the support of  $P_O$  is contained in the support of  $\mathcal{I}_{a,b}$ :

$$\frac{1}{2^{N}}\operatorname{Tr}([[P_{O}, H(t_{1})], ...H(t_{n})], P_{I} \otimes \gamma_{E})$$

$$= \frac{1}{2^{N}} \sum_{\mathbf{V} \in \mathcal{G}^{\mathcal{Q}}} \frac{1}{\mathbf{V}!} \sum_{\sigma \in S_{n}} \operatorname{Tr}(P_{O}, [P_{\mathbf{V}_{\sigma(1)}} B_{\mathbf{V}_{\sigma(1)}}(t_{1}), ..., [P_{\mathbf{V}_{\sigma(n)}} B_{\mathbf{V}_{\sigma(n)}}(t_{n}), P_{I} \otimes \gamma_{E}]]), \tag{A42}$$

where  $\mathcal{G}_n^O$  is a set of at most  $|\mathcal{G}_n^O| \leq (\mathfrak{d}_0 + 2)\mathfrak{d}(e\mathfrak{d})^n$  clusters of weight n.

*Proof.* We will follow the cluster expansion method outlined in [33, 115] to bound the number of terms in the sum. Let  $C_n$  be the set of all clusters of size n. Then, since we can view  $C_n$  as a collection of unordered indices in  $(\mathcal{P}_n \cup \mathcal{P}_{SE})^n$  and each ordered tuple on the left hand side will appear  $\mathbf{V}$ ! times in the sum over  $S_n$ , we obtain:

$$\frac{1}{2^{N}} \text{Tr}([[P_{O}, H(t_{1})], ..., H(t_{n})] P_{I} \otimes \gamma_{E}) = \frac{1}{2^{N}} \sum_{\mathbf{V} \in \mathcal{C}_{n}} \frac{1}{\mathbf{V}!} \sum_{\sigma \in S_{n}} \text{Tr}([[P_{O}, P_{\mathbf{V}_{\sigma(1)}} B_{\mathbf{V}_{\sigma(1)}}(t_{1})], ..., P_{\mathbf{V}_{\sigma(n)}} B_{\mathbf{V}_{\sigma(n)}}(t_{n})] P_{I} \otimes \gamma_{E}),$$
(A43)

Notice that for the sum above to vanish it is enough for one of the nested commutators to commute with all the terms that it is nested around. Prior works have made this precise and counted the number of non-vanishing terms in sums of this form [33]. To each cluster  $\mathbf{V}$  we associate a graph  $G_{\mathbf{V}}$  whose vertices are the elements a of  $\mathbf{V}$ , with  $\mu(a)$  vertices for each a, and an edge between vertices a, b if  $[P_aB_a(t), P_bB_b(t)] \neq 0$ . A cluster  $\mathbf{V}$  is said to be connected if  $G_{\mathbf{V}}$  is connected. Let  $\mathcal{G}_n$  be the set of connected clusters of size n. Consider the union of two clusters:  $\mathbf{W} = \mathbf{V}_1 \cup \mathbf{V}_2$ , satisfying  $\mu_{\mathbf{W}}(a) = \mu_{\mathbf{V}_1}(a) + \mu_{\mathbf{V}_2}(a)$ . We say that  $\mathbf{V}$  is completely connected to  $P_bB_a(t)$  if and only if  $G_{\mathbf{V} \cup \{(b,1)\}}$  is connected. Let the set of clusters of weight n that are connected to  $P_bB_b(t)$  be  $\mathcal{G}_n^b$ . In the following Lemma we collect some results from previous works that quantify the number of nonzero terms in the sum above.

**Lemma 9** (Adapted Proposition 3.6 [33], Lemma 1, 2 [115]). For any cluster  $\mathbf{V} \notin \mathcal{G}_n^b$  and distinct indices  $i_1, ..., i_n \in \{1, ..., n\}$ :

$$Tr([[P_O, P_{\mathbf{V}_{i_1}} B_{\mathbf{V}_{i_1}}(t_1)], ..., P_{\mathbf{V}_{i_n}} B_{\mathbf{V}_{i_n}}(t_n)] P_I \otimes \gamma_E) = 0,.$$
(A44)

Moreover,  $|\mathcal{G}_n^b| \leq (e\mathfrak{d})^n$ .

Therefore, in Eq. (A43) the only nonvanishing terms in the sum over  $C_n$  are those in  $\mathcal{G}_n^b$ , where  $P_bB_b(t)$  does not commute with with  $P_O$ . Since  $P_O$  is supported in  $\mathcal{I}_{a,b}$ , which overlaps with at most  $(\mathfrak{d}_0 + 2)(\mathfrak{d} + 1)$  Pauli strings in

 $\mathcal{P}_S \cup \mathcal{P}_{SE}$ , there are as many choices of  $P_b$ . Then, if we let  $\mathcal{G}_n^O := \bigcup_{[P_O, P_b B_b(t)] \neq 0} \mathcal{G}_n^b$ , the sum over  $\mathcal{C}_n$  is replaced by a sum over  $|\mathcal{G}_n^O| \leq (\mathfrak{d}_0 + 2)(\mathfrak{d} + 1)(e\mathfrak{d})^n$  terms:

$$(\mathbf{A43}) = \frac{1}{2^N} \sum_{\mathbf{V} \in \mathcal{G}_{\mathcal{O}}^{\mathcal{O}}} \frac{1}{\mathbf{V}!} \sum_{\sigma \in S_n} \text{Tr}([[P_O, P_{\mathbf{V}_{\sigma(1)}} B_{\mathbf{V}_{\sigma(1)}}(t_1)], ..., P_{\mathbf{V}_{\sigma(n)}} B_{\mathbf{V}_{\sigma(n)}}(t_n)] P_I \otimes \gamma_E), \tag{A45}$$

$$= \frac{1}{2^{N}} \sum_{\mathbf{V} \in \mathcal{G}_{\mathcal{O}}^{o}} \frac{1}{\mathbf{V}!} \sum_{\sigma \in S_{n}} \text{Tr}(P_{O}, [P_{\mathbf{V}_{\sigma(1)}} B_{\mathbf{V}_{\sigma(1)}}(t_{1}), ..., [P_{\mathbf{V}_{\sigma(n)}} B_{\mathbf{V}_{\sigma(n)}}(t_{n}), P_{I} \otimes \gamma_{E}]]). \tag{A46}$$

#### 4. Error analysis and sample complexity

We now estimate the error accumulated in correcting the contributions from the offset. Recall that we estimate the m-2-th kernel derivative  $K_{a,b}^{(m-2)}(0)$  from the m-derivative of the time traces  $B_{W,(O,I)}^{(m)}(0)$ . From Eq. (18) we obtain the precision at which we perform tomography on  $T_W^{(m)}$ :

$$\epsilon_{T,m} = \frac{1}{2^N} |\text{Tr}(P_O T_W^{(m)}(P_I)) - \text{Tr}(P_O \hat{T}_W^{(m)}(P_I))| = |B_{W,(O,I)}^{(m)}(0) - \hat{B}_{W,(O,I)}^{(m)}(0) + f_{W,(O,I)}^{(m)}(0) - \hat{f}_{W,(O,I)}^{(m)}| \le \epsilon_{S,m} + \epsilon_{f,m}, \tag{A47}$$

where  $\epsilon_{S,m}$ , m=0,...,M+2 is the precision in the derivative of the time trace  $B_{W,(O,I)}^{(m)}(0)$  obtained from the polynomial fit in Lemma 2 and  $\epsilon_{f,m}$  is the precision in reconstructing  $f_{W,(O,I)}^{(m)}$  in classical postprocessing, which we bound in Lemma 10. Moreover, Lemma 4 tells us that a precision  $\epsilon_{T,m}$  in the tomography observables leads to estimates of the real and imaginary parts of  $K_{a,b}^{(m-2)}(0)$  to the same precision:  $\epsilon_{K,m-2}=\epsilon_{T,m}$ . Therefore, we obtain:

$$\epsilon_{K,m-2} \le \frac{\epsilon_{S,M+2}}{d^{2(M+2-m)}} \frac{(2M+3)!!}{(2m+3)!!} + 3(1+\epsilon)^m (\mathfrak{d}_0+2)(\mathfrak{d}+1)(e\mathfrak{d})^m 2^{3m} m^{2(m+1)} \cdot \epsilon_{K,m-3}. \tag{A48}$$

Note that  $m \leq M + 2 \leq d$ , so the first term is less than  $\epsilon_{S,M+2}$ . This yields the following bound on the precision in the highest kernel derivative  $\epsilon_{K,M}$ :

$$\epsilon_{K,M} = e^{O(M^2 \log M)} (\epsilon_{S,M+2} + \epsilon_{K,0}). \tag{A49}$$

Recall that estimating  $K_{a,b}^{(0)}(0)$  requires computing the offset  $f_{\mathbb{1}^{\otimes N},(O,I)}^{(2)}$  from Eq.(A30):

$$f_{1^{\otimes N},(O,I)}^{(2)} = \frac{-4}{2^N} \text{Tr}([P_O, H_S][H_S, P_I]). \tag{A50}$$

Since  $\mathcal{I}_{\dashv, \downarrow}$  overlaps with at most  $(2 + \mathfrak{d}_{\circ})\mathfrak{d}$  terms in the Hamiltonian, we get that  $P_O, P_I$  can each commute with at most that many terms. Therefore,  $\epsilon_{K,0}$  is bounded by the precision in the Hamiltonian:

$$\epsilon_{K,0} \le \frac{\epsilon_{S,M+2}}{d^{2M}} \frac{(2M+3)!!}{7 \cdot 5 \cdot 3} + 4(\mathfrak{d}_0 + 2)^2 \mathfrak{d}^2 \epsilon_H$$
(A51)

Recall from Eq.(13) that the precision for Hamiltonian learning is related to the sample precision by:

$$\epsilon_H = \frac{1}{8} \epsilon_{S,1} \le \frac{\epsilon_{S,M+2}}{8d^{2(M+1)}} \frac{(2M+3)!!}{5 \cdot 3},\tag{A52}$$

so we finally obtain the bound on  $\epsilon_{K,M}$  depending only on sample precision:

$$\epsilon_{K,m} \leq e^{O(M^2 \log M)} \left( \epsilon_{S,M+2} + \frac{\epsilon_{S,M+2}}{d^{2M}} \frac{(2M+3)!!}{105} + 4(\mathfrak{d}_0 + 2)^2 \mathfrak{d}^2 \epsilon_H \right), 
\leq e^{O(M^2 \log M)} \left( 1 + \frac{(2M+3)!!}{105 \cdot d^{2M}} + \frac{(\mathfrak{d}_0 + 2)^2 \mathfrak{d}^2 (2M+3)!!}{30d^{2(M+1)}} \right) \epsilon_{S,M+2}, 
\leq O(e^{O(M^2 \log M)}) \epsilon_{S,M+2},$$
(A53)

where we used that, since  $M \leq d$ , the second and third summand decrease with d.

**Lemma 10.** Let  $\vec{x}$  be a vector of length  $M + 2\mathfrak{d}N(m-2)$ , containing the parameters of the Hamiltonian, as well as the real and imaginary parts of the kernel Taylor coefficients of degree 0, ..., m-3. Given estimates  $\hat{\vec{x}}$  satisfying  $||\hat{\vec{x}} - \vec{x}||_{\infty} < \epsilon$  we have:

$$|f_{\mathbb{1}^{\otimes N},(O,I)}^{(m)}(\vec{x}) - f_{\mathbb{1}^{\otimes N},(O,I)}^{(m)}(\hat{\vec{x}})| \le 3(1+\epsilon)^m (\mathfrak{d}_0 + 2)^{2m} \mathfrak{d}^{m(m+1)} 2^{3m} m^{m+2} \cdot \epsilon. \tag{A54}$$

The time complexity to compute the estimate is at most  $O((\mathfrak{d}_0+2)^m\mathfrak{d}^{\frac{m(m+1)}{2}}m^{\frac{3}{2}m+6}2^{-4m})$ .

*Proof.* Using the multivariate mean-value theorem, there is some  $s \in [0,1]$  such that:

$$f_{1\otimes N,(O,I)}^{(m)}(\vec{x}) - f_{1\otimes N,(O,I)}^{(m)}(\hat{\vec{x}}) = (\nabla_{\vec{x}} f_{1\otimes N,(O,I)}^{(m)}((1-s)\hat{\vec{x}} + s\vec{x})) \cdot (\vec{x} - \hat{\vec{x}}) \Rightarrow \tag{A55}$$

$$\Rightarrow |f_{\mathbb{1}^{\otimes N},(O,I)}^{(m)}(\vec{x}) - f_{\mathbb{1}^{\otimes N},(O,I)}^{(m)}(\hat{\vec{x}})| \le ||\nabla f_{\mathbb{1}^{\otimes N},(O,I)}^{(m)}((1-s)\hat{\vec{x}} + s\vec{x})||_1||\vec{x} - \hat{\vec{x}}||_{\infty}$$
(A56)

Where we used Hölder's inequality. As shown in Eq.(A41),  $f_{\mathbb{1}^{\otimes N},(O,I)}^{(m)}$  does not depend on all entries in  $\vec{x}$ , rather only those labelled by the index set  $\mathcal{G}_m^O$ , which is at most of size  $|\mathcal{G}_m^O| \leq (\mathfrak{d}_0+2)(\mathfrak{d}+1)(e\mathfrak{d})^m$ . Therefore, only as many entries in  $\nabla f_{\mathbb{1}^{\otimes N},(O,I)}^{(m)}$  are nonzero. We can then bound  $||\nabla f_{\mathbb{1}^{\otimes N},(O,I)}^{(m)}((1-d)\hat{\vec{x}}+s\vec{x})||_1 \leq (\mathfrak{d}_0+2)(\mathfrak{d}+1)(e\mathfrak{d})^m||\nabla f_{\mathbb{1}^{\otimes N},(O,I)}^{(m)}((1-d)\hat{\vec{x}}+s\vec{x})||_\infty$ . Using Lemma 11 this can be further bounded by:

$$|f_{\mathbb{1}^{\otimes N},(O,I)}^{(m)}(\vec{x}) - f_{\mathbb{1}^{\otimes N},(O,I)}^{(m)}(\hat{\vec{x}})| \le (\mathfrak{d}_0 + 2)(\mathfrak{d} + 1)(e\mathfrak{d})^m \cdot 3(1 + \epsilon)^m (\mathfrak{d}_0 + 2)(\mathfrak{d} + 1)(e\mathfrak{d})^m 2^{3m} m^{2(m+1)} \cdot \epsilon,$$

$$= 3(1 + \epsilon)^m (\mathfrak{d}_0 + 2)^2 (\mathfrak{d} + 1)^2 (e\mathfrak{d})^{2m} 2^{3m} m^{2(m+1)} \cdot \epsilon. \tag{A57}$$

In order to obtain a bound on the time to compute  $f_{1\otimes N,(O,I)}^{(m)}$  from Eq.(A41) we can follow a similar procedure to count the sums as done in Lemma 11. Taking into account the time required to compute  $v_{c,q}^{z,p}$  and the products of system parameters and kernels we obtain a time complexity  $O((\mathfrak{d}_0+2)(\mathfrak{d}+1)(e\mathfrak{d})^m m^{\frac{3}{2}m+6}2^{-4m})$ .

**Lemma 11.** Given the real value of the Hamiltonian parameters and the kernel's derivatives up to order m-3,  $\vec{x}$ , and an estimate  $\hat{\vec{x}}$  such that  $||\vec{x} - \hat{\vec{x}}||_{\infty} < \epsilon$ , the derivative  $\nabla f_{\mathbb{1}^{\otimes N},(O,I)}^{(m)}((1-s)\hat{\vec{x}} + s\vec{x})$  satisfies the following bound for all  $s \in [0,1]$ :

$$||\nabla f_{1\otimes N}^{(m)}|_{(O,I)}((1-s)\hat{\vec{x}}+s\vec{x})||_{\infty} \le 3(1+\epsilon)^{m}(\mathfrak{d}_{0}+2)(\mathfrak{d}+1)(e\mathfrak{d})^{m}2^{3m}m^{2(m+1)}. \tag{A58}$$

Proof. Let  $x_*$  be the coordinate that attains the maximum such that  $||\nabla f_{1\otimes N,(O,I)}^{(m)}((1-s)\hat{\vec{x}}+s\vec{x})||_{\infty} = |\partial_{x_*}f_{1\otimes N,(O,I)}^{(m)}((1-s)\hat{\vec{x}}+s\vec{x})|$ . Since  $f_{1\otimes N,(O,I)}^{(m)}(\vec{y})$  is a polynomial of degree at most m in every variable  $y_i$ , the derivative  $\partial_{x_*}f_{1\otimes N,(O,I)}^{(m)}(\vec{y})$  is a polynomial of degree at most m-1 in  $x_*$  and degree m in the other variables. Assume  $x_* = \text{Re}[K_{a,b}^{(u)}(0)]$  is a kernel parameter (the cases with the imaginary part and where it is a system parameter follow similarly). Using Eq.(A41) and the triangle inequality we can bound the derivative as:

$$|\partial_{x_*}(f_{1^{\otimes N},(O,I)}^{(m)}((1-s)\hat{\vec{x}}+s\vec{x}))| \leq \sum_{n=3}^m \sum_{\mathbf{V} \in \mathcal{G}_n^O} \frac{1}{\mathbf{V}!} \sum_{\sigma \in S_n} \sum_{l=0}^n \sum_{q \in Q(n,l)} \prod_{i \mid c_{q_i \in c_S}} |(1-s)\hat{\lambda}_{c_{q_i}} + s\lambda_{c_{q_i}}| \cdot \sum_{p \in \mathcal{P}_{2u_c}^2} \sum_{z_1 + \ldots + z_{u_c} = m-n} v_{c,q}^{z,p} \times v_{c,q}^{z,p} = v_{c,q}^{z,p} + v_{c,q}^{z,p} + v_{c,q}^{z,p} + v_{c,$$

$$d_{*,c,q}^{z,p} \cdot s|(1-s)\hat{x}_* + sx_*|_{d_{*,c,q}^{z,p}-1} \prod_{\substack{j=1\\c_{q'_{p_{j,1}}} \neq a, c_{q'_{p_{j,2}}} \neq b}}^{u_c} |(1-s)\hat{K}_{c_{q'_{p_{j,1}}} c_{q'_{p_{j,2}}}}^{(z_j)}(0) + sK_{c_{q'_{p_{j,1}}} c_{q'_{p_{j,2}}}}^{(z_j)}(0)|, \tag{A59}$$

where  $c_i = \mathbf{V}_{\sigma(i)}$ . Here we used  $|\frac{1}{2^N} \text{Tr}(PQ)| \leq 1$  for Pauli strings P, Q and let  $d_{*,c,q}^{z,p}$  be the degree of the kernel coefficient  $x_*$  in the product labeled by c, q, z, p. In order to bound the product of system coefficients we use  $|(1 - s)\hat{\lambda}_i + s\lambda_i| = |\lambda_i + (1 - s)(\hat{\lambda}_i - \lambda_i)| \leq 1 + \epsilon$ . We similarly bound  $|(1 - s)\hat{K}_{c_i,c_j}^{(z_j)} + sK_{c_i,c_j}^{(z_j)}| \leq \sqrt{2}(1 + \epsilon)$ , accounting for

the real and imaginary parts. So we obtain:

$$|\partial_{x_*}(f_{1\otimes N,(O,I)}^{(m)}((1-s)\hat{\vec{x}} + s\vec{x}))| \leq \sum_{n=3}^{m} \sum_{\mathbf{V} \in \mathcal{G}_n^O} \frac{1}{\mathbf{V}!} \sum_{\sigma \in S_n} \sum_{l=0}^{n} \sum_{q \in Q(n,l)} \sum_{p \in \mathcal{P}_{2u_c}^2} \sum_{z_1 + \dots + z_{u_c} = m-n} |v_{c,q}^{z,p}| d_{*,c,q}^{z,p}(\sqrt{2})^{u_c-1} (1+\epsilon)^{n-2u_c+u_c-1}$$
(A60)

We used that if the number of kernels is  $u_c$ , then the number of Hamiltonian parameters is  $n-2u_c$ . The highest degree of a Hamiltonian term  $d_{*,c,q}^{z,p}$  is  $n-2u_c \le n$  and the maximum number of kernels is  $\frac{n}{2}, \frac{n-1}{2}$  if n is even or odd, respectively, so  $u_c \le \lfloor \frac{n}{2} \rfloor$  we obtain:

$$|\partial_{x_*}(f_{1^{\otimes N},(O,I)}^{(m)}((1-s)\hat{\vec{x}} + s\vec{x}))| \le \sum_{n=3}^m n2^{\frac{1}{2}\lfloor \frac{n}{2} \rfloor} (1+\epsilon)^n \sum_{\mathbf{V} \in \mathcal{Q}_o^O} \frac{m!}{\mathbf{V}!} \sum_{l=0}^n \sum_{q \in Q(n,l)} \sum_{p \in \mathcal{P}_{2n}^2} \sum_{z_1 + \ldots + z_{uc} = m-n} |v_{c,q}^{z,p}|$$
(A61)

As discussed in Lemma 8,  $|\mathcal{G}_n^O| \leq (\mathfrak{d}_0 + 2)(\mathfrak{d} + 1)(e\mathfrak{d})^n$ . Since Q(n,l) entails choosing l distinct numbers among  $\{1,...,n\}$ ,  $|Q(n,l)| = \binom{n}{l}$ . We know that the number of partitions of  $\{1,...,2u_c\}$  grows as  $|\mathcal{P}_{2u_c}^2| = \frac{(2u_c)!}{2^{u_c}u_c!}$ . Since this is an increasing function of  $u_c \leq \lfloor \frac{n}{2} \rfloor$ , we can upper bound it by  $\frac{n!}{2^{\lfloor \frac{n}{2} \rfloor} \lfloor \frac{n}{2} \rfloor!}$ . From Lemma 12 we know that  $v_{c,q}^{z,p}$  is bounded by:

$$|v_{c,q}^{z,p}| \le \frac{2^m m!}{n! z_1! \dots z_u!},\tag{A62}$$

The sum over weak compositions can be simplified [83] using  $\sum_{z_1+...+z_{u_c}=m-n} \prod_{j=1}^{u_c} \frac{1}{z_j!} = \frac{u_c^{m-n}}{(m-n)!} \le \frac{\left(\frac{n}{2}\right)^{m-n}}{(m-n)!}$ . We will use  $\frac{1}{\mathbf{V}!} \le 1$  and bound:

$$|\partial_{x_*}(f_{\mathbb{1}^{\otimes N},(O,I)}^{(m)}((1-s)\hat{\vec{x}} + s\vec{x}))| \le m! \sum_{n=3}^m n2^{\frac{1}{2}\lfloor \frac{n}{2} \rfloor} (1+\epsilon)^n (\mathfrak{d}_0 + 2)(\mathfrak{d} + 1)(e\mathfrak{d})^n \times \\ \sum_{l=0}^n \binom{n}{l} \cdot \frac{n!}{2^{\lfloor \frac{n}{2} \rfloor} \lfloor \frac{l}{2} \rfloor!} \cdot \frac{2^m m!}{n!} \cdot 2^{n-m} \frac{n^{m-n}}{(m-n)!}, \tag{A63}$$

$$\leq (1+\epsilon)^m (\mathfrak{d}_0 + 2)(\mathfrak{d} + 1)(e\mathfrak{d})^m (m!)^2 \cdot 3 \cdot \sum_{n=3}^m 2^{2n} \frac{n^{m-n}}{\lfloor \frac{n}{2} \rfloor! (m-n)!}, \tag{A64}$$

where we used  $\sum_{l=0}^{n} {n \choose l} = 2^n$  and  $n \leq 3 \cdot 2^{\frac{1}{2} \lfloor \frac{n}{2} \rfloor}$  to simplify the factors of 2. We simplify the last sum using  ${m \choose n} \leq 2^m, m! \leq m^m$ :

$$(m!)^{2} \sum_{n=3}^{m} 2^{2n} \frac{n!}{\lfloor \frac{n}{2} \rfloor!} \frac{1}{n!(m-n)!} n^{m-n} \leq m! \cdot 2^{3m} \sum_{n=3}^{m} n^{\frac{n}{2}+1} n^{m-n} \leq m! \cdot 2^{3m} m^{m} \sum_{n=3}^{m} n^{1-\frac{n}{2}} \leq m! 2^{3m} m^{m+2} \leq 2^{3m} m^{2(m+1)}.$$

$$(A65)$$

**Lemma 12.** Let  $p_i(t) = \sum_{k=0}^{\infty} \frac{p_i^{(k)}(0)}{k!} t^k$  be Taylor series for i = 1, ..., u. Let  $s_1, ..., s_{2u} \in \{t_1, ..., t_n\}$  be distinct time variables. Then we can evaluate:

$$\partial_t^m \int_t^{2t} dt_1 \int_t^{t_1} dt_2 \dots \int_t^{t_{l-1}} dt_l \int_0^t dt_{l+1} \int_0^{t_{l+1}} dt_{l+2} \dots \int_0^{t_{n-1}} dt_n \prod_{i=1}^u p_i (s_{2i} - s_{2i-1}) \Big|_{t=0}$$

$$= \sum_{z_1 + \dots + z_n = m-n} v^{z,s} \prod_{i=1}^u p_i^{(z_i)}(0), \tag{A66}$$

where the coefficient  $v^{z,s}$ , with  $z_1 + ... + z_u = m - n \ge 0$  satisfies the upper bound:

$$|v^{z,s}| \le \frac{2^{m-n}m!}{(n-l)!l!z_1!...z_u!}.$$
(A67)

The coefficient  $v^{z,q}$  can be computed in time  $O(m^{l+1}n^2l^{3-l}u2^{4m-2n-2l})$ .

*Proof.* We use the absolute convergence of the Taylor series to rewrite their product as:

$$\prod_{i=1}^{u} p_{i}(s_{2i} - s_{2i-1}) = \prod_{i=1}^{u} \sum_{k=0}^{\infty} \frac{p_{i}^{(k)}(0)}{k!} (s_{2i} - s_{2i-1})^{k},$$

$$= \sum_{k=0}^{\infty} \sum_{z_{1} + \dots + z_{u} = k} \prod_{i=1}^{u} (s_{2i} - s_{2i-1})^{z_{i}} \prod_{i=1}^{u} \frac{p_{i}^{(z_{i})}(0)}{z_{i}!},$$

$$= \sum_{k=0}^{\infty} \sum_{z_{1} + \dots + z_{u} = k} \prod_{i=1}^{u} \sum_{j_{i} = 0}^{z_{i}} {z_{i} \choose j_{i}} s_{2i}^{j_{i}} (-s_{2i-1})^{z_{i} - j_{i}} \prod_{i=1}^{u} \frac{p_{i}^{(z_{i})}(0)}{z_{i}!}.$$
(A68)

After taking n integrals, we see that the k-th summand depends on time as  $t^{\sum_{i=1}^{u} z_i + n} = t^{k+n}$ . Therefore, if we take m > k + n derivatives, the k-th summand vanishes; while if we take m < k + n derivatives, the power of t will be  $\geq 1$ , so it vanishes by setting t = 0. Thus, only the summand k = m - n remains, so we obtain the following expression for  $v^{z,s}$ :

$$v^{z,s} = \partial_t^m \int_t^{2t} dt_1 \dots \int_t^{t_{l-1}} dt_l \int_0^t dt_{l+1} \dots \int_0^{t_{n-1}} dt_n \prod_{i=1}^u \sum_{j_i=0}^{z_i} {z_i \choose j_i} \frac{1}{z_i!} s_{2i}^{j_i} (-s_{2i-1})^{z_i-j_i} \Big|_{t=0},$$

$$= \sum_{j_1=0}^{z_1} \dots \sum_{j_n=0}^{z_n} (-1)^{\sum_i z_i - j_i} \prod_{i=1}^u {z_i \choose j_i} \frac{1}{z_i!} \partial_t^m \int_t^{2t} dt_1 \dots \int_t^{t_{l-1}} dt_l \int_0^t dt_{l+1} \dots \int_0^{t_{n-1}} dt_n \prod_{i=1}^u s_{2i}^{j_i} s_{2i-1}^{z_i-j_i} \Big|_{t=0}.$$
 (A69)

Using Lemma 13 and defining  $d_1, ..., d_n$  by  $\prod_{i=1}^u s_{2i}^{j_i} s_{2i-1}^{z_i-j_i} = \prod_{i=1}^n t_i^{d_i}$  we can write the integral as follows:

$$\int_{t}^{2t} dt_{1} \dots \int_{t}^{t_{l-1}} dt_{l} \prod_{i=1}^{l} t_{i}^{d_{i}} \int_{0}^{t} dt_{l+1} \dots \int_{0}^{t_{n-1}} dt_{n} \prod_{i=l+1}^{n} t_{i}^{d_{i}} = \int_{t}^{2t} dt_{1} \dots \int_{t}^{t_{l-1}} dt_{l} \prod_{i=1}^{l} t_{i}^{d_{i}} I_{n-l}(d^{[n-l]}, t),$$

$$= t^{n-l+||d^{[n-l]}||_{1}} \prod_{r=1}^{n-l} \frac{1}{r+||d^{[r]}||_{1}} \int_{t}^{2t} dt_{1} \dots \int_{t}^{t_{l-1}} dt_{l} \prod_{i=1}^{l} t_{i}^{d_{i}},$$
(A70)

and changing variables  $v_i = t_i - t, i = 1, ...l$  gives us:

$$\begin{split} &=t^{n-l+||d^{[n-l]}||_1}\prod_{r=1}^{n-l}\frac{1}{r+||d^{[r]}||_1}\int_0^t dv_1...\int_0^{v_{l-1}}dv_l\prod_{i=1}^l(v_i+t)^{d_i},\\ &=t^{n-l+||d^{[n-l]}||_1}\prod_{r=1}^{n-l}\frac{1}{r+||d^{[r]}||_1}\sum_{w_1=0}^{d_1}...\sum_{w_l=0}^{d_l}\binom{d_1}{w_1}...\binom{d_l}{w_l}t^{\sum_{i=1}^l d_i-w_i}\int_0^t dv_1...\int_0^{v_{l-1}}dv_l\prod_{i=1}^l v_i^{w_i}, \end{split} \tag{A71}$$

Using  $w = (w_1, ..., w_l)$ , the integrals are now  $I_l(w, t)$  and we can collect the powers of t:

$$t^{n-l+||d^{[n-l]}||_1} \cdot t^{\sum_{i=1}^l d_i - w_i} \cdot I_l(w,t) = t^{n-l+||d||_1 - ||w||_1} \cdot t^{l+||w||_1} \prod_{r=1}^l \frac{1}{r + ||w^{[r]}||_1} = t^{n+||d||_1} \prod_{r=1}^l \frac{1}{r + ||w^{[r]}||_1}. \tag{A72}$$

Recall that while we defined  $d_1, ..., d_n$  implicitly, we know that  $||d||_1 = ||z||_1 = m - n$ . After taking m derivatives with respect to t and setting t = 0 we obtain:

$$v^{z,s} = m! \sum_{j_1=0}^{z_1} \dots \sum_{j_u=0}^{z_u} (-1)^{\sum_{i=1}^u z_i - j_i} \prod_{i=1}^u {z_i \choose j_i} \frac{1}{z_i!} \prod_{r=1}^{n-l} \frac{1}{r + ||d^{[r]}||_1} \cdot \prod_{r=1}^l \frac{1}{r + ||w^{[r]}||_1}.$$
(A73)

We take the absolute value of this expression and upper bound it using the triangle inequality. The last two products can be upper bounded by the case d = (0, ..., 0):

$$\prod_{r=1}^{n-l} \frac{1}{r + ||d^{[r]}||_1} \cdot \prod_{r=1}^{l} \frac{1}{r + ||w^{[r]}||_1} \le \prod_{r=1}^{n-l} \frac{1}{r} \cdot \prod_{r=1}^{l} \frac{1}{r} \le \frac{1}{(n-l)!l!}.$$
(A74)

The remaining sums are upper bounded as follows, using that  $\sum_{i=1}^{u} z_i = m - n$ :

$$\sum_{j_1=0}^{z_1} \dots \sum_{j_n=0}^{z_n} \prod_{i=1}^u \binom{z_i}{j_i} \frac{1}{z_i!} = \prod_{i=1}^u \frac{\sum_{j_i=0}^{z_i} \binom{z_i}{j_i}}{z_i!} = \prod_{i=1}^u \frac{2^{z_i}}{z_i!} = \frac{2^{m-n}}{z_1! \dots z_u!}.$$
 (A75)

This yields the final bound:

$$|v^{z,s}| \le \frac{2^{m-n}m!}{(n-l)!l!z_1!...z_u!} \tag{A76}$$

From Eq. (A73) we can compute  $v^{z,s}$ . The factorial m! can be computed in time O(m). Similarly,  $\binom{d_1}{w_1}$  can be computed in time  $O(d_1)$  and using the arithmetic mean-geometric mean inequality yields that the product of binomial coefficients can be computed in time  $O(l \cdot (\frac{m-l}{l})^l)$ . The sum  $\sum_{i=1}^u z_i - j_i$  is computed in time O(u). The product  $\prod_{r=1}^l \frac{1}{r+||w^{(r)}||_1}$  can be computed in time  $O(l^2)$ . The number of terms in the sums over  $z_i$  can be bounded as above by  $4^{m-n}$ , and similarly the number of terms in sums over  $d_i$  is bounded by  $4^{m-l}$ . Therefore, we can compute  $v^{z,s}$  in time  $O(m^{l+1}n^2l^{3-l}u2^{4m-2n-2l})$ .

**Lemma 13.** Let  $d = (d_1, ..., d_n)$  be a vector of n nonnegative integers, and denote  $||d||_1 = \sum_{i=1}^n |d_i|$  the sum of its entries. Consider the integral

$$I_n(d,t) := \int_0^t dt_1 \dots \int_0^{t_{n-1}} dt_n \prod_{s=1}^n t_s^{d_s}.$$
 (A77)

Let  $d^{[r]}$  be the vector of the last r entries of d, then we have:

$$I_n(d,t) = t^{n+||d||_1} \prod_{r=1}^n \frac{1}{r+||d^{[r]}||_1}$$
(A78)

*Proof.* We use induction on n. Base case, n = 1:

$$I_1((d_1),t) = \int_0^t dt_1 t_1^{d_1} = \frac{1}{d_1 + 1} t^{d_1 + 1}.$$
 (A79)

Inductive step: we use the fact that  $(d_2, ..., d_n) = d^{[n-1]}$ .

$$I_n(d,t) = \int_0^t dt_1 t_1^{d_1} I_{n-1}(d^{[n-1]}, t_1) = \int_0^t dt_1 t_1^{d_1} t_1^{n-1+||d^{[n-1]}||_1} \prod_{r=1}^{n-1} \frac{1}{r+||(d^{[n-1]})^{[r]}||_1}, \tag{A80}$$

In the exponent of  $t_1$  we have  $d_1 + ||d^{[n-1]}||_1 = ||d||_1$ , and in the denominator we get  $(d^{[n-1]})^{[r]} = d^{[r]}$ , since  $r \le n-1$ . Therefore, using  $d = d^{[n]}$  we obtain:

$$I_n(d,t) = \frac{t^{n+||d||_1}}{n+||d||_1} \prod_{r=1}^{n-1} \frac{1}{r+||d^{[r]}||_1} = t^{n+||d||_1} \prod_{r=1}^n \frac{1}{r+||d^{[r]}||_1}.$$
 (A81)

## 5. Numerical observables

The N fermionic modes of the system and N modes of the bath are mapped to 4N Majorana modes, for i = 1, ..., N:

$$c_{2i-1} = a_i + a_i^{\dagger}, \qquad c_{2i} = i(a_i - a_i^{\dagger}).$$
 (A82)

$$c_{2(i+N)-1} = b_i + b_i^{\dagger}, \quad c_{2(i+N)} = i(b_i - b_i^{\dagger}).$$
 (A83)

We will compute time traces of the form  $O_{a,b,c,d}(t) = \text{Tr}(ic_ac_b\rho_{c,d}(t))$ , where  $\rho_{c,d}(0) = \frac{1}{2}(\mathbb{1} + ic_cc_d) \otimes \gamma$  and  $\gamma = (|0\rangle\langle 0|)^{\otimes 2N}$ . The time traces required to learn the derivatives of the kernel  $K_{i,j}(t)$  are:

If 
$$i \neq j : O_{2i-1,l,2j-1,l}$$
, where  $l \neq i,j$  (A84)

If 
$$i = j : O_{2i-1,l,2i-1,l}, O_{l,k,l,k}, O_{k,2i-1,k,2i-1}$$
 (A85)

where 
$$l, k \neq i, l \neq k$$
 (A86)

#### 6. Time evolution of local observables for constant time

In Appendix D of [34], they show that given a Lieb-Robinson bound on the Heisenberg evolution of local observables and a maximum evolution time  $t_{\text{max}}$ , the time evolution of local observables at constant times can be approximated by polynomials of controlled degree. In particular, in Proposition D.1 in [34] they show that for t = O(1), the expectation value of observables under the global evolution can be approximated by that of a local evolution. From this they derive their Theorem D.2, which also bounds the closeness of the derivatives. In order to obtain Lemma 1 we only need to change Proposition D.1 in their proof for an equivalent Lemma in the non-Markovian setting. In the non-Markovian case with unbounded system-environment Hamiltonian it is not expected that a Lieb-Robinson bound on operators holds, as there are initial system-environment states for which the Hamiltonian interaction terms are unbounded [70]. However, a Lieb-Robinson bound has been obtained for the initial states of the form  $\rho_S \otimes \gamma_E$  [70].

We introduce some notation to state this bound. Let a[l] be the set of sites that are within distance l of the Pauli string  $P_a$  and  $H_{a[l]} = \sum_{b:S_b \cap a[l] \neq \emptyset} \lambda_b P_b + \sum_{b:S_b \cap a[l] \neq \emptyset} P_b A_b(t)$ . Consider the Heisenberg evolution of an observable  $P_a$  under H(t) and the restricted Hamiltonian  $H_{a[l]}$ :  $P_a(t) = U^{\dagger}(t)P_aU(t), P_a(t;l) = U^{\dagger}_{a[l]}(t)P_aU_{a[l]}(t)$ , where  $U_{a[l]}(t) = \mathcal{T}\exp(-i\int_0^t H_{a[l]}(s)ds)$ . The physically relevant error for an initial state  $\rho(0)$  is  $\Delta_{P_a}(t;l) = |\mathrm{Tr}((P_a(t) - P_a(t;l))\rho(0))|$ , this measures the deviation in the observables for a specific initial state. In our case we only need to bound the error when the environment state is a Gaussian state.

**Lemma 14** (Adapted Proposition 1,[70]). Given  $P_a \subseteq \Lambda$ , a d-dimensional lattice, there exists  $v_{LR} > 0$  such that, for all initial states  $\rho_S \otimes \gamma_E$ , with  $\gamma_E$  a Gaussian state, the physically relevant error in the expectation value is bounded:

$$|\Delta_{P_a}(t;l)| = |\text{Tr}((P_a(t) - P_a(t;l))\rho_S \otimes \gamma_E)|,$$
  

$$\leq f(l) \exp(-l/a_0)(\exp(v_{LR}|t - t'|/a_0) - 1), \tag{A87}$$

where, for large l,  $f(l) \leq O(l^{d-1})$  and  $a_0 \leq k$ .

This Lieb-Robinson bound applies to our setting: the environment modes are geometrically local, can be described as a free bosonic field interacting only with the system and we assume that the kernel has finite memory in the sense of Eq. (9).

**Lemma 15** (Adapted Theorem E.1, Proposition E.1, Corollary E.1 [34], Theorem 1.2 [71]). Let p(t) be a polynomial of degree d defined on an interval [a,b] with  $a=d^{-2}$  and b=2+a,  $\epsilon_{S,M}>0$  a desired precision in the M-th derivative at 0. Then for  $\delta>0$ , sampling

$$O\left(d\log\left(\frac{d}{\delta}\right)\right),$$
 (A88)

i.i.d. points  $(x_i, y_i)$  from the Chebyshev measure on [a, b] satisfying

$$p(x_i) = y_i + w_i, |w_i| \le \epsilon_S = \epsilon_{S,M} \frac{(2M-1)!!}{3d^{2M}},$$
(A89)

for at least a fraction  $\alpha > \frac{1}{2}$  of the points is sufficient to obtain a polynomial  $\hat{p}$  satisfying

$$|p^{(m)}(0) - \hat{p}^{(m)}(0)| \le \epsilon_{S,M} \frac{(2M-1)!!}{d^{2M}} \frac{d^{2m}}{(2m-1)!!}, m = 0, 1, ..., M.$$
(A90)

*Proof.* Recall from Eq. E6 of [34] the following version of Markov brother's inequality: let  $q:[0,b]\to\mathbb{R}$  be a polynomial of degree d and let  $q^{(k)}$  be its k-th derivative. Then for  $0\leq a\leq b$ :

$$\max_{x \in [a,b]} \left| q^{(k)}(x) \right| \le \left| \frac{2}{b-a} \right|^k C_M(d,k) \max_{x \in [a,b]} |q(x)|, \text{ where } C_M(d,k) = \frac{d^2(d^2-1)(d^2-2^2)...(d^2-(k-1)^2)}{(2k-1)!!}, \quad (A91)$$

and  $(2k-1)!! = (2k-1)(2k-3) \cdot \dots \cdot 3 \cdot 1$  is the double factorial. By the Taylor expansion on  $x \in [0,a]$  we obtain:

$$q(x) = \sum_{k=0}^{d} q^{(k)}(a) \frac{(x-a)^k}{k!} \Rightarrow q^{(m)}(0) = \sum_{k=m}^{d} q^{(k)}(a) \frac{(-a)^{k-m}}{(k-m)!}.$$
 (A92)

We bound  $|q^{(m)}(0)|$  using the triangle inequality and the bound on  $|q^{(m)}(a)|$  from Eq.(A91):

$$\left| q^{(m)}(0) \right| \le \sum_{k=m}^{d} \left| q^{(k)}(a) \right| \frac{a^{k-m}}{(k-m)!} \le \sum_{k=m}^{d} \left| \frac{2}{b-a} \right|^{k} C_{M}(d,k) \max_{x \in [a,b]} |q(x)| \frac{a^{k-m}}{(k-m)!}. \tag{A93}$$

We use b = 2 + a,  $C_M(d, k) \le \frac{d^{2k}}{(2k-1)!!}$  and  $a = 1/d^2$ :

$$\left| q^{(m)}(0) \right| \le \max_{x \in [a,b]} |q(x)| \sum_{k=m}^{d} \frac{d^{2k}}{(2k-1)!!} \frac{d^{-2(k-m)}}{(k-m)!} \le \max_{x \in [a,b]} |q(x)| \frac{d^{2m+1}}{(2m-1)!!},\tag{A94}$$

where in the last inequality we bound the sum by the largest summand, k = m, times d.

By Theorem E.1 in [34], originally Corollary 1.5 in [103], for  $\delta > 0$ , sampling  $O(d \log(\frac{d}{\delta}))$  i.i.d. points  $(x_i, y_i)$  from the Chebyshev measure on [a, b] satisfying  $p(x_i) = y_i + w_i$ ,  $|w_i| \le \sigma$  for at least a fraction  $\alpha \ge 1/2$  of the points is sufficient to obtain a polynomial estimate  $\hat{p}$  satisfying  $\max_{x \in [a,b]} |p(x) - \hat{p}(x)| \le 3\sigma$  with success probability at least  $1 - \delta$ .

Now let  $q(x) = p(x) - \hat{p}(x)$ ,  $\epsilon_S := \sigma$ ,  $\epsilon_{S,M} := 3 \frac{d^{2M+1}}{(2M-1)!!} \epsilon_S$ , so we obtain:

$$|p^{(m)}(0) - \hat{p}^{(m)}(0)| \le 3\epsilon_S \frac{d^{2m+1}}{(2m-1)!!} = \epsilon_{S,M} \frac{(2M-1)!!}{d^{2M}} \frac{d^{2m}}{(2m-1)!!},\tag{A95}$$

and note that, since  $m \leq M \leq d$  we have

$$\frac{d^{2m}}{(2m-1)!!} \le \frac{d^{2M}}{(2M-1)!!},\tag{A96}$$

so all derivative estimates are at least as precise as the M-th derivative.

## Appendix B: Ensemble Hamiltonians

Recall that  $H_{\Lambda} = \sum_{a \in \mathcal{P}_S} \Lambda_a P_a$  is a geometrically local Hamiltonian on N spin- $\frac{1}{2}$  particles with Pauli strings  $P_a$  supported on at most k sites. The vector of coefficients  $\Lambda$  consists of jointly Gaussian random variables  $\Lambda = B \cdot Z + \lambda$ . We assume that the means are bounded  $|\lambda_a| \leq 1$  and the covariance matrix  $\Sigma = BB^T$  satisfies  $\Sigma_{aa} \leq 1$ . Given an observable O with  $||O|| \leq 1$ , let  $O_{\Lambda}(t)$  be its time evolution in the Heisenberg picture under  $H_{\Lambda}$  for time t and a specific draw of  $\Lambda$ .

## 1. Truncated series for local operators

Recall that, even though the measurement strategy is the same as in the non-Markovian case, we can not use the non-Markovian Lieb-Robinson bounds because the covariance matrix is not necessarily sparse and the kernels don't satisfy the finite memory condition. Moreover, we can not apply Hamiltonian Lieb-Robinson bounds, since the random variables  $\Lambda_a$  are not bounded and lead to unbounded Lieb-Robinson velocity. We show that the expected operator time evolution  $\mathbb{E}_{\Lambda}(O_{\Lambda}(t))$  can still be approximated by a low-degree polynomial.

**Lemma 16.** Let  $H_{\lambda} = \sum_{a=1}^{L} \Lambda_a P_a$  be a geometrically local Hamiltonian on N spin- $\frac{1}{2}$  particles with Pauli strings  $P_a$  supported on at most k sites.  $\{\Lambda_a\}_{a=1}^{L}$  are jointly Gaussian random variables with mean  $\{\lambda_a\}_{a=1}^{L}$  satisfying  $|\lambda_a| \leq 1$  and covariance matrix  $\Sigma$  satisfying  $|\Sigma_{aa}| \leq 1$  for i, j = 1, ..., L. Given an observable O with  $||O|| \leq 1$ , let  $\mathbb{E}_{\Lambda}(O_{\Lambda}(t))$  be its expected time evolution in the Heisenberg picture for time t. This has a convergent Taylor series for  $t \leq \left(\frac{6ec}{a} \max\left(1 + \sqrt{2}\sqrt{\log(\frac{2}{\epsilon}) + (d+2)\log(L)}, 10\right)\right)^{-1}$  and can be approximated to precision  $\epsilon > 0$  by a truncation of degree  $d \geq \log(\frac{1}{\epsilon})$ ,  $\mathbb{E}_{\Lambda,d}(O_{\Lambda}(t))$ :

$$||\mathbb{E}_{\Lambda}(O_{\Lambda}(t)) - \mathbb{E}_{\Lambda,d}(O_{\Lambda}(t))|| \le \epsilon. \tag{B1}$$

Asymptotically,  $t = O((\log(N) \cdot \log(1/\epsilon))^{-\frac{1}{2}}).$ 

Proof. Let  $O_{\Lambda}(t) = e^{itH_{\Lambda}}Oe^{-itH_{\Lambda}}$  be its time-evolution under  $H_{\Lambda}$  in the Heisenberg picture. Using the Baker-Campbell-Hausdorff formula and the remainder theorem, we can write the Taylor series for  $O_{\Lambda}(t) = e^{itH_{\Lambda}}Oe^{-itH_{\Lambda}}$  as a truncation to degree d,  $O_{d,\Lambda}(t)$ , and an integral remainder  $R_{d,\Lambda}(t)$ :

$$O_{\Lambda}(t) = O_{d,\Lambda}(t) + R_{d,\Lambda}(t), \text{ with } O_{d,\Lambda}(t) := \sum_{r=0}^{d} \frac{(it)^{r}}{r!} [(H_{\Lambda})^{r}, O], R_{d,\Lambda}(t) := \int_{0}^{t} O_{\Lambda}^{(d+1)}(\tau) \frac{(t-\tau)^{d}}{d!} d\tau.$$
 (B2)

Where  $O_{\Lambda}^{(d+1)}(t)$  is the d+1-th derivative of  $O_{\Lambda}(t)$ . This way we can find a truncated series for the expected operator  $\mathbb{E}_{\Lambda}(O_{\Lambda}(t)) = \mathbb{E}_{\Lambda}(O_{d,\Lambda}(t)) + \mathbb{E}_{\Lambda}(R_{d,\Lambda}(t))$ . Our goal is to obtain a bound on t such that the Taylor series converges and the truncation incurs an error at most  $\epsilon > 0$ :

$$||\mathbb{E}_{\Lambda}(O_{\Lambda}(t)) - \mathbb{E}_{\Lambda}(O_{d,\Lambda}(t))|| = ||\mathbb{E}_{\Lambda}(R_{d,\Lambda}(t))|| < \epsilon.$$
(B3)

We can bound the expectation of the remainder in two regimes: with high probability, all random variables  $\Lambda_b$  are bounded by a constant ( $|\Lambda_b| \leq \beta, \forall b$ , for some  $\beta \geq 1$ ). Then, since  $H_{\Lambda}$  is geometrically local we can use Lieb-Robinson bounds to bound the remainder. With low probability, some variable will be larger than  $\beta$  and the remainder will be large. Thus we need to pick  $\beta$  large enough that the probability is small to compensate. Let  $\beta > 0$  be a threshold and consider the event  $E: |\Lambda_b| \leq \beta, \forall b$ , i.e. the event that all  $|\Lambda_b|$  are bounded by  $\beta$ , and let the complementary event be  $E^c$ . Using Bayes' rule and the triangle inequality we obtain:

$$||\mathbb{E}_{\Lambda}(R_{d,\Lambda}(t))|| \le ||\mathbb{E}_{\Lambda}(R_{d,\Lambda}(t)|E)||\mathbb{P}(E) + ||\mathbb{E}_{\Lambda}(R_{d,\Lambda}(t)|E^c)||\mathbb{P}(E^c). \tag{B4}$$

We first bound the probabilities of a single  $\Lambda_b$  being outside the threshold  $\beta \geq 1$ . Recall that  $\Lambda_b \sim \mathcal{N}(\lambda_b, \Sigma_{bb})$ ,  $\Sigma_{bb} \leq 1, |\lambda_b| \leq 1, \forall b$ , so using the complementary error function bound  $\operatorname{erfc}(x) \leq e^{-x^2}$  we obtain:

$$\mathbb{P}(|\Lambda_b| > \beta) = \operatorname{erfc}\left(\frac{\beta - |\lambda_b|}{\sqrt{2\Sigma_{bb}}}\right) \le \exp\left(-\frac{(\beta - |\lambda_b|)^2}{2\Sigma_{bb}}\right) \le \exp\left(-\frac{(\beta - 1)^2}{2}\right). \tag{B5}$$

We can use the bound  $\mathbb{P}(E) \leq 1$ , while the probability of  $E^c$  is bounded by:

$$\mathbb{P}(E^c) = \mathbb{P}(\exists b : |\Lambda_b| > \beta) \le \sum_{b=1}^{L} \mathbb{P}(|\Lambda_b| > \beta) \le L e^{-\frac{(\beta-1)^2}{2}}.$$
 (B6)

From Lemmas 17, 18 we will consider  $\beta \geq 10$  and obtain the following bounds on the conditional expectations:

$$||E_{\Lambda}(R_{d,\Lambda}(t)|E)|| \le \frac{1}{1 - \frac{2ec\beta t}{a}} \left(\frac{2ec\beta t}{a}\right)^{d+1} \text{ if } t < \frac{a}{2ec\beta},\tag{B7}$$

$$||E_{\Lambda}(R_{d,\Lambda}(t)|E^c)|| \le \frac{(6tL)^{d+1}}{(d+1)\cdot d\cdot ...\cdot (\lfloor \frac{d}{2}\rfloor + 1)} \lfloor \frac{d+1}{2} \rfloor^{\frac{1}{2}}.$$
 (B8)

We find  $t, d, \beta$  such that both  $||E_{\Lambda}(R_{d,\Lambda}(t)|E)||$  and  $||E_{\Lambda}(R_{d,\Lambda}(t)|E)||L \cdot \exp(-\frac{(\beta-1)^2}{2})$  are smaller than  $\frac{\epsilon}{2}$ . We set  $t = \frac{1}{3} \frac{a}{2ec\beta} < \frac{a}{2ec\beta}$ , which is required for convergence in event E, and  $d \ge \log(\frac{1}{\epsilon})$ . This suffices to show  $||E_{\Lambda}(R_{d,\Lambda}(t)|E)|| \le \frac{\epsilon}{2}$ :

$$||E_{\Lambda}(R_{d,\Lambda}(t)|E)|| \le \frac{1}{1 - \frac{2ec\beta t}{a}} \left(\frac{2ec\beta t}{a}\right)^{d+1} \le \frac{1}{2}3^{-d} \le \frac{1}{2}e^{-d} = \frac{\epsilon}{2}.$$
 (B9)

To bound  $||E_{\Lambda}(R_{d,\Lambda}(t)|E^c)||\mathbb{P}(E^c)|$  it suffices to use  $\beta = \max(1 + \sqrt{2}\sqrt{\log(\frac{2}{\epsilon}) + (d+2)\log(L)}, 10)$ :

$$||E_{\Lambda}(R_{d,\Lambda}(t)|E^{c})||\mathbb{P}(E^{c})| < \frac{(6t)^{d+1}}{(d+1) \cdot d \cdot \dots \cdot (\lfloor \frac{d}{2} \rfloor + 1)} \left\lfloor \frac{d+1}{2} \right\rfloor^{\frac{1}{2}} \cdot (L^{d+2} \cdot e^{-\frac{1}{2}(\beta - 1)^{2}}) < \frac{\epsilon}{2}.$$
(B10)

The last product is  $\frac{\epsilon}{2}$  by the choice of  $\beta$ , and the rest is less than 1 by the choice of t. Thus for  $t \leq \left(\frac{6ec}{a} \max\left(1 + \sqrt{2}\sqrt{\log(\frac{2}{\epsilon}) + (d+2)\log(L)}, 10\right)\right)^{-1}$  the truncation converges and Eq. B3 holds.

Since the expected observable can be well approximated by a polynomial of low degree, we can find a polynomial fit to the time trace  $\frac{1}{2^N}\mathbb{E}_{\Lambda}(\text{Tr}(P_ae^{-itH_{\Lambda}}P_be^{itH_{\Lambda}}))$  using the analysis from the non-Markovian case. Since we need to do tomography on the second order of the Dyson series, i.e. two nested commutators, to obtain estimate  $\Sigma_{a,b}$ , the same measurement protocol as in the non-Markovian case allows us to obtain estimates for  $\lambda_a, \Sigma_{a,b}$ . By estimating  $\mathbb{E}_{\Lambda}(\Lambda_a\Lambda_b) = \Sigma_{a,b} + \lambda_a\lambda_b$  and  $\lambda_a, \lambda_b$  to precision  $\frac{\epsilon}{3}$ , we can learn  $\Sigma_{a,b}$  to precision  $\epsilon$ :

$$|\hat{\Sigma}_{a,b} - \Sigma_{a,b}| = |\widehat{\lambda_a \lambda_b} - \mathbb{E}_{\Lambda}(\Lambda_a \Lambda_b) - \hat{\lambda}_a \hat{\lambda}_b + \lambda_a \lambda_b| \le |\widehat{\lambda_a \lambda_b} - \mathbb{E}_{\Lambda}(\Lambda_a \Lambda_b)| + |\hat{\lambda}_a \hat{\lambda}_b - \lambda_a \lambda_b| \le \frac{\epsilon}{3} + \frac{2\epsilon}{3} = \epsilon$$
(B11)

We used the following bound for the second term:

$$|\hat{\lambda}_a \hat{\lambda}_b - \lambda_a \lambda_b| = |\hat{\lambda}_a \lambda_b - \hat{\lambda}_a \lambda_b + \hat{\lambda}_a \hat{\lambda}_b - \lambda_a \lambda_b| = |\hat{\lambda}_a (\lambda_b - \hat{\lambda}_b) + \lambda_b (\lambda_a - \hat{\lambda}_a)| \stackrel{(1)}{\leq} |\hat{\lambda}_a| \frac{\epsilon}{3} + |\lambda_b| \frac{\epsilon}{3} \stackrel{(2)}{\leq} \frac{2\epsilon}{3}$$
(B12)

In (1) we used the triangle inequality and in (2) we used  $|\lambda_b|, |\hat{\lambda}_a| \leq 1$ .

Therefore, our total sample complexity is the same as for the non-Markovian case, except that the overhead due to the offset is only  $\epsilon \mapsto \frac{\epsilon}{3}$ :

$$O\left(\frac{2 \cdot 9((\mathfrak{d}_0 + 2)(s + \mathfrak{d})\mathfrak{d}^2 + 1)}{\epsilon_S^2} \cdot \log\left(\frac{L \cdot 2 \cdot 3^{2k_{SE} + \mathfrak{d}_0 - 2}}{\delta}\right)\right). \tag{B13}$$

And since we only need to estimate up to the 2-nd derivative of the time trace using Eq. (A50):

$$\epsilon_{K,0} \le \left(\frac{1}{d^4} + \frac{4(\mathfrak{d}_0 + 2)^2 \mathfrak{d}^2}{8d^6}\right) \epsilon_{S,4} = \left(1 + \frac{4(\mathfrak{d}_0 + 2)^2 \mathfrak{d}^2}{8d^2}\right) 3\epsilon_S.$$
 (B14)

Finally, in order to estimate the covariance to precision  $\epsilon_{K,0}$  we use a number of samples:

$$O\left(\frac{2\cdot 9^2((\mathfrak{d}_0+2)(s+\mathfrak{d})\mathfrak{d}^2+1)\left(1+\frac{4(\mathfrak{d}_0+2)^2\mathfrak{d}^2}{8d^2}\right)^2}{2\epsilon_{K,0}^2}\cdot \log\left(\frac{L\cdot 2\cdot 3^{2k_{SE}+\mathfrak{d}_0-2}}{\delta}\right)\right). \tag{B15}$$

**Lemma 17.** In event E all the random variables satisfy  $|\Lambda_a| \leq \beta$ . For time  $t < \frac{a}{2ec\beta}$ , where a, c are constants from the Lieb-Robinson bound, the Taylor series for  $O_{\Lambda}(t)$  converges. A truncation to degree d,  $O_{\Lambda,d}(t)$  will yield an error:

$$||\mathbb{E}_{\Lambda}(R_{d,\Lambda}(t)|E)|| \le \frac{1}{1 - \frac{2ec\beta t}{a}} \left(\frac{2ec\beta t}{a}\right)^{d+1}.$$
(B16)

*Proof.* Since  $H_{\Lambda}$  is geometrically local and all variables are bounded, the following Lieb-Robinson bound holds:

**Theorem 1.** (Lieb-Robinson bound) Let A, B be observables acting on subsystems X, Y. Their commutator is bounded:

$$||[A, B]|| \le 2||A||||B||c \cdot exp(-a \cdot d(X, Y)),$$
 (B17)

where a, c are constants and d(X,Y) is the distance between subsystems X,Y.

The single-commutator Lieb-Robinson bound leads to the following Lieb-Robinson bound on nested commutators:

$$\sum_{a_1,\dots,a_d} ||[P_{a_1},\dots[P_{a_d},A]]|| \le \sum_{a_1,\dots,a_d} (2c)^d ||A|| \min_{a_j} (e^{-a \cdot d(P_{a_j},A)}) \le (2c)^d ||A|| \sum_{a_1,\dots,a_d} (e^{-a \cdot d(P_{a_1},A)} \cdot \dots \cdot e^{-a \cdot d(P_{a_d},A)})^{\frac{1}{d}},$$
(B18)

$$= (2c)^{d} ||A|| \left( \sum_{a_1} e^{-\frac{a}{d} \cdot d(P_{a_1}, A)} \right) \cdot \dots \cdot \left( \sum_{a_d} e^{-\frac{a}{d} \cdot d(P_{a_d}, A)} \right) \stackrel{(1)}{\leq} (2c)^{d} ||A|| \left( \frac{d}{a} \right)^{d} = \left( \frac{2c}{a} \right)^{d} d^{d} ||A||. \tag{B19}$$

In the first line we used that the harmonic mean upper bounds the minimum function,  $\min(x_1, ..., x_d) \leq (x_1 \cdot ... \cdot x_d)^{\frac{1}{d}}$ , and in (1) we used Lemma 12 from [102].

We can finally bound  $||\mathbb{E}_{\Lambda}(R_{d,\Lambda}(t)|E)||$  using that  $\mathbb{E}_{\Lambda}(|\prod_{j=1}^r \Lambda_{a_j}|||\Lambda_b| \leq \beta, \forall b) \leq \beta^r$ :

$$R_{d,\Lambda}(t) = O_{\Lambda}(t) - O_{d,\Lambda}(t) = \sum_{r=m+1}^{\infty} \frac{(it)^r}{r!} [(H)^r, O] \Rightarrow$$
(B20)

$$\Rightarrow ||\mathbb{E}_{\Lambda}(R_{d,\Lambda}(t)|E)|| = \left|\left|\mathbb{E}_{\Lambda}\left(\sum_{r=m+1}^{\infty} \frac{(it)^r}{r!} \sum_{i_1,\dots,i_r} \Lambda_{i_1} \dots \Lambda_{i_r}[P_{i_r},\dots[P_{i_1},O]\dots]\right|E\right)\right|\right| \leq$$
(B21)

$$\leq \sum_{r=m+1}^{\infty} \frac{t^r}{r!} \sum_{i_1,...,i_r} |\mathbb{E}_{\Lambda}(\Lambda_{i_1}...\Lambda_{i_r}|E)| \cdot ||[P_{i_r},...[P_{i_1},O]...]|| \leq \sum_{r=m+1}^{\infty} \frac{t^r}{r!} \beta^r \sum_{i_1,...,i_r} ||[P_{i_r},...[P_{i_1},O]...]|| \leq (B22)$$

$$\leq \sum_{r=m+1}^{\infty} \frac{t^r}{r!} \beta^r \left(\frac{2c}{a}\right)^r r^r ||O|| < \sum_{r=m+1}^{\infty} \left(\frac{2ec\beta t}{a}\right)^r, \text{ converges if } t < \frac{a}{2ec\beta}$$
 (B23)

In the last line we used Eq.(B19) and  $\frac{r^r}{r!} < e^r$ . When the last expression converges,  $||\mathbb{E}_{\Lambda}(R_{d,\Lambda}(t)|E)|| \le \frac{1}{1-\frac{2ec\beta t}{a}}(\frac{2ec\beta t}{a})^{m+1}$ .

**Lemma 18.** In event  $E^c$  there is at least one of the random variables  $\Lambda$  that is larger than  $\beta$  in norm. Suppose that  $\beta \geq 12$ , then a truncation to degree d of the Heisenberg evolution  $O_{\Lambda}(t)$  will yield an error:

$$||\mathbb{E}(R_{d,\Lambda}(t)|E^c)|| \le \frac{(6tL)^{d+1}||O||}{(d+1)\cdot d\cdot \dots \cdot (|\frac{d}{2}|+1)} \left\lfloor \frac{d+1}{2} \right\rfloor^{\frac{1}{2}}.$$
 (B24)

*Proof.* Recall that  $R_{d,\Lambda}(t) = \int_0^t O_{\Lambda}^{(d+1)}(\tau) \frac{(t-\tau)^d}{d!} d\tau$  is the integral remainder of the truncation of the Heisenberg time evolution  $O_{\Lambda}(t)$  to degree d. By the triangle inequality we get:

$$||\mathbb{E}_{\Lambda}(R_{d,\Lambda}(t)|E^c)| \le \int_0^t E_{\Lambda}(||O_{\Lambda}^{(d+1)}(\tau)|||E^c) \frac{(t-\tau)^d}{d!} d\tau.$$
 (B25)

We first bound  $||O_{\Lambda}^{(d+1)}(t)||$  using  $O_{\Lambda}^{(d+1)}(t) = i^{d+1}[(H_{\Lambda})^{d+1}, O_{\Lambda}(t)]$ :

$$||O_{\Lambda}^{(d+1)}(t)|| = ||i^{d+1}[(H_{\Lambda})^{d+1}, O_{\Lambda}(t)]|| = \left| \left| \sum_{i_{1}, \dots, i_{d+1}} \Lambda_{i_{1}} \dots \Lambda_{i_{d+1}} [P_{i_{d+1}}, \dots [P_{i_{1}}, O_{\Lambda}(t)] \dots] \right| \right|,$$

$$\leq \sum_{i_{1}, \dots, i_{d+1}} |\Lambda_{i_{1}} \dots \Lambda_{i_{d+1}}| \cdot ||[P_{i_{d+1}}, \dots [P_{i_{1}}, O_{\Lambda}(t)] \dots]||,$$

$$\leq \sum_{i_{1}, \dots, i_{d+1}} |\Lambda_{i_{1}} \dots \Lambda_{i_{d+1}}| \cdot 2^{d+1} ||O_{\Lambda}(t)|| = 2^{d+1} ||O|| \sum_{i_{1}, \dots, i_{d+1}} |\Lambda_{i_{1}} \dots \Lambda_{i_{d+1}}|.$$
(B26)

We upper bound the commutators by  $2^{d+1}$ , since  $||P_a|| = 1$ , and use that  $||O_{\Lambda}(t)|| = ||O||$  for all  $\Lambda, t$  by unitarity. We now bound the expectation of the random variables. Using Hölder's inequality we obtain the upper bound:

$$\mathbb{E}(|\Lambda_{i_1}...\Lambda_{i_{d+1}}||E^c) \le \prod_{k=1}^{d+1} \mathbb{E}(|\Lambda_{i_k}|^{d+1}|E^c)^{\frac{1}{d+1}} \le \max_k \mathbb{E}(|\Lambda_{i_k}|^{d+1}|E^c). \tag{B27}$$

In the event  $E^c$  there is at least one random variable  $\Lambda_a$  satisfying  $|\Lambda_a| \geq \beta$ . We now consider event F, where all of them satisfy it:  $|\Lambda_a| > \beta$  for all a.

$$\mathbb{E}(|\Lambda_{i_k}|^{d+1}|E^c) = \mathbb{E}(|\Lambda_{i_k}|^{d+1}|F)P(F|E^c) + \mathbb{E}(|\Lambda_{i_k}|^{d+1}|F^c)P(F^c|E^c),$$

$$\leq \mathbb{E}(|\Lambda_{i_k}|^{d+1}||\Lambda_{i_k}| > \beta)P(F|E^c) + \beta^{d+1}P(F^c|E^c). \tag{B28}$$

The right term drops out, since  $P(F^c|E^c) = 0$  because  $F^c \cap E^c = \emptyset$ : a random variable can't be both less than or equal to  $\beta$  and strictly larger than  $\beta$ . We bound the left term using that the marginal probability distribution of  $\Lambda_{i_k}$  is  $\mathcal{N}(\lambda_{i_k}, \Sigma_{i_k i_k})$ , with  $|\lambda_{i_k}| \leq 1$ ,  $\Sigma_{i_k, i_k} \leq 1$  and Lemma 20:

$$\mathbb{E}(|\Lambda_{i_k}|^{d+1}||\Lambda_{i_k}| > \beta) \le 2\frac{((\beta+1)^2+1)}{\beta^2-1} \exp\left(-\frac{(\beta-1)^2}{4} + 2\beta\right) \left\lfloor \frac{d+1}{2} \right\rfloor^{\frac{1}{2}} \left\lfloor \frac{d}{2} \right\rfloor! \cdot 3^{d+1}. \tag{B29}$$

Using  $P(F|E^c) \leq 1$  and considering  $\beta \geq 10$  we can simplify the dependence on  $\beta$ :

$$\mathbb{E}(|\Lambda_{i_1}...\Lambda_{i_{d+1}}|E^c) \le 2\left\lfloor \frac{d+1}{2} \right\rfloor^{\frac{1}{2}} \left\lfloor \frac{d}{2} \right\rfloor! \cdot 3^{d+1}.$$
(B30)

We can now perform the integral above:

$$||\mathbb{E}_{\Lambda}(R_{d,\Lambda}(t)|E^{c})|| \leq \int_{0}^{t} E_{\Lambda}(||O_{\Lambda}^{(d+1)}(\tau)|||E^{c}) \frac{(t-\tau)^{d}}{d!} d\tau,$$

$$\leq \int_{0}^{t} 2^{d+1}||O|| \sum_{i_{1},...,i_{d+1}} \mathbb{E}_{\Lambda}(|\Lambda_{i_{1}}...\Lambda_{i_{d+1}}||E^{c}) \frac{(t-\tau)^{d}}{d!} d\tau = \frac{(2t)^{d+1}}{(d+1)!}||O|| \sum_{i_{1},...,i_{d+1}} \mathbb{E}_{\Lambda}(|\Lambda_{i_{1}}...\Lambda_{i_{d+1}}||E^{c}),$$

$$\leq \frac{(2t)^{d+1}}{(d+1)!}||O||L^{d+1} \left\lfloor \frac{d+1}{2} \right\rfloor^{\frac{1}{2}} \left\lfloor \frac{d}{2} \right\rfloor! \cdot 3^{d+1} \leq \frac{(6tL)^{d+1}||O||}{(d+1) \cdot d \cdot ... \cdot (\left\lfloor \frac{d}{2} \right\rfloor + 1)} \left\lfloor \frac{d+1}{2} \right\rfloor^{\frac{1}{2}}$$
(B31)

In the last line we used that there are  $L^{d+1}$  terms in the sum in the second line and Eq.(B30).

**Lemma 19.** Let  $Z \sim \mathcal{N}(\mu, \sigma^2)$  be a Gaussian random variable,  $m \geq 1$  an integer,  $\beta \geq 1$  a threshold. Then:

$$\mathbb{E}(|Z|^m||Z| \ge \beta) \le 2\frac{((\beta + |\mu|)^2 + \sigma^2)\sigma^2}{\beta^2 - |\mu|^2} \exp\left(-\frac{(\beta - |\mu|)^2}{4\sigma^2} + \frac{2\beta|\mu|}{\sigma^2}\right) \left\lfloor \frac{m}{2} \right\rfloor^{\frac{1}{2}} \left\lfloor \frac{m-1}{2} \right\rfloor ! (2\sigma + |\mu|)^m. \tag{B32}$$

*Proof.* Notice that we can write  $Z = X + \mu$ , where  $X \sim \mathcal{N}(0, \sigma^2)$ :

$$\mathbb{E}(|Z|^m||Z| \ge \beta) \le \sum_{n=0}^m \binom{m}{n} |\mu|^{m-n} \mathbb{E}(|X|^n||Z| \ge \beta) = \sum_{n=0}^m \binom{m}{n} |\mu|^{m-n} \mathbb{E}(|X|^n||X| \ge \beta - |\mu|) \frac{\mathbb{P}(|X| \ge \beta - |\mu|)}{\mathbb{P}(|Z| \ge \beta)},$$
(B33)

where we used the definition of conditional expectation in the last step. We will bound the fraction using the two-sided bounds on the Gaussian tail given by the Mills ratio:

$$\frac{t}{t^2 + \sigma^2} \frac{1}{\sqrt{2\pi} \sigma} e^{-\frac{t^2}{2\sigma^2}} \le \mathbb{P}(|X| \ge t) \le \frac{2\sigma}{\sqrt{2\pi} t} e^{-\frac{t^2}{2\sigma^2}}, \qquad t > 0.$$
 (B34)

Since  $\mathbb{P}(|Z| \geq \beta) \geq \mathbb{P}(|X| - |\mu| \geq \beta)$  by the triangle inequality, it suffices to bound:

$$\frac{\mathbb{P}(|X| \ge \beta - |\mu|)}{\mathbb{P}(|X| \ge \beta + |\mu|)} \le 2 \frac{((\beta + |\mu|)^2 + \sigma^2)\sigma^2}{\beta^2 - |\mu|^2} \exp\left(\frac{(\beta + |\mu|)^2 - (\beta - |\mu|)^2}{2\sigma^2}\right) = 2 \frac{((\beta + |\mu|)^2 + \sigma^2)\sigma^2}{\beta^2 - |\mu|^2} \exp\left(\frac{2\beta|\mu|}{\sigma^2}\right). \quad (B35)$$

We can now use Lemma 20 to bound the expectation value:

$$\mathbb{E}(|X|^n||X| \ge \beta - |\mu|) \le \left\lfloor \frac{n}{2} \right\rfloor^{\frac{1}{2}} \left\lfloor \frac{n-1}{2} \right\rfloor ! (2\sigma)^n e^{-\frac{(\beta - |\mu|)^2}{4\sigma^2}}.$$
 (B36)

Finally, this yields the result:

$$\mathbb{E}(|Z|^{m}||Z| \ge \beta) \le 2\frac{((\beta + |\mu|)^{2} + \sigma^{2})\sigma^{2}}{\beta^{2} - |\mu|^{2}} \exp\left(\frac{2\beta|\mu|}{\sigma^{2}}\right) \exp\left(-\frac{(\beta - |\mu|)^{2}}{4\sigma^{2}}\right) \sum_{n=0}^{m} {m \choose n} |\mu|^{m-n} \left\lfloor \frac{n}{2} \right\rfloor^{\frac{1}{2}} \left\lfloor \frac{n-1}{2} \right\rfloor ! (2\sigma)^{n}, \tag{B37}$$

$$\leq 2\frac{((\beta+|\mu|)^2+\sigma^2)\sigma^2}{\beta^2-|\mu|^2}\exp\left(\frac{2\beta|\mu|}{\sigma^2}\right)\exp\left(-\frac{(\beta-|\mu|)^2}{4\sigma^2}\right)\left\lfloor\frac{m}{2}\right\rfloor^{\frac{1}{2}}\left\lfloor\frac{m-1}{2}\right\rfloor!(2\sigma+|\mu|)^m. \tag{B38}$$

**Lemma 20.** Let  $Z \sim \mathcal{N}(0, \sigma^2)$  be a Gaussian random variable,  $m \geq 1$  an integer,  $\beta \geq 0$  a threshold. Then:

$$\mathbb{E}(|Z|^m||Z| \ge \beta) \le \left\lfloor \frac{m}{2} \right\rfloor^{\frac{1}{2}} \left\lfloor \frac{m-1}{2} \right\rfloor ! (2\sigma)^m e^{-\frac{\beta^2}{4\sigma^2}}$$
(B39)

*Proof.* We write the conditional moment in terms of the incomplete Gamma function:

$$\mathbb{E}(|Z|^m||Z| \ge \beta) = \int_{-\infty}^{\infty} |z|^m \mathbb{P}(z||z| \ge \beta) dz = 2 \int_{\beta}^{\infty} z^m \mathbb{P}(z) dz = 2 \int_{\beta}^{\infty} z^m \frac{e^{-\frac{z^2}{2\sigma^2}}}{\sqrt{2\pi\sigma^2}} dz =$$
(B40)

$$= \frac{2 \cdot 2^{\frac{m-1}{2}} \cdot \sigma^m}{\sqrt{2\pi}} \int_{\frac{\beta^2}{2\sigma^2}}^{\infty} t^{\frac{m-1}{2}} e^{-t} dt = \frac{2^{\frac{m}{2}} \sigma^m}{\sqrt{\pi}} \Gamma\left(\frac{m+1}{2}, \frac{\beta^2}{2\sigma^2}\right)$$
(B41)

In the second line we used the change of variables  $z = \sigma(2t)^{\frac{1}{2}}, dz = \sigma(2t)^{\frac{-1}{2}}dt$  and the definition of the upper incomplete Gamma function  $\Gamma(s,x) = \int_x^\infty t^{s-1}e^{-t}dt$ . For positive integer s we have:

$$\Gamma(s,x) = (s-1)!e^{-x} \sum_{k=0}^{s-1} \frac{x^k}{k!} \le (s-1)!e^{-x} 2^{s-1} e^{\frac{x}{2}} = 2^{s-1} (s-1)!e^{-\frac{x}{2}}$$
(B42)

If m is even, then  $s=\frac{m+1}{2}$  is not an integer. Let s=k+r be the decomposition of a real number s into its integer, k, and decimal,  $0 \le r < 1$ , parts. The ratio  $\frac{\Gamma(s,x)}{\Gamma(s)}$  is monotonically increasing in s for s>0, x>0 [112], so  $\Gamma(k+r,x) \le \frac{\Gamma(k+r)}{\Gamma(k+1)}\Gamma(k+1,x)$  and we can use Gautschi's inequality  $\frac{\Gamma(k+r)}{\Gamma(k+1)} < k^{r-1}$  to obtain the bound  $\Gamma(r+d,x) < r^{d-1}\Gamma(r+1,x)$ . Using  $s=\frac{m+1}{2}$  with m even,  $k=\frac{m}{2}, r=\frac{1}{2}$  and we get  $\Gamma(\frac{m+1}{2},x) < (\frac{m}{2})^{-\frac{1}{2}}\Gamma(\frac{m}{2}+1,x)$ . Therefore, we obtain the bounds:

$$m \text{ odd}: \mathbb{E}(Z^m || Z| \ge \beta) = \frac{2^{\frac{m}{2}} \sigma^m}{\sqrt{\pi}} \Gamma\left(\frac{m+1}{2}, \frac{\beta^2}{2\sigma^2}\right) \le \frac{2^{\frac{m}{2}} \sigma^m}{\sqrt{\pi}} \left(\frac{m-1}{2}\right) ! 2^{\frac{m-1}{2}} e^{-\frac{\beta^2}{4\sigma^2}} < (2\sigma)^m \left(\frac{m-1}{2}\right) ! e^{-\frac{\beta^2}{4\sigma^2}}$$

$$m \text{ even}: \mathbb{E}(Z^m || Z| \ge \beta) < \frac{2^{\frac{m}{2}} \sigma^m}{\sqrt{\pi}} \left(\frac{m}{2}\right)^{-\frac{1}{2}} \Gamma\left(\frac{m}{2} + 1, \frac{\beta^2}{2\sigma^2}\right) \le \frac{2^{\frac{m}{2}} \sigma^m}{\sqrt{\pi}} \left(\frac{m}{2}\right)^{-\frac{1}{2}} \left(\frac{m}{2}\right) ! 2^{\frac{m}{2}} e^{-\frac{\beta^2}{4\sigma^2}} < (2\sigma)^m \left(\frac{m}{2}\right)^{\frac{1}{2}} \left(\frac{m}{2} - 1\right) ! e^{-\frac{\beta^2}{4\sigma^2}}$$

$$(B44)$$

Using the floor function we see that  $\lfloor \frac{m-1}{2} \rfloor$  is  $\frac{m-1}{2}$  for m odd and  $\frac{m}{2}-1$  for m even, so we get the global bound:

$$\mathbb{E}(|Z|^m||Z| \ge \beta) \le \left\lfloor \frac{m}{2} \right\rfloor^{\frac{1}{2}} \left\lfloor \frac{m-1}{2} \right\rfloor ! (2\sigma)^m e^{-\frac{\beta^2}{4\sigma^2}}$$
(B45)